AD_____

Award Number: W81XWH-08-1-0076

TITLE: Articular Cartilage Repair Through Muscle Cell-Based Tissue Engineering

PRINCIPAL INVESTIGATOR: Johnny Huard

CONTRACTING ORGANIZATION: Children's Hospital of Pittsburgh
Pittsburgh, PA 15224

REPORT DATE: March 2011

TYPE OF REPORT: Annual

PREPARED FOR: U.S. Army Medical Research and Materiel Command
Fort Detrick, Maryland 21702-5012

REPORT DOCUMENTATION PAGE

Form Approved
OMB No. 0704-0188

1. REPORT DATE *(DD-MM-YYYY)*	**2. REPORT TYPE**	**3. DATES COVERED** *(From - To)*
01-03-2011	Annual	1 MAR 2010 - 28 FEB 2011

4. TITLE AND SUBTITLE

Articular Cartilage Repair Through Muscle Cell-Based Tissue Engineering

5a. CONTRACT NUMBER

5b. GRANT NUMBER

W81XWH-08-1-0076

5c. PROGRAM ELEMENT NUMBER

6. AUTHOR(S)

Johnny Huard

E-Mail: jhuard@pitt.edu

5d. PROJECT NUMBER

5e. TASK NUMBER

5f. WORK UNIT NUMBER

7. PERFORMING ORGANIZATION NAME(S) AND ADDRESS(ES)

Children's Hospital of Pittsburgh
Pittsburgh, PA 15224

8. PERFORMING ORGANIZATION REPORT NUMBER

9. SPONSORING / MONITORING AGENCY NAME(S) AND ADDRESS(ES)

U.S. Army Medical Research and Materiel Command
Fort Detrick, Maryland 21702-5012

10. SPONSOR/MONITOR'S ACRONYM(S)

11. SPONSOR/MONITOR'S REPORT NUMBER(S)

12. DISTRIBUTION / AVAILABILITY STATEMENT

Approved for Public Release; Distribution Unlimited

13. SUPPLEMENTARY NOTES

14. ABSTRACT

Abstract on next page.

15. SUBJECT TERMS

Articular Cartilage Repair, Fibrocartilage prevention, Muscle-derived Stem Cells, BMP-4, VEGF, Angiogenisis, sFLT-1

16. SECURITY CLASSIFICATION OF:			**17. LIMITATION OF ABSTRACT**	**18. NUMBER OF PAGES**	**19a. NAME OF RESPONSIBLE PERSON**
a. REPORT	**b. ABSTRACT**	**c. THIS PAGE**			USAMRMC
U	U	U	UU	86	**19b. TELEPHONE NUMBER** *(include area code)*

Abstract:
Using the modified preplate technique, we have isolated a population of early myogenic progenitor cells from postnatal skeletal muscle that display stem cell characteristics. We have shown that these 'muscle-derived stem cells' (MDSCs) can differentiate toward myogenic, osteogenic, chondrogenic, neurogenic, and hematopoietic lineages. Specifically, MDSCs cultured in chondrogenic medium can undergo chondrogenic differentiation *in vitro*, and MDSCs delivered to osteochondral defects display good cell survival and can differentiate into chondrocytes that improve the healing of articular cartilage. We also have observed that bone morphogenetic protein 4 (BMP4) promotes chondrogenic differentiation of MDSCs *in vitro* and *in vivo* and that this cytokine can trigger chondrogenic differentiation of other populations of muscle-derived cells, including myoblasts (late myogenic progenitor cells) and fibroblasts. The proposed project will investigate the use of these populations of muscle-derived cells as novel cell sources for articular cartilage repair in osteochondral defects created in nude rats. We will investigate the *in vitro* chondrogenic potential of various populations of mouse muscle-derived cells (fibroblastic cells and early and late myogenic progenitor cells) expressing BMP4 and determine the regenerative capacity of these cells after implantation in rat articular cartilage defects. We then will explore the relative contributions of these muscle-derived cells' long-term proliferation, survival, and self-renewal to their regenerative capacity after transplantation into the cartilage defects (**Technical Objective #1**). Next, we will determine the contributions of angiogenesis and scar tissue formation to the regenerative capacity of the muscle-derived cells and to the overall quality of the cartilage generated within the treated osteochondral defects (**Technical Objective #2**). This project will increase our understanding of the basic biology of muscle cell populations and their possible role in chondrogenic regeneration, and may lead to the development of new techniques to improve cartilage regeneration via the transplantation of muscle-derived cells.

Technical Objective #1: Evaluate different fractions of cells obtained from mouse skeletal muscle to identify the cell population with the greatest chondrogenic potential and the greatest capacity for cartilage regeneration.

> ***Hypothesis:*** *Different populations of cells obtained from skeletal muscle, when transduced to express bone morphogenetic protein 4 (BMP4), will exhibit different capacities for cartilage regeneration.*

Technical Objective #2**: Determine the relative contributions of angiogenesis and fibrosis on the capacity of muscle-derived cells to regenerate articular cartilage.**

> ***Hypothesis****: The promotion of angiogenesis and the prevention of fibrosis will improve the persistence and quality of regenerated cartilage.*

Relevance: This project will increase our understanding of the basic biology of muscle cell populations and their possible role in chondrogenic regeneration, and may lead to the development of new techniques to improve cartilage regeneration via the transplantation of muscle-derived cells.

Table of Contents

Articular Cartilage Repair through Muscle Cell–Based Tissue Engineering
(Johnny Huard)
Contract #: W81XWH-08-1-0076

Introduction

Using the modified preplate technique, we have isolated a population of early myogenic progenitor cells from postnatal skeletal muscle that display stem cell characteristics. We have shown that these 'muscle-derived stem cells' (MDSCs) can differentiate toward myogenic, osteogenic, chondrogenic, neurogenic, and hematopoietic lineages. Specifically, MDSCs cultured in chondrogenic medium can undergo chondrogenic differentiation *in vitro*, and MDSCs delivered to osteochondral defects display good cell survival and can differentiate into chondrocytes that improve the healing of articular cartilage. We also have observed that bone morphogenetic protein 4 (BMP4) promotes chondrogenic differentiation of MDSCs *in vitro* and *in vivo* and that this cytokine can trigger chondrogenic differentiation of other populations of muscle-derived cells, including myoblasts (late myogenic progenitor cells) and fibroblasts. The proposed project will investigate the use of these populations of muscle-derived cells as novel cell sources for articular cartilage repair in osteochondral defects created in nude rats. We will investigate the *in vitro* chondrogenic potential of various populations of mouse muscle-derived cells (fibroblastic cells and early and late myogenic progenitor cells) expressing BMP4 and determine the regenerative capacity of these cells after implantation in rat articular cartilage defects. We then will explore the relative contributions of these muscle-derived cells' long-term proliferation, survival, and self-renewal to their regenerative capacity after transplantation into the cartilage defects (**Technical Objective #1**). Next, we will determine the contributions of angiogenesis and scar tissue formation to the regenerative capacity of the muscle-derived cells and to the overall quality of the cartilage generated within the treated osteochondral defects (**Technical Objective #2**). This project will increase our understanding of the basic biology of muscle cell populations and their possible role in chondrogenic regeneration, and may lead to the development of new techniques to improve cartilage regeneration via the transplantation of muscle-derived cells.

Relevance: This project will increase our understanding of the basic biology of muscle cell populations and their possible role in chondrogenic regeneration, and may lead to the development of new techniques to improve cartilage regeneration via the transplantation of muscle-derived cells.

Body:

1) Technical Objectives:

Technical Objective #1: Evaluate different fractions of cells obtained from mouse skeletal muscle to identify the cell population with the greatest chondrogenic potential and the greatest capacity for cartilage regeneration.

Hypothesis: Different populations of cells obtained from skeletal muscle, when transduced to express bone morphogenetic protein 4 (BMP4), will exhibit different capacities for cartilage regeneration.

Technical Objective #2: Determine the relative contributions of angiogenesis and fibrosis on the capacity of muscle-derived cells to regenerate articular cartilage.

Hypothesis: The promotion of angiogenesis and the prevention of fibrosis will improve the persistence and quality of regenerated cartilage.

Progress from 3-1-08 to 2-28-10:

1) It was observed that fibrogenic cells residing in the fascia (fascia-derived cells [FDCs]) in the skeletal muscle are chondrogenic progenitor cells. By definition, the fascia of skeletal muscle is epimysium that covers the entire body of skeletal muscle. We hypothesized that cells located in endomysium and perimysium also possess chondrogenic potential; however, physically separating the endomysium and perimysium tissues from skeletal muscle is too difficult to be accomplished. Since endomysium and perimysium tissues are contained in the skeletal muscle, muscle derived cells (MDCs) would contain cells from endomysium and perimysium as well as other populations of cells. The characteristics and chondrogenic differentiation of MDCs have been investigated and human FDCs have also been examined. Characterization of MDCs demonstrated that they contain at least two populations of cells, FDCs and a population of myogenic cells. Chondrogenic differentiation displayed by muscle derived cells (MDCs) implies that either FDCs, a population of myogenic cells, or both MDCs and FDCs have chondrogenic potential. Mixtures of FDCs and rat L6 myoblasts demonstrated FDCs are the chondrogenic progenitor cell fraction of MDCs, but the myogenic cell fraction of MDCs plays little role in chondrogenesis. Findings about rat FDCs are also supported by the positive chondrogenic differentiation displayed by human FDCs. **(Refer to Appendix 1** [Abstract])

   Intramuscular injection of bone morphogenetic protein (BMP) has been shown to induce ectopic bone formation. As in developmental bone formation, a chondrogenic phase is typically observed in this process, which suggests that there may exist a chondrogenic sub-population of cells residing in skeletal muscle. Identification and isolation of this population could yield an important cell source for cartilage tissue engineering. Two prospective cell populations were isolated from rat skeletal muscle: fascia-derived cells (FDCs) extracted from gluteus maximus muscle fascia and muscle-derived cells (MDCs) isolated from the muscle body. Both were investigated for their cell surface marker profile (flowcytometry analysis), proliferation rate, and myogenic and chondrogenic potentials. The majority of FDCs expressed mesenchymal cell markers (CD29, CD59, and CD90) but not endothelial cell markers (CD34, CD31, CD144, vWF, Flk-1 and CD146). FDCs underwent chondrogenic differentiation after BMP-4 treatment in vitro, but not myogenic differentiation when cultured in myogenic differentiation medium. Sorting on the basis of CD29 and CD146 expression demonstrated that chondrogenic potential correlated poorly with CD29 expression and negatively with CD146. In fact, unsorted FDCs demonstrated significantly higher chondrogenic potential as well as proliferation rates than all other sub-populations studied. Although MDCs were similar to FDCs in term of cell surface marker profile and chondrogenic potential, they expressed the myogenic cell marker desmin and readily underwent myogenic differentiation in vitro. However, this result is likely confounded by the presence of FDC-like cells residing in the muscle peri- and endomysium. To clarify the role of muscle derived myogenic cells in chondrogenesis, mixed pellets varying ratios of FDCs and L6 myoblasts were formed and studied for chondrogenic potential. Results suggest that myoblasts did not participate in chondrogenesis. Further studies of human FDCs demonstrated the presence of similar cell displaying a low myogenic potential and capable of chondrogenesis. From this study we conclude that non-myogenic cells residing in the fascia of skeletal muscle have chondrogenic potential and may represent a novel cell donor source for cartilage regeneration and repair. (**Manuscript under preparation**, **Entitled: Identification and characterization of chondrogenic progenitor cells in post natal skeletal muscle: the role of fascia derived cells in chondrogenesis**)

2) We explored possible differences in muscle derived stem cell (MDSC) chondrogenic differentiation in vitro and articular cartilage (AC) regeneration in vivo between murine male MDSCs (M-MDSCs) and female MDSCs (F-MDSCs). Three different populations of M- and F-MDSCs obtained via a modified preplate technique, were compared for their in vitro chondrogenic potential using pellet culture. The cells with or

without retroviral transduction to express bone morphogenetic protein 4 (BMP4) were assayed. The influence of both the expression of stem cell markers (stem cell antigen 1, SCA-1) and the in vitro expansion level on the chondrogenic potential of M-and F-MDSCs was also determined. Lastly, BMP4-transduced M- and F-MDSCs were applied to a full-thickness AC defect of a nude rat femur. In addition to qualitative macroscopic examination, a histological grading scale of Safranin O-fast green staining was used to evaluate the quality of the repaired tissue.

Our results indicate that with and without BMP4 gene transduction, M-MDSCs produced significantly larger pellets with a richer extracellular matrix when compared to F-MDSCs. Although Sca1 purification influences the chondrogenic potential of MDSCs, especially M-MDSCs, it appears that long term culturing does not influence the chondrogenic potential of M-MDSCs, but does influence F-MDSCs. In vivo macroscopic and histological evaluations demonstrate that M-MDSC repair AC defects in a more effective manner than F-MDSCs, at all time points tested. **(Refer to Appendix 2, Matsumoto T, et al. A&R 2008)**

3) We investigated the effect of VEGF stimulation and the effect of blocking VEGF with its antagonist, sFlt1, on chondrogenesis using skeletal muscle-derived stem cells (MDSCs). The direct effect of VEGF on the *in vitro* chondrogenic ability of mouse MDSCs was tested using a pellet culture system followed by quantitative real time PCR and histological analyses. Next, the effect of VEGF on chondrogenesis within the synovial joint was tested using genetically engineered MDSCs implanted into the rat osteochondral defect. In this model, MDSCs, transduced with a retroviral vector to express BMP4, were co-implanted with MDSCs transduced to express either VEGF or sFlt1 (a VEGF antagonist) to provide a gain- and loss-of VEGF function experimental design. Histological scoring was used to compare cartilage formation among the treatment groups.

Hyaline-like cartilage matrix production was observed in both VEGF-treated and VEGF-blocked (sFlt1-treated) pellet cultures, but real-time PCR revealed that sFlt1 treatment improved the expression of chondrogenic genes in MDSCs that were stimulated to undergo chondrogenic differentiation with BMP4 and TGF-β3. *In vivo* testing of articular cartilage repair showed that VEGF-transduced MDSCs caused an arthritic change in the knee joint, and sFlt1 improved the MDSC-mediated repair of articular cartilage, compared to BMP4 alone. **(Refer to Appendix 3, Kubo S, et al. A&R 2009)**

4) Osteoarthritis (OA), a chronic degenerative joint disorder worldwide and characterized by articular cartilage destruction and osteophyte formation, affects over 40 million individuals in the United States alone. Stem cells are attractive because of their superior capacity for self renewal, proliferation, and survival post-implantation. Several studies have suggested that stem cells can undergo chondrogenesis and repair articular cartilage in experimental cartilage injury models, including studies using muscle derived stem cells (MDSCs). We have already reported that bone morphogenic protein 4 (BMP4) transduced MDSCs improve cartilage regeneration in the *in vitro* pellet culture and the *in vivo* cartilage defect model. The control of angiogenesis such as using sFlt1, vascular endothelial growth factor (VEGF) antagonist, during the chondrogenic differentiation of stem cells is also an important issue to consider especially for the persistence of the regenerate cartilage. Based on these backgrounds, the series of experiments is designed to clarify the therapeutic efficacy of BMP4 and sFlt1 transduced MDSCs for the repair of articular cartilage after OA.

Macroscopic and histological evaluation of the joint: *In vivo* testing of articular cartilage regeneration showed macroscopically and histologically that VEGF transduced MDSCs prevented but sFlt1 improved the B4-mediated MDSC regeneration of articular cartilage compared to the B4 alone, as confirmed by histological scores.

Contribution of MDSCs in cartilage regeneration and repair: Double IHC of Col2 and GFP or β-gal demonstrated that VEGF transduced MDSCs prevented but sFlt1 improved chongenic differentiation of MDSC and intrinsic chondrogenesis , compared to BMP4 alone.

Chondrocyte apoptosis and proliferation analyses: TUNEL stain and BrdU assay demonstrated that sFlt1-transduced MDSCs, unlike VEGF expressing cells, lead to less apoptosis and more proliferation compared to B4 alone.

Mixed pellet culture: In vitro mixed co-culture showed BMP4 treated group produced significantly larger pellets with hyaline cartilage-like matrix production than all other groups, confirmed by the chondrogenic differentiation capacity of MDSCs using qPCR and qIHC of Col2 and GFP or β-gal. FISH showed no fusion between OA chondrocytes and MDSCs and higher intrinsic chondrogenesis in BMP4 treated group.

Separated pellet culture: In vitro separated co-culture showed BMP4 treated group produced significantly larger pellets with hyaline cartilage-like matrix production than all other groups. (**Refer to Appendices 4 and 5, Matsumoto T, et al. Artritis Rheum, 2009**).

5) Over the past number of years it has become increasingly clear that the role of the donor cells participation in the repair process is not fully elucidated. In fact, in numerous animal models we have shown that the implantation of BMP4 expressing MDCs improves AC repair; however, the repair process is mediated primarily by the chemo-attraction of host cells. Therefore, we have started to more closely analyze these chemo-attracted host derived cells that appear at the injury site after MDC implantation. We want to determine the tissue of origin of the host cells that participate in the AC regeneration processes and have begun preliminary experiments designed to determine if the host cells could originate from the bone marrow or possibly the intra-articular synovial tissue. We are planning to investigate the role that donor MDC survival plays in the AC repair process even though the donor cells do not actively participate in chondrogenic differentiation but instead seem to vigorously chemo-attract host cells which are the primary cell source for the newly regenerated AC tissue. To this end we plan to investigate approaches to improve cell survival and the contribution that the donor cells play in the repair process. This is important since OA typically affects older patients and the host cells of aged patients may have a reduction in their tissue regenerative potential. To date we have preliminary results that compare the cartilage regenerative ability of the MDCs in synovectomized rats that have had an OA injury created with MIA, and compared them to rats with intact synovial membranes. The MDCs that were intracapsularly injected had half of the cells transduced with sflt-1 and the other half transduced with BMP4, which was the best transduction regime determined previously (**Appendices 1 and 4**). The cells were also transduced with either GFP or LacZ to track the fate of the donor cells. Briefly, the study methodology that we followed was: 1) Rat OA models were created using MIA, 2) Two weeks after MIA injection a synovectomy was performed in half of the rats as previously described [*Miyamoto A, et al. The role of the synovium in repairing cartilage defects. Knee Surg Sports Traumatol Arthrosc. 200], 3)* Three days after surgery 5x10E5 MDCs were injected (50:50 sflt-1:BMP4 transduced), 4) Four weeks after MDC injection the rats were sacrificed and their knee joints assessed. **Figure 1** shows a macroscopic evaluation of the two groups. Macroscopic evaluation of the synovectomy(-) group showed well-healed articular surfaces, some parts of the joints included osteophyte formation. However, the synovectomy(+) group showed marked arthritis including synovial hypertrophy and osteophyte formation.

FIGURE 1

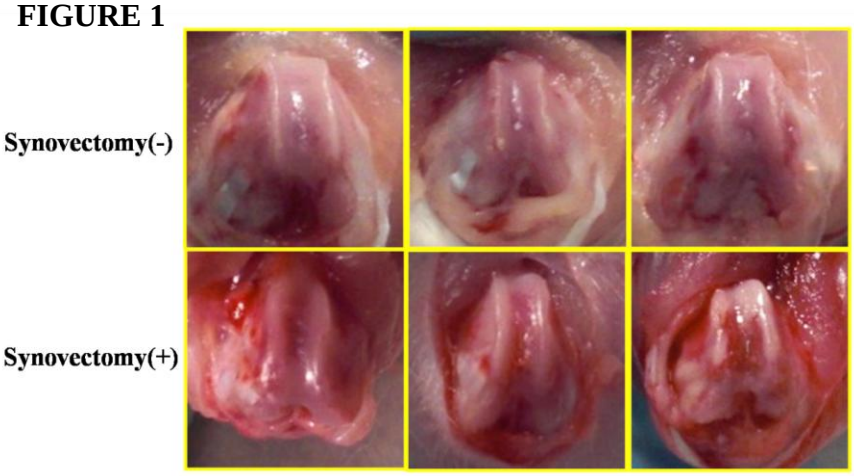

Macroscopic evaluation (4W)
(Treated with sFlt1/BMP4-MDSC)

Histologic assessment demonstrated that Safranin O–positive hyaline-like cartilage was present in the synovectomy(-) group. However, Safranin O–positive hyaline-like cartilage was less prominent in the synovectomy(-) group **(Figure 2)**.

FIGURE 2

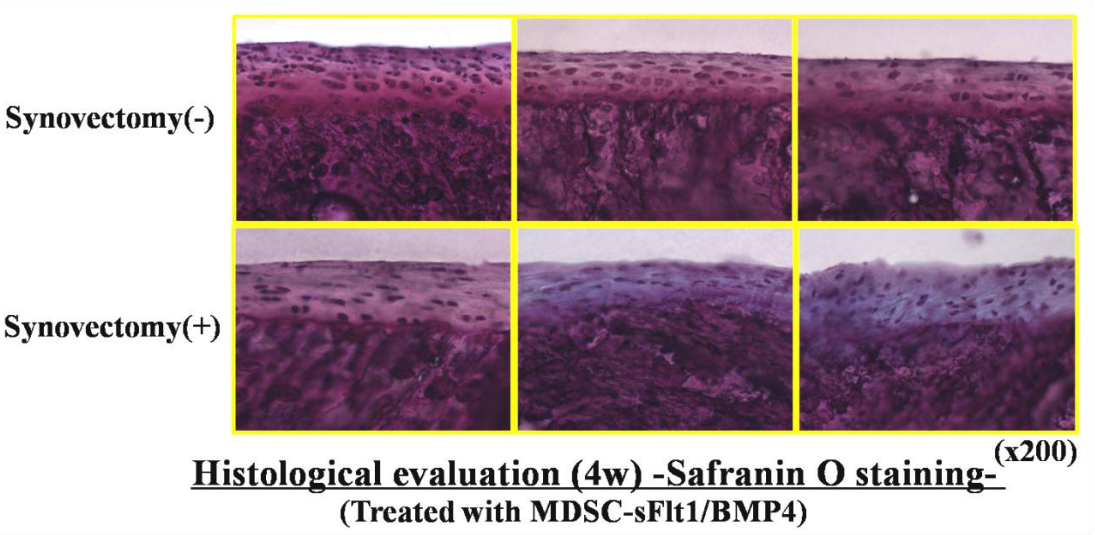

A previously described histological grading scale was used to evaluate the quality of the repaired tissue. Four weeks after transplantation, the total score in the synovectomy(-) group was significantly lower than that in the synovectomy(+) group. Note that a lower score in this grading scale represents better cartilage (synovectomy(-) group, 5.2±1.0. synovectomy(+) group, 11.0±1.7. $P<0.05$, respectively) **(Figure 3)**.

FIGURE 3

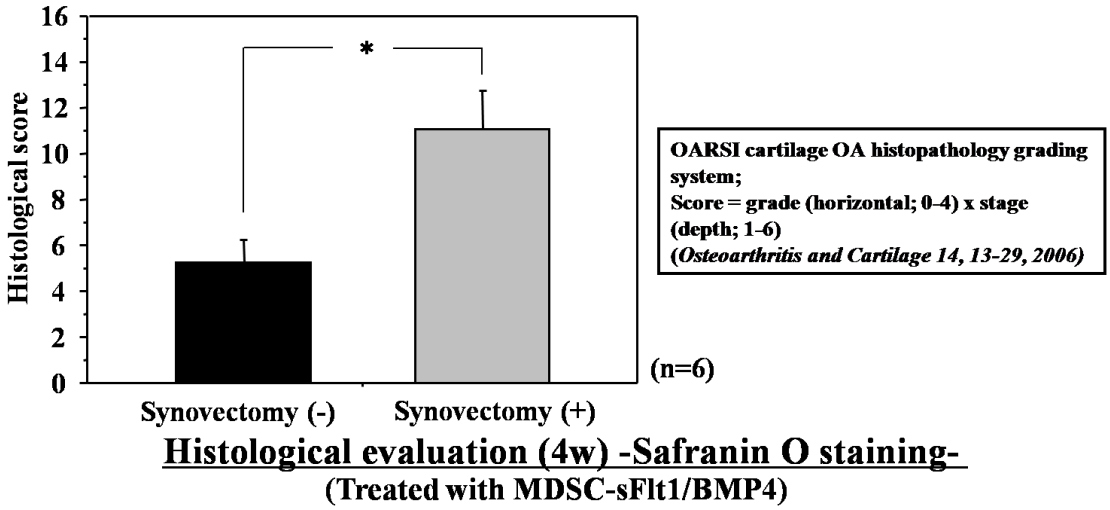

These preliminary results strongly support the fact that some factor emanating from the synovium is essential for proper regeneration of OA injured articular cartilage. More investigation is necessary to determine exactly how the synovial tissue is participating in the repair process. It could be both the deployment of cells from the synovial tissue that actually participate in the remodeling of the AC and/or the paracrine release of essential factors that aide in the healing process and potentially attract other cell types from the host. These results are being included in a paper currently under preparation.

Current Progress from 3-1-10 to 2-28-11:

1) Intramuscular injection of bone morphogenetic protein (BMP) has been shown to induce ectopic bone formation. As in ectopic bone formation, a chondrogenic phase is typically observed in this process, which suggests that there may exist a chondrogenic sub-population of cells residing in skeletal muscle. It is observed that fibrogenic cells residing in the fascia (FDCs) in the skeletal muscle are chondrogenic progenitor cells. By definition, the fascia of skeletal muscle is epimysium that covers the entire body of skeletal muscle. We hypothesized that cells located in endomysium and perimysium also possess chondrogenic potential; however, physically separating the endomysium and perimysium tissues from skeletal muscle is too difficult to be accomplished. Since endomysium and perimysium tissues are contained in the skeletal muscle, muscle derived cells (MDCs) would contain cells from endomysium and perimysium as well as other populations of cells. The characteristics and chondrogenic differentiation of MDCs have been investigated and human FDCs have also been examined.

Two prospective cell populations were isolated from rat skeletal muscle: fascia-derived cells (FDCs), extracted from gluteus maximus muscle fascia, and muscle-derived cells (MDCs), isolated from the muscle body. Both populations were investigated for their cell surface marker profile (flowcytometry analysis), proliferation rates, as well as their myogenic and chondrogenic potentials. The majority of FDCs expressed mesenchymal stromal cell markers (CD29, CD59, and CD90) but not endothelial cell markers (CD34, CD31, CD144, vWF, Flk-1 and CD146). FDCs underwent chondrogenic differentiation after BMP-4 treatment in vitro, but not myogenic differentiation when cultured in myogenic differentiation medium. Sorting on the basis of CD29 and CD146 expression demonstrated that chondrogenic potential correlated poorly with CD29 and CD146 expression. In fact, the unsorted FDCs demonstrated a significantly higher chondrogenic potential and proliferation rate compared to all the other sub-populations studied. Although MDCs were similar to the FDCs in terms of their cell surface marker profile and chondrogenic potential, they expressed the myogenic cell marker desmin and readily underwent myogenic differentiation in vitro; however, the chondrogenic potential of the MDCs is confounded by the presence of FDC-like cells (fibroblasts) residing in the muscle peri- and endomysium. To clarify the role of the muscle derived myogenic cells in chondrogenesis, mixed pellets with varying ratios of FDCs and L6 myoblasts were formed and studied for chondrogenic potential. Our results indicated that the chondrogenic potential of the FDCs decreased with the increased ratio of myogenic to FDCs supporting the role of FDCs in chondrogenesis. Additonal studies of human FDCs also demonstrated the presence of similar cells displaying a high chondrogenic potential with a low myogenic potential. Taken together, our results suggest that non-myogenic cells residing in the fascia of skeletal muscle have a strong chondrogenic potential and may represent a novel donor cell source for cartilage regeneration and repair (**see Appendices 1 and 6**).

2) As you can see above in **Figure 2,** our results indicate a significant decrease in the repair process when the synovial lining is removed but the repair process is not completely inhibited. We would expect to achieve similar results using the MDSCs in the osteochondral defect, and we posit that the repair process can also be mediated, at least in part, by cells other than synovial derived cells such as bone marrow derived cells. We are analyzing the role of bone marrow derived cells in the AC repair process after MDSCs implantation. To block the possible reparative cells from the bone marrow, we propose to inject a sclerosing agent (such as ethanol or sodium morrhuate) into the femoral and tibia medullary canal 1 week before the induction of OA via ACL transection. These agents will cause sclerosis of the vessels in the medullary canal and will alter the bone marrow cells, as previously describe. Briefly, the distal metaphysis in the femur and the proximal metaphysis in the tibia will be palpated and identified. Using a percutaneous stab incision, a 20G needle will be inserted into the femoral and tibia canals and advanced by hand, reaming to a depth of 1.5 cm. The needle will be then extracted and a larger bore needle (18 G) will be used to ream the canals further. After reaming, the needle will be left in the canal to be used for sclerosing agent delivery. 25µl either 100% ethanol or 5% sodium morrhuate solution will be slowly injected into the medullary spaces. As the agents are slowly injected, the needle will be retracted from the canal. The cortical bone will be closed with bone wax to avoid leakage of the injection, and

the muscle fascias and skin will be sutured. These agents will alter bone marrow cells in the medullary canal and will reduce/negate their participation in AC repair. As a pilot study, 200µl of pure ethanol was injected into medullary canal of one femur through an 18 G needle that was inserted via intra-trochanter fossa. After 2, 4, and 6 weeks, both femurs were collected and the number of nucleated cells within the ethanol injected femur were counted and compared with the number present in the untreated control femur. The number of nucleated cells in the ethanol treated femur was significantly reduced (**Fig. 3**). Furthermore, the colony forming units (CFU) per million nucleated cells in ethanol injected femur was also significantly decreased when compare with control femur (**Fig. 3**). These results demonstrated our ability to perform this set of studies in order to reduce bone marrow involvement during the AC repair process after MDSC transplantation.

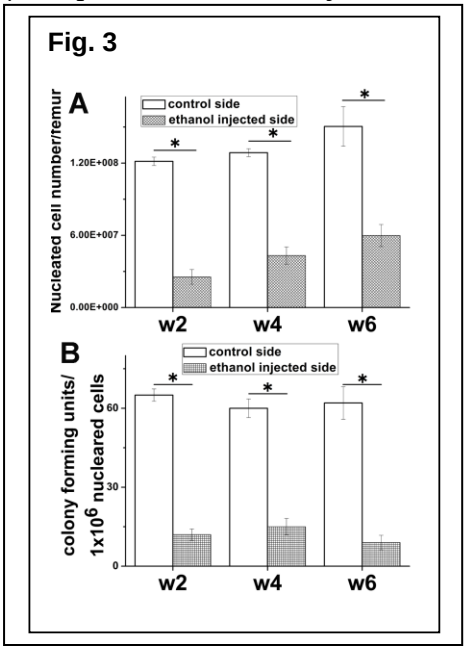

We also initiated experiments to determine whether Platelet Rich Plasma (PRP) as a substance that can be added to the MDSCs to further promote AC repair in the OA model. In fact, PRP is a natural biomaterial that can be obtained autogenously or allogeneically. PRP contains more than 30 bioactive components (growth factors and cytokines) that can promote healing of various tissues including cartilage. Several growth factors that can be found abundantly in PRP, including TGF-β and IGF have been found capable of enhancing chondrocyte proliferation and extracellular matrix synthesis. PRP itself also has the potential to stimulate chondrocyte proliferation, differentiation and matrix biosynthesis both *in vitro, in vivo, and in clinical trials*. A recent study also showed that PRP could be a potential treatment option for OA because of its anti-inflammatory effect. Several studies have shown that PRP can promote the proliferation of bone marrow-derived mesenchymal stem cells (MSCs), adipose tissue-derived MSCs, and peripheral blood precursors *in vitro*. We have observed a beneficial effect of PRP in the proliferation of human MDSCs which will be presented at the upcoming 2011 Orthopaedic Research Society meeting as a poster (Hongshuai Li, et al.)

We have recently shown that the dilution of MDSCs within PRP (30 µl) improves AC repair, after injection into the joint fluid, when compared to non-PRP-treated MDSCs (**Fig. 4**). The improvement of AC repair, through the histological grading system, with the addition of PRP was not only observed with non-transduced MDSCs but also with MDSCs transduced to express BMP4 and sFlt-1(**Fig. 4**). We therefore propose to use PRP with the best group described above (MDSC or MDSC stimulated with sFlt-1/BMP4 proteins) to further improve AC repair after OA. PRP will be isolated via the following procedure. The blood of the donor rats will be drawn into tubes containing 3.2% sodium citrate. PRP will be isolated from the blood via a double centrifugation technique that has been previously described. The blood sample will be centrifuged at 160 g for 20 min at 22 °C to separate the plasma containing the platelets from the red cells. The plasma will be drawn off the top and centrifuged at 22 °C for an additional 15 min at 400 g to separate the platelets. The platelet-poor plasma (PPP) will be drawn off the top, leaving the PRP. 30 µl of the PRP will be used to dilute the chosen MDSC group prior to implantation into the joint fluid.

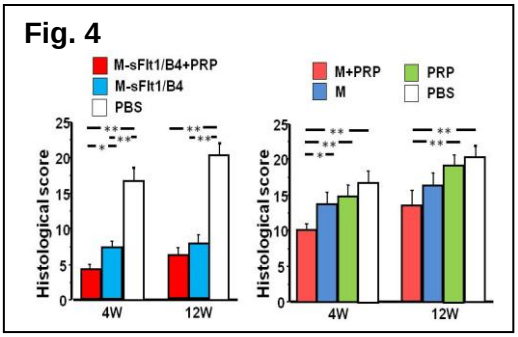

3) Platelet-rich plasma (PRP) provides an invaluable source of and growth factors for potential enhancement of multi-potent progenitor cells which reside in skeletal muscle, termed muscle derived progenitor cells (MDPCs),.for use in tissue reconstruction of muscle, bone, cartilage, and other musculoskeletal tissues. The influence of PRP on the growth and differentiation of hMDPCs is still not clear. In this study, we

investigated the effect of an allogenic PRP on human MDPCs (Pre-plated MDPCs, Myo-endothelial cells, and Pericytes) proliferation and differentiation.

Six whole blood donations were used to prepare one pooled PRP derived from buffy coats. The platelet concentration in the pooled PRP was standardized to 2×10^6 platelets per microliter (10 times above baseline) by centrifugation and re-suspension in platelet poor plasma (PPP). The platelet-released supernatants were prepared by activating PRP with one unit of human thrombin per ml cell suspension. Three different hMDPCs were used for this study. Human pre-plated MDPCs that were isolated by pre-plate technique were brought from Cook, Inc. Myoendothelial cells ($CD45^-$, $CD56^+$, $CD146^-$, $CD144^+$, $CD34^+$) and pericytes ($CD45^-$, $CD56^-$, $CD146^+$, $CD144^-$ $CD34^-$) were obtained by muscle biopsy from three donors, and surface markers were sorted by FACS. The influences of an *in vitro* PRP microenvironment on the proliferation and differentiation of hMDPCs were investigated. First, we tested if PRP can promote the proliferation of hMDPCs and if PRP can be used for *ex-vivo* expansion of hMDPCs instead of FBS by short-term and long-term proliferation assays, and the expression of human mesenchymal stem cell marker genes were analyzed by RT-PCR. Second, we investigated which growth factor within PRP play a main role in promoting the proliferation by neutralization assay. Third, we studied the influence of PRP on the differentiation of hMDPCs both in *ex-vivo* expansion phase and differentiation-induction phase.

Both short-term and long-term cell proliferation and number of performed cell doublings were enhanced in cultures supplemented with PRP, either with or without the concomitant addition of FBS. Growth factor neutralization assay revealed that PDGF within PRP mainly contributed the mitogenic effects. Osteogenic, chondrogenic, and myogenic differentiation abilities were maintained in the cells that expanded within PRP. Furthermore, most of the stem cell markers were steady expressed by the hMDPCs when expanded in 20% PRP. For some of the stem cell markers, the expression levels were even higher than in the cells expanded in FBS. Interestingly, osteogenic, chondrogenic, and myogenic differentiation efficiency of hMDPCs were dramatically decreased when PRP was present in the induction medium, and the differentiation ability was regained when PRP was removed from the induction medium. And the inhibition effects were related to the proliferation of the hMDPCs during differentiation induction.

This study demonstrates direct effects of PRP on hMDPCs without the additional effect of systemic factors. Together these findings indicate a potential usage of PRP with hMDPCs for tissue engineering. First, PRP can be used as a supplement for *ex vivo* expansion of hMDPCs. Second, PRP could be a possible augmentative agent for *in vivo* stem cell therapy since the growth factors released by PRP can support the proliferation of the hMDPCs and keep them in an early undifferentiated stage at their initial transplantation; once the platelets have lost their activity, the MDPCs will regain their responsiveness to the local micro-environmental stimuli and differentiate into functional tissue cells.

4) Viral vectors can be applied for the genetic modification of stem cells; however, due to the fact that transduction reduces the proliferation and differentiation of adult stem cells it limits stem cell therapy modalities. Rats are commonly used for animal modeling in regenerative medicine to investigate bone and cartilage repair. Recombinant adeno-associated viral (rAAV) vectors have great advantages; however, in our previous studies, low-efficiency transduction of rAAV vectors was observed in rat muscle-derived stem cells (MDSCs). To monitor gene transfer efficiency and to image *in vivo* implanted MDSCs, we recently developed a novel retro-vector that efficiently expresses a red fluorescent protein (RFPn) reporter with a nuclear localization signal. The purpose of this study is to test whether high-efficiency transduction in rat MDSCs can be achieved, even after the cells have split many generations. Moreover, the red reporter in the nucleus avoids green fluorescent background in hard and soft tissues.

The retro-viral vector carrying the RPFn gene was controlled by a CMV promoter. The vector was generated in a packaging cell line (GP2-293), according to standard protocol. The virus-containing supernatant was harvested 48 hours post-co-transfection, and activity was determined in the packaging cell line. MDSCs were isolated from GFP transgenic rats and cultured in regular proliferation medium with 50% cell fluency. A solution of 50% collected medium, containing the virus, and 50% regular medium was used to infect rat MDSCs. The cells were passed daily to keep 50% density until day 21. The live, infected cells were routinely monitored by fluorescent microscopy to evaluate the transduction efficiency in daughter cells, and they were compared with FACS-sorted cells via red fluorescent marker

Figure 1.

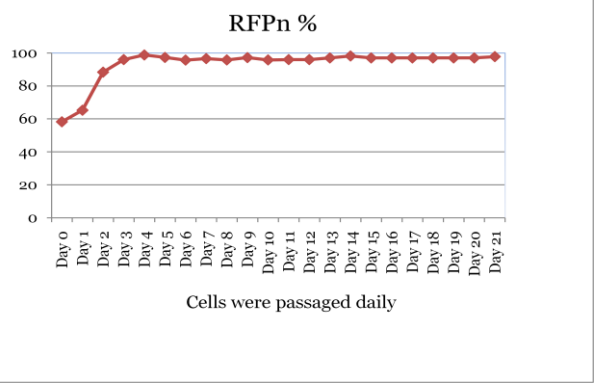

In this study, we counted over 500 cells per day, to qualitatively analyze RFPn transduction efficiency in rat MDSCs. As shown in Figure 1, RFPn expression in rat MDSCs was observed over 21 days. We found that the percentage rose from 60% to over 90% from day1 to day3, and it plateaued around 97% until day 21. We also did side-by-side comparison of the transduction efficiency between the unsorted RFPn-infected cells and sorted RFPn-infected. Interestingly, we did not find a significant difference (See Figure 2).

Figure 2.

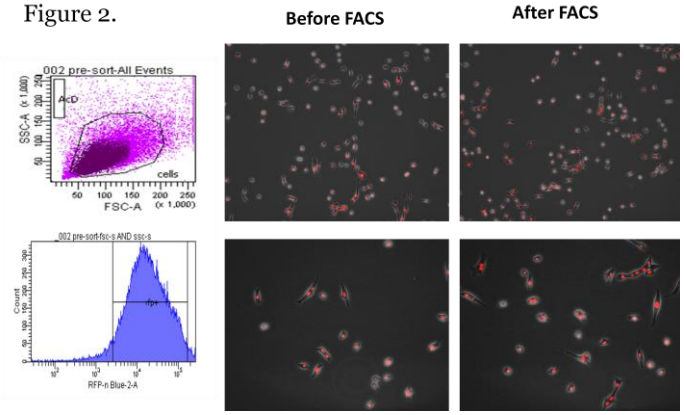

FACS sorting via cell or reporter markers is a common process concentrating the cells that express target genes. In this preliminary study, we demonstrate that this novel retro-viral vector is very suitable for gene transfer in rat MDSCs, even though we do not need FACS to sort cells.

Additional Experiments currently underway:

1) We have recently isolated different populations of muscle derived cells by the pre-plate technique. Fibroblastic cells (PP1), myoblastic cells (PP2-3), and MDSCs (PP6) and have transduced them with Retro-BMP-4-GFP.
2) We are currently testing the chondrogenic capacities of the transduced cell populations both in monolayer and pellet cultures.
3) Protein expression assay, RT-PCR, collagen and proteoglycan deposition etc. will be evaluated and compared among all the cell populations.
4) We are testing the cell proliferation kinetics of the transduced MDCs both under normoxia and hypoxia condition (5% oxygen).
5) We are testing the cell survival rates of the transduced MDCs both under oxidative stress (H_2O_2 induced), and inflammatory stress (TNF-alpha induced) conditions.
6) All three populations of cells will be transplanted into osteochondral defects created in nude rats. The cell engraftment, cell survival, induction of angiogenesis and cartilage-specific ECM production within and around the regenerated cartilage at different time points (4, 8, 16, and 24 weeks after cell transplantation) will be evaluated and compared among the groups.

Key Research Accomplishments to date

- Demonstrated that MDCs contain FDCs and a population of myogenic cells.
- Demonstrated that MDCs possess lower chondrogenic potential than FDCs.
- Demonstrated that non-myogenic cells residing in the fascia of skeletal muscle have chondrogenic potential and may represent a novel cell donor source for cartilage regeneration and repair.
- Demonstrated that Male MDSCs have a greater chondrogenic potential than Female-derived MDSCs
- Demonstrated that VEGF inhibits the chondrogenic potential of BMP4 transduced MDSCs
- Demonstrated that sFLT improves chondrogenic potential of BMP4 transduced MDSCs and inhibits apoptosis.
- Demonstrated that sFLT /BMP4 transduced MDSCs were superior to MDSCs transduced with only BMP4 or VEGF and BMP4 at chondrogenic regeneration after osteoarthritis was induced in rats
- Demonstrated that Human FDCs showed more fibrogenic staining and strong chondrogenic potential.
- Demonstrated that an intact synovium is essential for the proper healing of OA injured articular cartilage.
- Demonstrated that a Human Cell counter-part to the murine MDSCs were capable of differentiating toward a chondrogenic lineage and form articular cartilage.
- Two prospective cell populations of cells were isolated from rat skeletal muscle: fascia-derived cells (FDCs), extracted from gluteus maximus muscle fascia, and muscle-derived cells (MDCs), isolated from the muscle body. Both populations were investigated for their cell surface marker profiles.
- Demonstrated that pure myogenic cells (myoblasts) have a very poor chonrogenic potential and that fascia derived cells have an excellent chondrogenic potential.
- Demonstrated the direct effects that PRP had on hMDPCs without the additional effect of systemic factors for use in the culturing process to increase expansion efficiency prior to use in cartilage repair.
- Developed a Red Fluorescent Protein AAV vector which efficiently transduced MDSCs for use in tracking the cells post-transplantation.

Reportable Outcomes

1. **Li, GH; Zheng, B; Meszaros, LB;Corsi, KA; Usas, A; Huard, J.** Identification and Characterization of Chondrogenic Progenitor Cells in Adult Skeletal Muscle. Orthopeadic Research Society Annual Meeting Feb 2009 (Abstract). **(Appendix 1)**

2. **Matsumoto T, Kubo S, Meszaros L, Corsi K, Cooper G, Li G, Usas A, Osawa A, Fu F, Huard J**. The influence of sex on the chondrogenic potential of muscle-derived stem cells. A&R 2008 Dec; **58(12)3809-3819. (Appendix 2)**

3. **Kubo S, Cooper G, Phillippi J, Corsi K, Usas A, Li G, Freddie F, Huard J.** Blocking VEGF with sFlt1 improves the chondrogenic regeneration capacity of skeletal muscle-derived stem cells. A&R 2009 Jan; 60(1):155-165. **(Appendix 3)**

4. **Matsumoto, T ; Cooper, GM; Gharaibeh, B; Meszaros, L; Li G; Usas A; Fu, FH; Huard, J.** Cartilage Repair after Osteoarthritis through Intra-articular Injection of Muscle Stem Cells Expressing BMP4 and sFlt1. Orthopeadic Research Society Annual Meeting Feb 2009 (Abstract). **(Appendix 4)**

5. **Matsumoto T, Cooper G, Gharaibeh B, Meszaros L, Li G, Usas A, Fu F, Huard J.** Cartilage repair in a rat model of osteoarthritis through intraarticular transplantation of muscle-derived stem cells expressing bone morphogenetic protein 4 and soluble Flt-1. **Artritis Rheum;** Published Online: Apr 29 2009 (p 1390-1405), PMID: 19404941 [PubMed - indexed for MEDLINE]. (**Appendix 5**)

6. **Bo Zheng, Guangheng Li, Bridget M Deasy, Jonathan B Pollett, Bin Sun, Lauren Drowley, Burhan Gharaibeh, Arvydas Usas, Alison Logar, Bruno Peault, Johnny Huard.** Clonal Analysis of Human Myoendothelial Cells Reveals Stem Cell Characteristics. **In Submission to J of Mol Cell Biol.**

7. **Guangheng Li, Bo Zheng, Laura B Meszaros, Joseph B Vella, Arvydas Usas, and Tomoyuki Matsumoto, Johnny Huard.** Identification and characterization of chondrogenic progenitor cells in the fascia of post natal skeletal muscle. **In Submission to J of Mol Cell Biol.**

8. **Li H, Usas A, Chen W, Gao X, Huard J** The Influence of Platelet-Rich Plasma on *In-vitro* Proliferation, and on Osteogenic, Chondrogenic, and Myogenic Differentiation of Human Muscle Derived Progenitor Cells, Orthopaedic Research Society Annual Meeting, Jan 13-16, 2011.

Conclusions:

1) Fibrogenic cells which reside in fascia and similar tissues in the skeletal muscles contain a population of chondrogenic progenitor cells. Fascia of skeletal muscle could be the tissue from which cells could be harvested for cartilage repair. Future research will focus on isolating these cells and using them to repair cartilage.

2) Our study demonstrated that sex influences the chondrogenic differentiation and AC regeneration potential of MDSCs, with M-MDSCs displaying more chondrogenic differentiation and better cartilage regeneration potential than F-MDSCs after cartilage injury.

3) sFlt1 gene therapy improved BMP4- and TGF-β3-induced chondrogenic gene expression of MDSCs *in vitro*, and improved the persistence of repaired articular cartilage by preventing vascularization and bone invasion into the repaired articular cartilage.

4) Our results suggest that MDSC-based gene/cell therapy involving sFlt1 and BMP4 repaired articular cartilage after OA mainly by having a beneficial effect on chondrogenesis by the donor and host cells as well as by preventing angiogenesis which eventually prevent cartilage resorption, resulting in a persistent cartilage regeneration and repair.

5) Some factor(s) emanating from the synovium are essential for the proper regeneration of OA injured articular cartilage. It could be both the deployment of cells from the synovial tissue that actually participate in the remodeling of the AC and/or the paracrine release of essential factors that aide in the healing process and potentially attract other cell types from the host.

6) We have demonstrated that human myoendothelial --a potential human counterpart cell population to the murine MDSCs-- cells possess fundamental properties of stem cells, including self-renewal, clonogenic and multipotent properties (including chondrogenic) *in vitro* and *in vivo.*

7) Synovial cells and bone marrow contain progenitor cells that play a role in MDSC mediated articular cartilage repair

8) Platelet Rich Plasma may represent a substance that can improve the chondrogenic potential of MDSC and their usage for AC repair.

9) Use of a novel RFP-AAV vector can efficiently transduce MDSCs so the cells can be effectively track post-transplantation.

Appendices

Appendix 1: Li, GH; Zheng, B; Meszaros, LB;Corsi, KA; Usas, A; Huard, J. Identification and Characterization of Chondrogenic Progenitor Cells in Adult Skeletal Muscle. Orthopeadic Research Society Annual Meeting Feb 2009 (Abstract).

Appendix 2: Matsumoto T, Kubo S, Meszaros L, Corsi K, Cooper G, Li G, Usas A, Osawa A, Fu F, Huard J. The influence of sex on the chondrogenic potential of muscle-derived stem cells. A&R 2008 Dec; 58(12)3809-3819.

Appendix 3: Kubo S, Cooper G, Phillippi J, Corsi K, Usas A, Li G, Freddie F, Huard J. Blocking VEGF with sFlt1 improves the chondrogenic regeneration capacity of skeletal muscle-derived stem cells. A&R 2009 Jan; 60(1):155-165.

Appendix 4: Matsumoto, T ; Cooper, GM; Gharaibeh, B; Meszaros, L; Li G; Usas A; Fu, FH; Huard, J. Cartilage Repair after Osteoarthritis through Intra-articular Injection of Muscle Stem Cells Expressing BMP4 and sFlt1. Orthopeadic Research Society Annual Meeting Feb 2009 (Abstract).

Appendix 5: Matsumoto T, Cooper G, Gharaibeh B, Meszaros L, Li G, Usas A, Fu F, Huard J. Cartilage repair in a rat model of osteoarthritis through intraarticular transplantation of muscle-derived stem cells expressing bone morphogenetic protein 4 and soluble Flt-1. Artritis Rheum; Published Online: Apr 29 2009 (p 1390-1405), PMID: 19404941 [PubMed - indexed for MEDLINE].

Appendix 6: Guangheng Li, Bo Zheng, Laura B Meszaros, Joseph B Vella, Arvydas Usas, and Tomoyuki Matsumoto, Johnny Huard. Identification and characterization of chondrogenic progenitor cells in the fascia of post natal skeletal muscle. In Submission to J of Mol Cell Biol.

Appendix 7: Li H, Usas A, Chen W, Gao X, Huard J. The Influence of Platelet-Rich Plasma on *In-vitro* Proliferation, and on Osteogenic, Chondrogenic, and Myogenic Differentiation of Human Muscle Derived Progenitor Cells, Orthopaedic Research Society Annual Meeting, Jan 13-16, 2011 (Poster).

Identification and Characterization of Chondrogenic Progenitor Cells in Adult Skeletal Muscle

*Li, GH; *Zheng, B; *Meszaros, LB; *Corsi, KA; *Usas, A; +*Huard, J

+*Stem Cell Research Center, Children's Hospital of Pittsburgh of UPMC and Department of Orthopaedic Surgery, University of Pittsburgh, Pittsburgh, PA

Senior author: jhuard@pitt.edu

INTRODUCTION:

It is observed that fibrogenic cells residing in the fascia (FDCs) in the skeletal muscle are chondrogenic progenitor cells (ORS abstract, 2006, 2007).By definition, the fascia of skeletal muscle is epimysium that covers the entire body of skeletal muscle. In the present study, we hypothesized that cells located in endomysium and perimysium also possess chondrogenic potential (Fig.1). However, physically separating the endomysium and perimysium tissues from skeletal muscle is too difficult to be accomplished. Since endomysium and perimysium tissues are contained in the skeletal muscle, muscle derived cells (MDCs) would contain cells from endomysium and perimysium as well as other populations of cells. The characteristics and chondrogenic differentiation of MDCs were investigated and human FDCs were also examined in the present study.

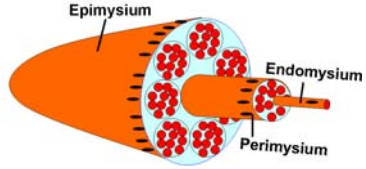

Fig1. Diagram of skeletal muscle structure

METHODS:

Freshly isolated rat MDCs were analyzed by flow cytometry. They were immunostained by desmin, vimentin and MyoD and their chondrogenic potential was evaluated under the treatment of BMP4 and TGFβ3. Chondrogenic potential of mixed FDCs and rat L6 myoblasts in different ratios (1:0, 4:1, 1:1, 1:4, 0:1 of FDCs to L6 cells) was also investigated. Finally, human FDCs were isolated and characterized, and their chondrogenic potential was also investigated.

RESULTS:

1. MDCs contain FDCs and a population of myogenic cells (Fig.2).
2. MDCs possess strong chondrogenic potential (Fig .2).
3. Chondrogenic assay of mixed FDCs and rat L6 myoblasts in different ratios showed chondrogenic potential is inversely proportional to the percentage of L6 cells (Fig.3).
4. Human FDCs showed more fibrogenic staining and strong chondrogenic potential (Fig.4).

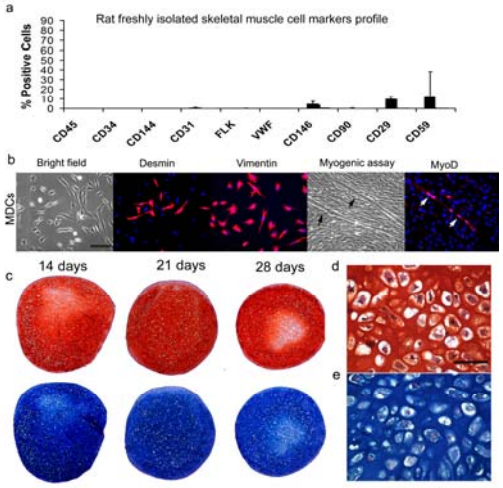

Fig2. (a) Surface marker profile of freshly isolated MDCs. (b) Phenotypic characterization of MDCs. MDCs acquire spindle-shape in vitro. Immunostaining for desmin (red) shows positive cells found in the MDCs. Blue color stains the cells' nuclei. Vimentin (red) staining shows all cells (nuclei, blue) are positive. Myogenic assay shows that myotubes form (arrows). Immunostaining for MyoD (red) shows the positive staining in nuclei of a myotube (arrows). (c) Chondrogenic assay demonstrates positive chondrogenic differentiation of MDCs with safranin O and Alcian blue staining, respectively. (d, e) Under higher magnification, typical chondrocytes which occupy lacunae within the safranin O positively stained (red) and Alcian blue/ nuclear fast red (blue) cartilage matrix can be observed in the MDCs pellet.

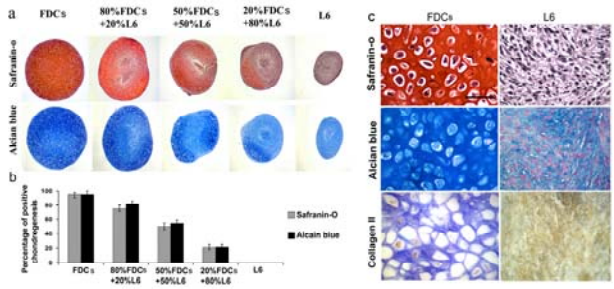

Fig3.(a) With safranin-O and Alcian blue staining, pellets of mixed FDCs and rat myoblast L6 showed decreasing chondrogenic potential with increasing percentage of L6 cells. FDCs display the strongest chondrogenic potential, whereas L6 cells show no chondrogenic differentiation. (b) Quantification of positive area of safranin-O and Alcian blue shows similar results. (c) Under higher magnification, results showed chondrogenic differentiation of FDCs and no chondrogenic differentiation in the L6 group by safranin-O, Alcian blue and collagen II staining.

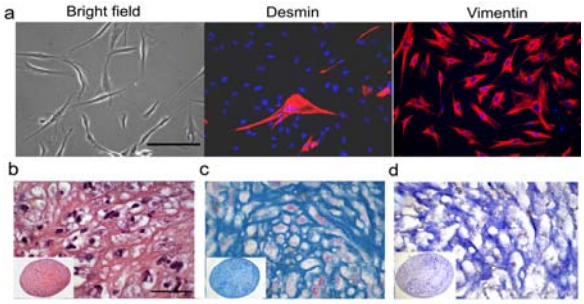

Fig4. (a) Freshly isolated human FDCs acquire fibroblasts shape in vitro. Immunostaining for desmin (red) shows very few are positive. Vimentin (red) staining shows most of cells (nuclei, blue) are positive. (b,c,d) With safranin-O, Alcian blue and collagen II staining, human FDC pellets show positive staining and typical chondroctyes

DISCUSSION:

Characterization of MDCs demonstrated that they contain at least two populations of cells, FDCs and a population of myogenic cells. Chondrogenic differentiation displayed by muscle derived cells (MDCs) implies that either FDCs, a population of myogenic cells, or both have chondrogenic potential. Mixtures of FDCs and rat L6 myoblasts demonstrated FDCs are the chondrogenic progenitor cell fraction of MDCs, but the myogenic cell fraction of MDCs plays little role in chondrogenesis. Findings about rat FDCs are also supported by the positive chondrogenic differentiation displayed by human FDCs.

In summary, this study shows that fibrogenic cells which reside in fascia and similar tissues in the skeletal muscles contain a population of chondrogenic progenitor cells. Fascia of skeletal muscle could be the tissue from which cells could be harvested for cartilage repair. Future research will focus on isolating these cells and using them to repair cartilage

ACKNOWLEDGMENTS

This work was supported by funding from the Henry J. Mankin Endowed Chair for Orthopaedic Research at the University of Pittsburgh, the William F. and Jean W. Donaldson Chair at Children's Hospital of Pittsburgh, the Hirtzel Foundation, and the National Institutes of Health (R01 AR47973 awarded to J.H.).

ARTHRITIS & RHEUMATISM
Vol. 58, No. 12, December 2008, pp 3809–3819
DOI 10.1002/art.24125

Appendix 2

The Influence of Sex on the Chondrogenic Potential of Muscle-Derived Stem Cells

Implications for Cartilage Regeneration and Repair

Tomoyuki Matsumoto,[1] Seiji Kubo,[1] Laura B. Meszaros,[2] Karin A. Corsi,[2] Gregory M. Cooper,[2] Guangheng Li,[2] Arvydas Usas,[2] Aki Osawa,[1] Freddie H. Fu,[3] and Johnny Huard[1]

Objective. **To explore possible differences in muscle-derived stem cell (MDSC) chondrogenic differentiation in vitro and articular cartilage regeneration in vivo between murine male MDSCs (M-MDSCs) and female MDSCs (F-MDSCs).**

Methods. **Three different populations of M- and F-MDSCs (n = 3 of each sex) obtained via preplate technique, which separates cells based on their variable adhesion characteristics, were compared for their in vitro chondrogenic potential using pellet culture. Cells were assayed with and without retroviral transduction to express bone morphogenetic protein 4 (BMP-4). The influence of both expression of stem cell marker Sca1 and in vitro expansion on the chondrogenic potential of M- and F-MDSCs was also determined. Additionally, BMP-4–transduced M- and F-MDSCs were applied to a full-thickness articular cartilage defect (n = 5 each) on the femur of a nude rat, and the quality of the repaired tissue was evaluated by macroscopic and histologic examination.**

Results. **With and without BMP-4 gene transduction, M-MDSCs produced significantly larger pellets with a richer extracellular matrix, compared with F-MDSCs. Sca1 purification influenced the chondrogenic potential of MDSCs, especially M-MDSCs. Long-term culture did not affect the chondrogenic potential of M-MDSCs but did influence F-MDSCs. M-MDSCs repaired articular cartilage defects more effectively than did F-MDSCs at all time points tested, as assessed both macroscopically and histologically.**

Conclusion. **Our findings demonstrate that sex influences the chondrogenic differentiation and articular cartilage regeneration potential of MDSCs. Compared with female MDSCs, male MDSCs display more chondrogenic differentiation and better cartilage regeneration potential.**

Articular cartilage damage is difficult to treat because the tissue lacks a blood, nerve, and lymph supply and has limited intrinsic capacity to repair. Injury-related full-thickness articular cartilage defects or large defects caused by osteoarthritis (OA) may require substantial surgical treatments, including bone stimulation techniques (multiple perforations, abrasions, and microfractures) in which subchondral bone is broken to facilitate repair of cartilage damage caused by bone marrow–derived cells and cytokines. However, these methods result in the presence of fibrocartilage in repaired tissue. There is currently no widely accepted treatment for the repair of these lesions, except for total knee arthroplasty. Since the clinical introduction of autologous chondrocyte implantation by Brittberg and colleagues (1) as an alternative to mosaicplasty, many

Supported by the US Department of Defense (contract W81XWH-08-0076), the William F. and Jean W. Donaldson Chair at the Children's Hospital of Pittsburgh (Dr. Huard), and the Henry J. Mankin Endowed Chair in Orthopaedic Surgery at the University of Pittsburgh (Dr. Huard).

[1]Tomoyuki Matsumoto, MD, PhD, Seiji Kubo, MD, Aki Osawa, MD, PhD, Johnny Huard, PhD: Children's Hospital of Pittsburgh and University of Pittsburgh, Pittsburgh, Pennsylvania; [2]Laura B. Meszaros, BS, Karin A. Corsi, PhD, Gregory M. Cooper, PhD, Guangheng Li, MD, PhD, Arvydas Usas, MD: Children's Hospital of Pittsburgh, Pittsburgh, Pennsylvania; [3]Freddie H. Fu, MD: University of Pittsburgh, Pittsburgh, Pennsylvania.

Drs. Matasumoto and Kubo contributed equally to this work.

Dr. Huard has received consulting fees from Cook MyoSite, Inc. (more than $10,000).

Address correspondence and reprint requests to Johnny Huard, PhD, Children's Hospital of Pittsburgh, 4100 Rangos Research Center, 3705 Fifth Avenue, Pittsburgh, PA 15213-2582. E-mail: jhuard@pitt.edu.

Submitted for publication June 13, 2008; accepted in revised form August 29, 2008.

have reported the clinical effectiveness of implanting autologous culture-expanded chondrocytes for cartilage regeneration (2). However, due to dedifferentiation or loss of reparative ability of chondrocytes during culture, the utility of transplanted chondrocytes is still unclear (3–5).

Stem cells, due to their ability to differentiate toward various lineages, have become an important tool in regenerative medicine and tissue engineering. Adult stem cells and progenitor cells for mesenchymal lineages from various tissues and organs, such as bone marrow (6), peripheral blood or blood vessels (7), adipose tissue (8), synovium (4), umbilical cord blood (9), and skeletal muscle (10), have been described. For cartilage regeneration and repair, stem cells are an attractive cell source due to their superior capacity for self-renewal, proliferation, and response to stress (11,12). Results of several studies have suggested that various stem cells have potential for cartilage regeneration and repair in experimental cartilage injury models (13–15). Recently, autologous stem cell–based tissue engineering has been used clinically for cartilage repair and regeneration (16,17). Our group has identified and isolated muscle-derived stem cells (MDSCs) from mouse skeletal muscle (12). MDSCs could potentially be a novel cell source for cartilage tissue engineering. They are known to have multilineage differentiation potential, including the ability to differentiate into skeletal muscle, bone, neural, endothelial, and hematopoietic tissue (12,18–23). We have previously shown that muscle-derived cells, including MDSCs, can undergo chondrogenesis in vivo and in vitro (24,25).

Variations in the characteristics of stem cells isolated from animals of different sexes have been recently investigated (26–28), and our group has demonstrated a sex difference in skeletal muscle regeneration and osteogenesis mediated by MDSCs (29,30). Therefore, we performed a series of experiments to examine whether there are differences in chondrogenic potential of male MDSCs (M-MDSCs) and female MDSCs (F-MDSCs) that could potentially influence their use in articular cartilage tissue engineering applications.

MATERIALS AND METHODS

MDSC isolation and culture. MDSCs were isolated from the hind limb skeletal muscle of 3-week-old C57.BL10 mice (The Jackson Laboratory, Bar Harbor, ME) via a modified preplate technique that has been described previously (10,31). The sex of the animals was determined anatomically at the time of isolation, and the sex of the cells was later confirmed by fluorescence in situ hybridization (FISH). M-MDSC and F-MDSC populations were cultured on collagen-coated flasks in proliferation medium containing phenol red–free Dulbecco's modified Eagle's medium (DMEM; Invitrogen, San Diego, CA) supplemented with 110 mg/liter sodium pyruvate (Sigma-Aldrich, St. Louis, MO), 584 mg/liter L-glutamine, 10% fetal bovine serum, 10% horse serum, 1% penicillin/streptomycin (all from Invitrogen), and 0.5% chick embryo extract (Accurate, Westbury, NY). Cells were trypsinized and replated at a density of 250 cells/cm^2 until sufficient numbers of cells from all populations were available for the chondrogenic assays. All cells used in this study, except for cells examined with long-term culturing (described below), were passaged <30 times.

Characterization of MDSCs. Three M-MDSC populations (M1, M2, and M3) and 3 F-MDSC populations (F1, F2, and F3) were characterized by flow cytometry for CD34 and Sca1 expression. MDSCs were labeled with rat anti-mouse Sca1 (phycoerythrin) and CD34 (biotin) monoclonal antibodies (BD Biosciences, San Jose, CA). A separate portion of cells was treated with equivalent amounts of isotype control antibodies. Both fractions were washed and labeled with streptavidin–allophycocyanin; 7-aminoactinomycin D was added to exclude nonviable cells from analysis. Sca1 and CD34 expression was determined by flow cytometry with fluorescence-activated cell sorting (FACS) (FACSAria; Becton Dickinson, Mountain View, CA). Cell sex was confirmed by FISH with degenerate oligonucleotide-primed polymerase chain reaction (PCR)–labeled Y probes.

Retroviral transduction of MDSCs. M1 MDSCs and F1 MDSCs were retrovirally transduced with human bone morphogenetic protein 4 (BMP-4) and green fluorescent protein vector as described previously (32) and compared with nontransduced MDSCs for in vitro chondrogenesis by pellet culture ($n = 3$ of each sex). The transduced cells were cultured for 2 weeks before use in experiments, and the medium on these transduced cells was sampled to determine the level of transgene expression. The amount of BMP-4 secreted from the transduced cells was estimated with a BMP-4 bioassay, as previously described (33).

Purification of Sca1+ and Sca1− cells. Based on the significant difference in Sca1 expression between M-MDSCs and F-MDSCs, the Sca1+ and Sca1− fractions of BMP-4–transduced M1 and F1 populations were sorted by FACS (FACSAria), and each fraction was tested for chondrogenesis by pellet culture ($n = 3$ of each sex).

Population doublings. To compare short- and long-term proliferation potential, M-MDSCs and F-MDSCs were plated in 25-cm^2 collagen-coated flasks, and routine cell expansion was performed every 2–3 days. At each passage, cells were replated to a density of 225 cells/cm^2. The number of population doublings for each subculturing was calculated as the $\log_2 (N/N_0)$. This process was repeated for >150 population doublings. Karyotyping was performed as previously described (32), for 2 M-MDSC populations (M1 and M2) and 2 F-MDSC populations (F1 and F2). All populations of M-MDSCs and F-MDSCs that were expanded to 30 population doublings, 90 population doublings, and 150 population doublings were characterized by FACS, and chondrogenesis was assessed by pellet culture.

Pellet culture. Pellet culture was performed as described previously (34). Cells (2.5×10^5) were centrifuged at 2,500 revolutions per minute for 5 minutes in 0.5 ml of

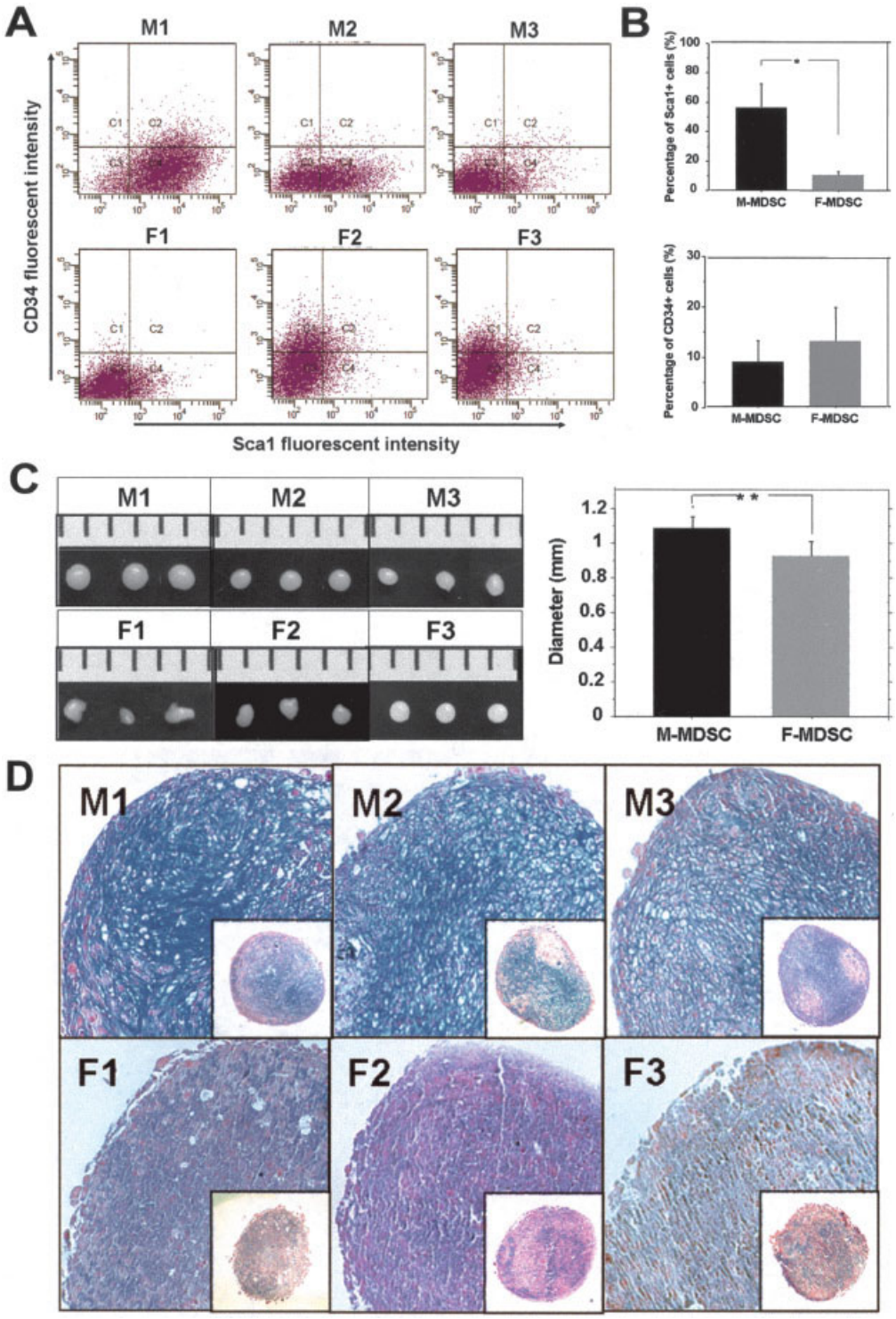

Figure 1. In vitro characterization of muscle-derived stem cells (MDSCs). **A,** Flow cytometric analysis of 6 MDSC populations (male MDSC [M-MDSC] 1–3 [M1–M3] and female MDSC [F-MDSC] 1–3 [F1–F3]). **B,** Quantification of the flow cytometric results, demonstrating that the percentage of Sca1+ cells was significantly higher in M-MDSCs than in F-MDSCs, with no significant difference between the 2 cell populations in the number of CD34+ cells. **C,** Measurement of the pellets produced by M-MDSCs and F-MDSCs (ruler is in mm). **D,** Alcian blue staining, demonstrating that pellets of M-MDSCs produced richer extracellular matrix–like hyaline cartilage than did F-MDSCs (original magnification × 200; × 40 in **insets**). Bars in **B** and **C** show the mean and SEM. $* = P < 0.05$; $** = P < 0.01$.

standard chondrogenic medium containing DMEM supplemented with 1% penicillin/streptomycin, $10^{-7}M$ dexamethasone, 50 μg/ml ascorbate-2-phosphate, 40 μg/ml proline, 100 μg/ml pyruvate, and insulin–transferrin–selenium (1% BD ITS+Premix; Becton Dickinson). The pellets in the experiments characterizing the BMP-4 response of MDSCs were cultured in chondrogenic medium supplemented with 10 ng/ml transforming growth factor β3 (TGFβ3; R&D Systems, Minneapolis, MN), and those in experiments investigating Sca1 purification and population doublings were cultured in chondrogenic medium supplemented with 10 ng/ml TGFβ3 and 50 ng/ml BMP-4. Pellets were incubated at 37°C in 5% CO_2 for 14 days, and the medium was changed every 2–3 days.

Assessment of chondrogenesis. Pellets were fixed overnight in 10% neutral buffered formalin, dehydrated, embedded in paraffin, and sectioned in 5-μm–thick slices. Pellet sections were deparaffinized, placed in 3% acetic acid for 3 minutes, and transferred into Alcian blue solution for 30 minutes. The slides were rinsed with running tap water for 10 minutes and counterstained with nuclear fast red.

Quantitative real-time PCR analysis of pellet cultured cells. Messenger RNA was isolated using the RNeasy Plus Kit, according to the instructions of the manufacturer (Qiagen, Valencia, CA). After RNA extraction, quantitative real-time PCR analysis of all populations from different population doublings was carried out as previously described (35,36). Gene expression levels were calculated based on the difference in threshold cycle. All target genes were normalized to the housekeeping gene 18S; 18S primers and probes were designed by and purchased from Applied Biosystems (Foster City, CA). Primers and probes were designed for type II collagen, SOX9, and type X collagen, according to GenBank sequence. All target gene primers and probes were purchased from Integrated DNA Technologies (Coralville, IA). For quantitative PCR assays, the coefficient of variation calculated from triplicate assays was within 3%. Primers and probes were as follows: mouse type II collagen forward primer AAG-TCA-CTG-AAC-AAC-CAG-ATT-GAG-A, reverse primer AAG-TGC-GAG-CAG-GGT-TCT-TG, TaqMan probe ATC-CGC-AGC-CCC-GAC-GGC-T; mouse SOX9 forward primer CGG-CTC-CAG-CAA-GAA-CAA-G, reverse primer TGC-GCC-CAC-ACC-ATG-A, TaqMan probe ACG-TCA-AGC-GAC-CCA-TGA-ACG-C; mouse type X collagen forward primer TAC-TTA-CAC-GGA-TGG-AGA-CCA-TGT-T, reverse primer ATC-CAG-TTG-ACT-ACT-GGT-GCA-ATT-T, TaqMan probe AAC-CCT-CTT-TTC-GGA-TTA-ACC-CTG-CGA-GTT.

Articular cartilage defect model and cell transplantation. All animal experiments were approved by the Animal Research and Care Committee at Children's Hospital of Pittsburgh. Fifteen 12-week-old female nude rats (NIH-*Whn* NIHRNU-M; Taconic, Germantown, NY) were used in this study. The animals were anesthetized by exposure to 3% isoflurane and O_2 gas (1.5 liter/minute) delivered through an inhalation mask. The knee joint was exposed by medial parapatellar incision, and the trochlear groove was exposed by lateral dislocation of the patella. A 1.8-mm outer diameter trephine drill was used to create bilateral osteochondral defects (1.8 × 2.0 mm) in the trochlear groove of each femur as previously described (25). BMP-4–transduced M1 MDSCs and F1 MDSCs (5×10^5) were mixed with fibrin glue (Tisseel VH; Baxter Healthcare Hyland Immuno, Glendale, CA) and applied to the articular cartilage defect in both knees. As a control, fibrin glue without cells was used. After macroscopic examination, 5 distal femora in each group were dissected at weeks 4, 8, and 16 and embedded in paraffin. Specimens were stained with Safranin O–fast green, and the histologic grading scale described by O'Driscoll et al (37) was used to evaluate the quality of the repaired tissue.

Statistical analysis. Comparisons between 2 groups were performed using unpaired *t*-tests. Comparisons among 3 populations were performed by one-way analysis of variance except for comparisons of histologic scores, which were performed by Kruskal-Wallis analysis. Post hoc analysis was performed with Fisher's protected least significant difference test. *P* values less than 0.05 were considered significant.

RESULTS

In vitro MDSC characterization. Flow cytometric analysis with 6 populations demonstrated that the percentage of Sca1+ cells was significantly higher in M-MDSCs than in F-MDSCs (mean ± SEM 56.0 ± 15.4% versus 9.4 ± 1.9%) ($P < 0.05$), with no significant difference in the number of CD34+ cells (M-MDSCs 8.8 ± 4.5%, F-MDSCs 13.0 ± 6.6%) (Figures 1A and B). M-MDSCs also produced significantly larger pellets than F-MDSCs when cultivated in chondrogenic medium (mean ± SEM 1.06 ± 0.04 mm versus 0.85 ± 0.02 mm) ($P < 0.01$) (Figure 1C). Alcian blue staining demonstrated that pellets of M-MDSCs produced more extracellular matrix (ECM) that closely resembled hyaline-like cartilage, when compared with F-MDSCs (Figure 1D).

Effect of BMP-4 transduction and Sca1 purification on the chondrogenic potential of M- and F-MDSCs. Similar to the observations in nontransduced cells, BMP-4 transduction of M-MDSCs produced pellets with significantly larger diameter than was observed with BMP-4 transduction of F-MDSCs (mean ± SEM 1.30 ± 0.03 mm in BMP-4–transduced M-MDSCs, 1.05 ± 0.03 mm in nontransduced M-MDSCs, 0.94 ± 0.07 mm in BMP-4–transduced F-MDSCs, and 0.79 ± 0.05 mm in nontransduced F-MDSCs) ($P < 0.01$, BMP-4–transduced M-MDSCs versus nontransduced M-MDSCs; $P < 0.05$, BMP-4-transduced MDSCs versus BMP-4–transduced F-MDSCs; $P < 0.05$, nontransduced MDSCs versus nontransduced F-MDSCs) (Figure 2A). Alcian blue staining demonstrated that pellets of BMP-4–expressing M-MDSCs produced more ECM compared with F-MDSCs (Figure 2B).

Purification of Sca1+ M-MDSCs produced significantly larger pellets than were produced by Sca1−

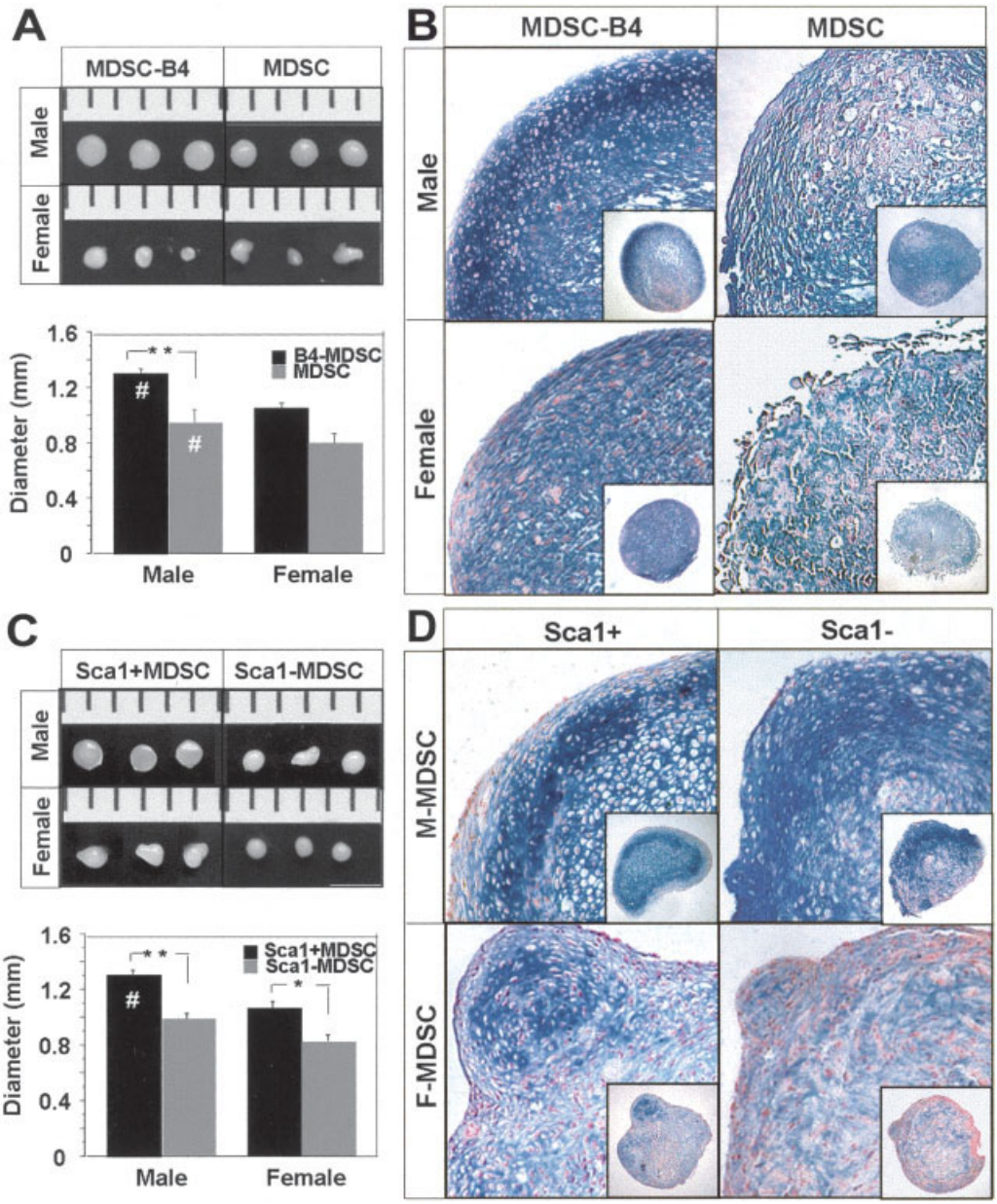

Figure 2. Effects of bone morphogenetic protein 4 (BMP-4) transduction and Sca1 purification. **A,** Measurement of the chondrogenic pellets produced by BMP-4–transduced MDSCs (MDSC-B4) and nontransduced MDSCs. BMP-4–transduced M-MDSCs produced significantly larger chondrogenic pellets compared with nontransduced M-MDSCs and BMP-4–transduced F-MDSCs. **B,** Alcian blue staining, demonstrating that after BMP-4 transduction, the extracellular matrix (ECM) was richer in pellets of M-MDSCs compared with F-MDSCs (original magnification × 200). **C,** Measurement of the chondrogenic pellets produced by Sca1+ and Sca1− MDSCs. In both male and female MDSCs, purified Sca1+ cells produced significantly larger pellets than Sca1− cells. **D,** Alcian blue staining, demonstrating that Sca1+ cells isolated from both male and female MDSCs produced richer ECM than the Sca1− cell fractions (original magnification × 200; × 40 in **insets**). Rulers in **A** and **C** are in mm; bars in **A** and **C** show the mean and SEM. $* = P < 0.05$; $** = P < 0.01$. # $= P < 0.05$ versus female cells. See Figure 1 for other definitions.

M-MDSCs or by the Sca1+ and Sca1− fractions of F-MDSCs (mean ± SEM 1.29 ± 0.03 mm in Sca1+ M-MDSCs, 0.96 ± 0.05 mm in Sca1− M-MDSCs, 1.05 ± 0.07 mm in Sca1+ F-MDSCs, and 0.81 ± 0.03 mm in Sca1− F-MDSCs) ($P < 0.01$, Sca1+ M-MDSCs versus Sca1– M-MDSCs; $P < 0.05$, Sca1+ F-MDSCs

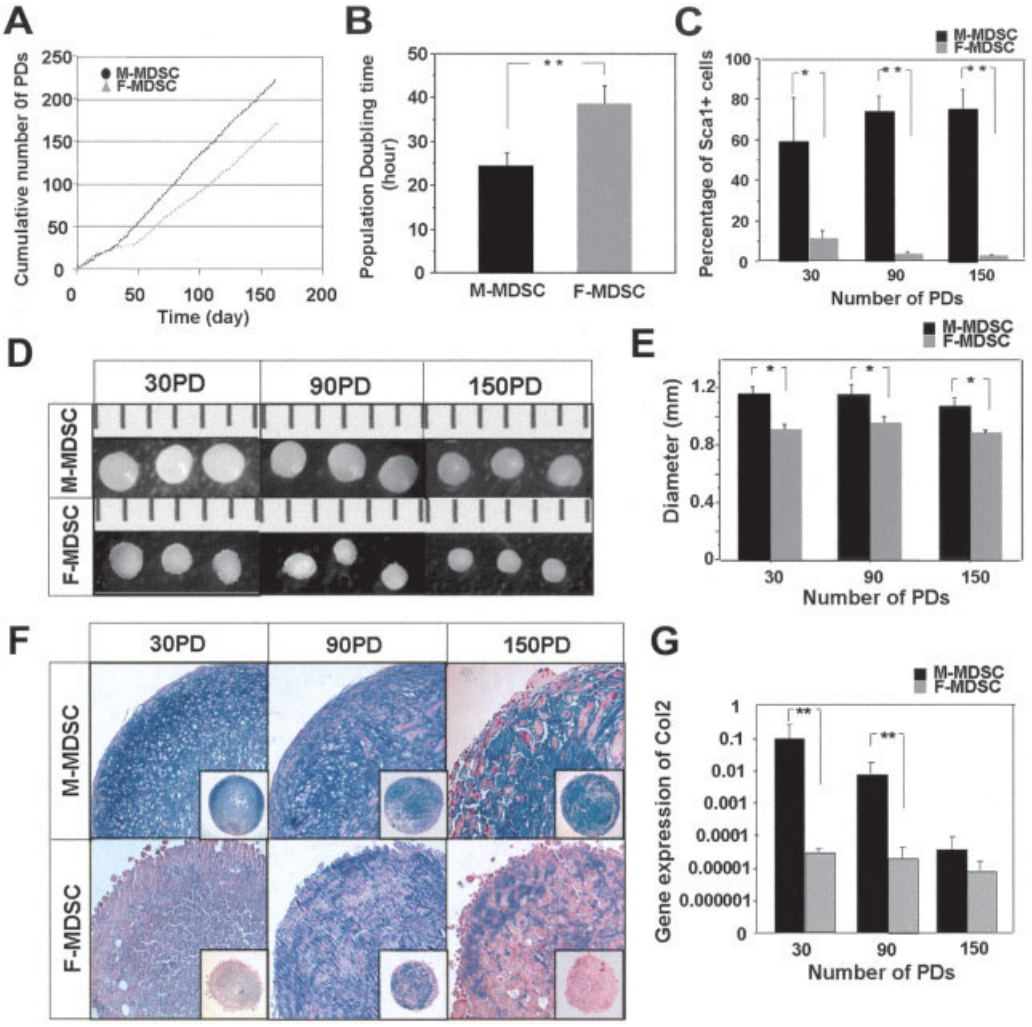

Figure 3. Effect of culturing on the chondrogenic potential of MDSCs. **A** and **B,** Numbers of population doublings (PDs) over time, and time required for population doubling. A decrease in population doubling times was observed with expansion of both male and female MDSCs. **C,** Quantitative results of flow cytometric analysis, demonstrating that the number of Sca1-expressing cells, at all population doublings, was significantly higher in M-MDSCs than in F-MDSCs. **D** and **E,** Measurement of chondrogenic pellets after 30, 90, and 150 population doublings (ruler is in mm). **F,** Alcian blue staining, demonstrating that M-MDSCs produced larger pellets with richer extracellular matrix compared with F-MDSCs at all population doublings, with decreased chondrogenic potential with cell expansion in both cell populations (original magnification × 200; × 40 in **insets**). **G,** Quantitative results of real-time polymerase chain reaction analysis, demonstrating significantly higher type II collagen (Col2) gene expression by M-MDSCs versus F-MDSCs at all population doublings, with a reduction in type II collagen expression with increasing population doubling. Bars in **B, C, E,** and **G** show the mean and SEM. $* = P < 0.05$; $** = P < 0.01$. See Figure 1 for other definitions.

versus Sca1− F-MDSCs; $P < 0.05$, Sca1+ M-MDSCs versus Sca1+ F-MDSCs) (Figure 2C). Alcian blue staining revealed that the Sca1+ fraction of M-MDSCs produced more ECM than Sca1− M-MDSCs, as well as more ECM than either Sca1+ or Sca1− F-MDSCs (Figure 2D).

Influence of expansion on the chondrogenic potential of M- and F-MDSCs. Analysis of short-term kinetics showed that M-MDSC and F-MDSC populations had similar population doubling times over a 3-day period, as previously described (12). However, after moderate expansion over 14 days or extended expansion over 3 months (>150 population doublings), M-MDSC populations exhibited significantly shorter population doubling time than their female counterparts (mean ± SEM 24.6 ± 2.7 hours versus 38.5 ± 4.2 hours; $P < 0.01$) (Figures 3A and B). Flow cytometric analysis revealed that expression of Sca1 at all population doublings was

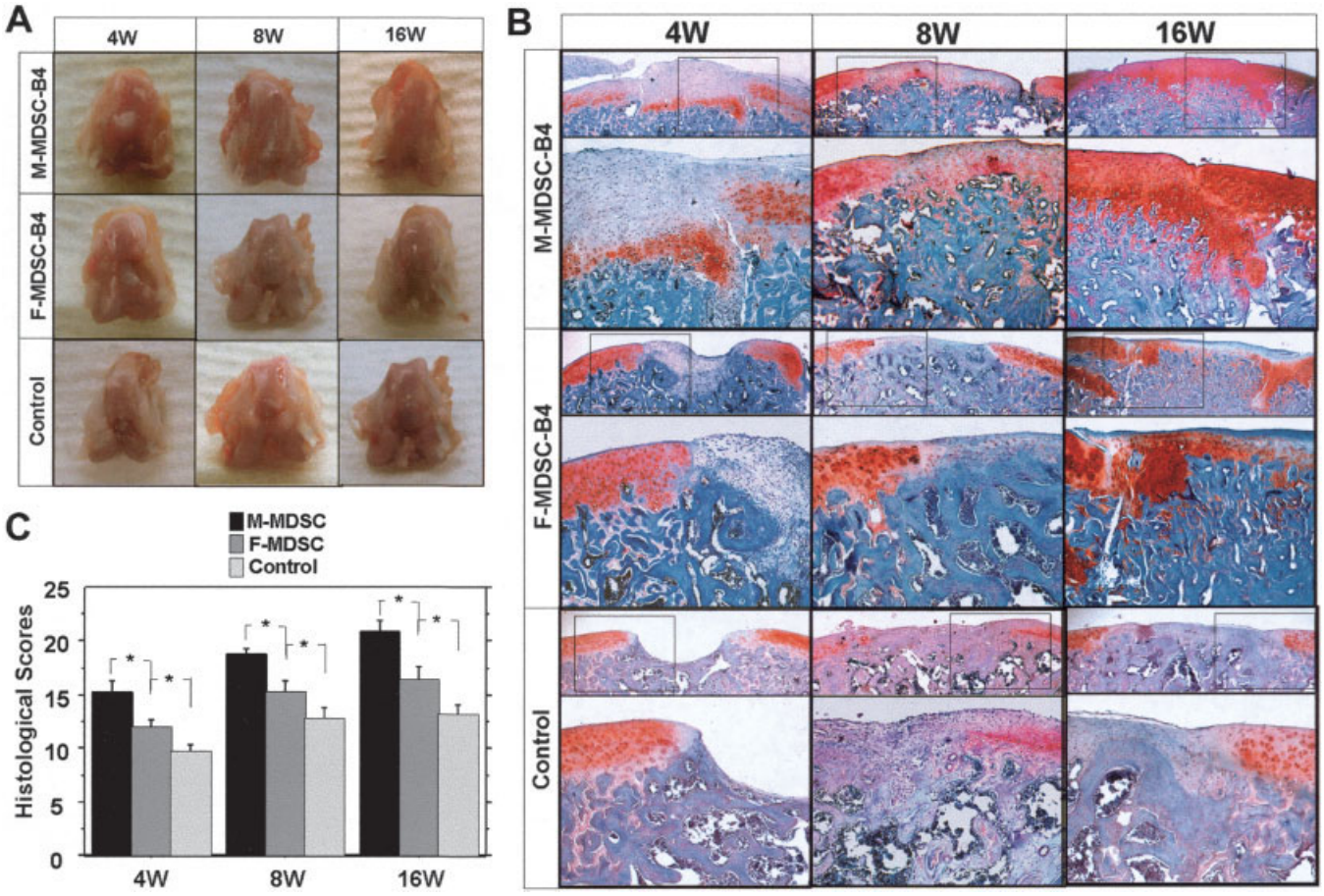

Figure 4. In vivo cartilage regeneration with bone morphogenetic protein 4 (BMP-4)–expressing MDSC treatment in the rat articular cartilage defect model. **A,** Macroscopic appearance, showing that the cartilage surface was partially filled at week 4, and the defect had become entirely covered by week 16, in the BMP-4–transduced MDSC (MDSC-B4)–treated group; however, a visible defect was still present in the BMP-4–transduced F-MDSC–treated group at all time points tested. **B,** Safranin O staining. At week 4, Safranin O–positive hyaline cartilage was observed in the defects in the group treated with BMP-4–expressing M-MDSCs, and the subchondral area was replaced by bone or cartilage, whereas fibrous tissue only partially filled the defects in the group treated with BMP-4–expressing F-MDSCs. Eight weeks after treatment, defects in the group treated with BMP-4–expressing F-MDSCs still exhibited partial healing and were covered with fibrous tissue, with minimal Safranin O–positive areas. In the group treated with BMP-4–expressing M-MDSCs, the defects were fully covered and well-integrated with cartilaginous tissue, which showed slight positivity for Safranin O. By week 16, treatment with BMP-4–expressing M-MDSCs had induced complete healing, with highly Safranin O–positive hyaline cartilage, whereas the group treated with BMP-4–expressing F-MDSCs showed incomplete healing, with limited Safranin O–positive hyaline cartilage. Larger images are higher-magnification views of the boxed areas (original magnification $\times$ 100 in lower portion of each panel; $\times$ 40 in upper portion of each panel with boxed area). **C,** O'Driscoll histologic scores. Scores in regenerated tissue from the BMP-4–expressing M-MDSC treatment group were significantly better than those in tissue from the BMP-4–expressing F-MDSC treatment group at 4, 8, and 16 weeks after transplantation. However, the F-MDSC treatment group showed significantly better scores than the control group. Bars show the mean and SEM. $* = P < 0.05$. See Figure 1 for other definitions.

significantly higher in M-MDSCs than in F-MDSCs (in male cells, mean $\pm$ SEM 64.7 $\pm$ 17.1%, 73.7 $\pm$ 8.3%, and 75.3 $\pm$ 10.3% at 30, 90, and 150 population doublings, respectively; in female cells, 10.0 $\pm$ 3.3%, 2.7 $\pm$ 1.2%, and 1.9 $\pm$ 0.7%, respectively) ($P < 0.01$, M-MDSCs versus F-MDSCs at 90 and 150 population doublings; $P < 0.05$, M-MDSCs versus F-MDSCs at 30 population doublings) (Figure 3C). There was no significant difference in CD34 expression at all population doublings between M- and F-MDSCs (in male cells, 4.03 $\pm$ 2.98%, 8.18 $\pm$ 4.29%, and 35.50 $\pm$ 21.88% at 30, 90, and 150 population doublings, respectively; in female cells, 5.77 $\pm$ 2.79%, 5.63 $\pm$ 0.82%, and 11.47 $\pm$ 3.81%, respectively).

Significantly larger pellets were produced with M-MDSCs than with F-MDSCs at all population doublings, with a decreasing trend over time (in male cells, mean ± SEM 1.16 ± 0.1 mm, 1.16 ± 0.08 mm, and 1.07 ± 0.06 mm at 30, 90, and 150 population doublings, respectively; in female cells, 0.91 ± 0.03 mm, 0.96 ± 0.04 mm, and 0.89 ± 0.02 mm, respectively) ($P < 0.05$, M-MDSCs versus F-MDSCs at all population doublings) (Figures 3D and E). Alcian blue staining also demonstrated that pellets of M-MDSCs showed decreasing production of ECM with passage, while F-MDSCs showed poor ECM production at all population doublings (Figure 3F).

Real-time PCR analysis demonstrated that type II collagen gene expression was significantly higher in M-MDSCs than in F-MDSCs; however, this trend decreased with increasing population doubling (in male cells, mean ± SEM 0.12 ± 0.092, 0.0071 ± 0.0053, and 0.000039 ± 0.000033 at 30, 90, and 150 population doublings, respectively; in female cells, 0.000026 ± 0.0000050, 0.000018 ± 0.000011, and 0.0000071 ± 0.0000039, respectively) ($P < 0.01$, M-MDSCs versus F-MDSCs at 30 and 90 population doublings) (Figure 3G). There were no differences in SOX9 or type X collagen gene expression between M-MDSCs and F-MDSCs at any population doubling (data not shown).

Cartilage regeneration. In the in vivo transplantation model, macroscopic assessment demonstrated that tissue was beginning to fill the cartilage surface at week 4, and the defect had become smooth and entirely covered by week 16 in the group treated with BMP-4–transduced M-MDSCs. However, a visible defect was present in the group treated with BMP-4–transduced F-MDSCs at all time points tested (Figure 4A).

Histologic assessment by Safranin O staining at week 4 demonstrated that defects in the group treated with BMP-4–expressing M-MDSCs contained Safranin O–positive hyaline cartilage and the subchondral area was replaced by bone or cartilage, whereas defects in the group treated with BMP-4–expressing F-MDSCs were partially filled with fibrous tissue (Figure 4B). Eight weeks after treatment, defects in the group treated with BMP-4–expressing F-MDSCs showed eburnated bone covered by thin fibrous tissue, with few Safranin O–positive areas. In contrast, defects in the group treated with BMP-4–expressing M-MDSCs were covered and well-integrated with cartilaginous tissue, which showed slightly positive staining with Safranin O (Figure 4B). At week 16, treatment with BMP-4–expressing M-MDSCs had induced good healing and the defect was covered with highly Safranin O–positive hyaline cartilage, whereas the BMP-4–expressing F-MDSC group showed incomplete healing and some Safranin O–positive hyaline cartilage limited to the border of the defect (Figure 4B). In the control group, there was no Safranin O–positive hyaline cartilage in the area of the defect at any time point up to 16 weeks after transplantation (Figure 4B).

O'Driscoll histologic scores in regenerated tissue from the group treated with BMP-4–expressing M-MDSCs were significantly better than those in the BMP-4–expressing F-MDSC treatment group at 4, 8, and 16 weeks after transplantation (Figure 4C). However, the F-MDSC treatment group showed significantly better scores than the control group (mean ± SEM histologic score at 4 weeks, 8 weeks, and 16 weeks, respectively, 15.2 ± 1.0, 18.8 ± 0.5, and 20.8 ± 1.0 in the group treated with BMP-4–expressing M-MDSCs; 12.0 ± 0.6, 15.2 ± 1.0, and 16.4 ± 1.2 in the group treated with BMP-4–expressing F-MDSCs; 9.6 ± 0.7, 12.8 ± 1.0, and 13.2 ± 0.8 in controls) ($P < 0.05$, M-MDSC–treated group versus F-MDSC–treated group and F-MDSC–treated group versus controls, at all time points) (Figure 4C).

DISCUSSION

To examine the difference in chondrogenic potential between M-MDSCs and F-MDSCs, we isolated MDSCs from 3 male and 3 female mice and tested these cells for chondrogenesis both in vitro and in vivo. MDSCs have previously been shown to have chondrogenic potential (24,25), especially after BMP-4 transduction. BMP-4 has also been demonstrated to enhance potential for chondrogenesis in vitro and in vivo in cell types other than MDSCs (38–40). It has also been reported that the combined effect of TGFβ3 and BMP-4 or BMP-2 on chondrogenic pellet size is greater than that of each growth factor administered separately (41,42). Consequently, we used TGFβ3 in all experiments, and BMP-4 was either added to the chondrogenic media or cells were retrovirally transduced to produce BMP-4 and cultured in chondrogenic media. Under these conditions, both M-MDSCs and F-MDSCs underwent chondrogenic differentiation. Interestingly, in experiments using chondrogenic media without BMP-4, M-MDSCs produced significantly larger pellets with richer ECM resembling hyaline-like cartilage compared with F-MDSCs. Our findings suggest that MDSCs can undergo chondrogenesis even without BMP-4, and that this phenomenon is more pronounced in M-MDSCs than F-MDSCs.

Various types of stem cells have been shown, by FACS analysis, to highly express Sca1, and these stem cells also have chondrogenic potential (43–45). Our group previously reported that MDSCs express the stem cell surface marker CD34 as well as Sca1 (10). Characterization by FACS analysis in the present study demonstrated that the number of Sca1+ cells was significantly higher in M-MDSCs than F-MDSCs; however, there was no significant difference in the number of CD34+ cells. We also compared the chondrogenic potential (pellet culture) of M-MDSC and F-MDSC populations sorted on the basis of Sca1 expression. In both M- and F-MDSCs, the Sca1+ fractions were more chondrogenic than the Sca1− fractions. In addition, the male Sca1+ cells showed substantially more chondrogenic potential in pellet culture than did female Sca1+ cells. Since M-MDSCs contain more Sca1+ cells than do F-MDSCs, we cannot exclude the possibility that the differential chondrogenic potential observed between M-MDSCs and F-MDSCs is related to the subpopulation of Sca1+ cells.

We have previously demonstrated the effect of BMP-4 on MDSC chondrogenesis in vitro and in vivo (25), and in the present study, we compared the differences in BMP-4 response of M-MDSCs and F-MDSCs, using a retroviral transduction method. BMP-4–transduced M-MDSCs produced significantly larger pellets with richer ECM than did pellets of BMP-4–transduced F-MDSCs.

When cultured in chondrogenic medium with TGFβ3 and BMP-4, M-MDSCs produced significantly larger pellets with richer ECM than did F-MDSCs, at all population doublings. The chondrogenic potential of M-MDSCs was maintained even after long-term culture (high population doubling), while the F-MDSCs lost their chondrogenic potential with expansion. Interestingly, real-time PCR analysis demonstrated that chondrogenic pellets of M-MDSCs showed significantly higher gene expression of type II collagen compared with F-MDSCs, even though all MDSCs (regardless of population doubling number) showed significantly decreasing expression with culturing. After 2 weeks in culture, there was weak expression of type X collagen and SOX9 in all pellets, but there was no significant difference in expression of these genes between M- and F-MDSCs. These findings indicate that M-MDSCs maintain a higher rate of self-renewal and have more chondrogenic potential than F-MDSCs at all population doublings, even though MDSCs of both sexes display a reduction of chondrogenic potential with culturing.

In an in vivo osteochondral defect model, treatment with both M- and F-MDSCs demonstrated some ability to potentiate cartilage regeneration, adding to the findings of our previous study using only F-MDSCs (25). However, M-MDSC treatment led to greater cartilage regeneration than F-MDSC treatment. At week 16, macroscopic and histologic assessment demonstrated that treatment with BMP-4–transduced M-MDSCs produced good articular cartilage healing with highly Safranin O–positive hyaline cartilage. However, at 16 weeks, the BMP-4–transduced F-MDSC group still showed visible defects and only faintly Safranin O–positive hyaline cartilage, which was limited to the border of the defect. The histologic score at this time point was significantly better with BMP-4–transduced M-MDSC treatment compared with BMP-4–transduced F-MDSC treatment. Overall, in both in vivo and in vitro chondrogenic models, sex-related differences between M- and F-MDSCs were observed.

Sex differences in stem cell treatments for cartilage repair could have great clinical impact. OA is diagnosed more frequently in women than in men, especially in the population over 50 years old (46). Sex- and age-related differences in OA are well described and considered to be a key aspect of development and discovery of new treatments. Sex differences in knee geometry (47,48) and biomechanical properties (49) are well known, but it is not known if these differences contribute to the disparity in the prevalence of OA between men and women. Researchers have attempted to identify differences at the cellular level between OA in men and OA in women. Although the in vivo cartilage defect model used in the present study may not directly reflect OA progression, it does demonstrate the effectiveness of MDSCs in repairing full-thickness cartilage defects, which could possibly occur with OA. Although the role of host sex was not examined in this study, stem cell sex differences in healing of cartilage defects could lead to different clinical treatments of OA in men and women.

Some limitations of this study should be noted. First, we used murine muscle–derived cells, not human cells, and all male and female cells used in this study were from healthy mice. Results using cells from older human OA patients could be different. Second, although we demonstrated the chondrogenic potential of BMP-4–transduced MDSCs using in vitro and in vivo approaches, we did not test other BMPs, including BMP-2, BMP-6, or BMP-7. These BMPs could be investigated in the future.

In conclusion, our results suggest that M-MDSCs have higher chondrogenic potential in vitro and induce

more cartilage regeneration in an in vivo osteochondral defect model than do F-MDSCs. We also observed that M-MDSCs maintain their chondrogenic potential even at high population doublings, in contrast to observations with F-MDSCs. The fact that M-MDSCs contain a higher number of Sca1+ cells and maintain chondrogenic potential throughout the time of culturing may contribute to the observed sex difference in the chondrogenic potential of MDSCs. These results further the understanding of the chondrogenic potential of MDSCs and may contribute to the development of new therapeutic strategies for cartilage repair and regeneration.

ACKNOWLEDGMENTS

We would like to thank Burhan Gharaibeh and Jessica Tebbets for technical support. We are also grateful for assistance from James Cummins and Michele Keller.

AUTHOR CONTRIBUTIONS

Dr. Huard had full access to all of the data in the study and takes responsibility for the integrity of the data and the accuracy of the data analysis.

Study design. Matsumoto, Kubo, Li, Fu, Huard.
Acquisition of data. Matsumoto, Kubo, Corsi, Li, Usas, Osawa.
Analysis and interpretation of data. Meszaros, Corsi, Cooper, Li, Usas, Osawa, Huard.
Manuscript preparation. Matsumoto, Meszaros, Corsi, Cooper, Li, Fu, Huard.
Statistical analysis. Matsumoto, Kubo, Meszaros, Cooper, Huard.
Project oversight. Huard.

REFERENCES

1. Brittberg M, Lindahl A, Nilsson A, Ohlsson C, Isaksson O, Peterson L. Treatment of deep cartilage defects in the knee with autologous chondrocyte transplantation. N Engl J Med 1994;331: 889–95.
2. Browne JE, Anderson AF, Arciero R, Mandelbaum B, Moseley JB Jr, Micheli LJ, et al. Clinical outcome of autologous chondrocyte implantation at 5 years in US subjects. Clin Orthop Relat Res 2005:237–45.
3. Benz K, Breit S, Lukoschek M, Mau H, Richter W. Molecular analysis of expansion, differentiation, and growth factor treatment of human chondrocytes identifies differentiation markers and growth-related genes. Biochem Biophys Res Commun 2002;293: 284–92.
4. De Bari C, Dell'Accio F, Tylzanowski P, Luyten FP. Multipotent mesenchymal stem cells from adult human synovial membrane. Arthritis Rheum 2001;44:1928–42.
5. Richter W. Cell-based cartilage repair: illusion or solution for osteoarthritis. Curr Opin Rheumatol 2007;19:451–6.
6. Pittenger MF, Mackay AM, Beck SC, Jaiswal RK, Douglas R, Mosca JD, et al. Multilineage potential of adult human mesenchymal stem cells. Science 1999;284:143–7.
7. Kuznetsov SA, Mankani MH, Gronthos S, Satomura K, Bianco P, Robey PG. Circulating skeletal stem cells. J Cell Biol 2001;153: 1133–40.
8. Zuk PA, Zhu M, Ashjian P, De Ugarte DA, Huang JI, Mizuno H, et al. Human adipose tissue is a source of multipotent stem cells. Mol Biol Cell 2002;13:4279–95.
9. Sarugaser R, Lickorish D, Baksh D, Hosseini MM, Davies JE. Human umbilical cord perivascular (HUCPV) cells: a source of mesenchymal progenitors. Stem Cells 2005;23:220–9.
10. Qu-Petersen Z, Deasy B, Jankowski R, Ikezawa M, Cummins J, Pruchnic R, et al. Identification of a novel population of muscle stem cells in mice: potential for muscle regeneration. J Cell Biol 2002;157:851–64.
11. Oshima H, Payne TR, Urish KL, Sakai T, Ling Y, Gharaibeh B, et al. Differential myocardial infarct repair with muscle stem cells compared to myoblasts. Mol Ther 2005;12:1130–41.
12. Deasy BM, Gharaibeh BM, Pollett JB, Jones MM, Lucas MA, Kanda Y, et al. Long-term self-renewal of postnatal muscle-derived stem cells. Mol Biol Cell 2005;16:3323–33.
13. Wakitani S, Yamamoto T. Response of the donor and recipient cells in mesenchymal cell transplantation to cartilage defect. Microsc Res Tech 2002;58:14–8.
14. Wakitani S, Goto T, Pineda SJ, Young RG, Mansour JM, Caplan AI, et al. Mesenchymal cell-based repair of large, full-thickness defects of articular cartilage. J Bone Joint Surg Am 1994;76: 579–92.
15. Koga H, Muneta T, Ju YJ, Nagase T, Nimura A, Mochizuki T, et al. Synovial stem cells are regionally specified according to local microenvironments after implantation for cartilage regeneration. Stem Cells 2007;25:689–96.
16. Wakitani S, Imoto K, Yamamoto T, Saito M, Murata N, Yoneda M. Human autologous culture expanded bone marrow mesenchymal cell transplantation for repair of cartilage defects in osteoarthritic knees. Osteoarthritis Cartilage 2002;10:199–206.
17. Kuroda R, Ishida K, Matsumoto T, Akisue T, Fujioka H, Mizuno K, et al. Treatment of a full-thickness articular cartilage defect in the femoral condyle of an athlete with autologous bone-marrow stromal cells. Osteoarthritis Cartilage 2007;15:226–31.
18. Cao B, Zheng B, Jankowski RJ, Kimura S, Ikezawa M, Deasy B, et al. Muscle stem cells differentiate into haematopoietic lineages but retain myogenic potential. Nat Cell Biol 2003;5:640–6.
19. Jankowski RJ, Deasy BM, Cao B, Gates C, Huard J. The role of CD34 expression and cellular fusion in the regeneration capacity of myogenic progenitor cells. J Cell Sci 2002;115(Pt 22):4361–74.
20. Lee JY, Qu-Petersen Z, Cao B, Kimura S, Jankowski R, Cummins J, et al. Clonal isolation of muscle-derived cells capable of enhancing muscle regeneration and bone healing. J Cell Biol 2000;150:1085–100.
21. Peng H, Wright V, Usas A, Gearhart B, Shen HC, Cummins J, et al. Synergistic enhancement of bone formation and healing by stem cell-expressed VEGF and bone morphogenetic protein-4. J Clin Invest 2002;110:751–9.
22. Shen HC, Peng H, Usas A, Gearhart B, Cummins J, Fu FH, et al. Ex vivo gene therapy-induced endochondral bone formation: comparison of muscle-derived stem cells and different subpopulations of primary muscle-derived cells. Bone 2004;34:982–92.
23. Wright V, Peng H, Usas A, Young B, Gearhart B, Cummins J, et al. BMP4-expressing muscle-derived stem cells differentiate into osteogenic lineage and improve bone healing in immunocompetent mice. Mol Ther 2002;6:169–78.
24. Adachi N, Sato K, Usas A, Fu FH, Ochi M, Han CW, et al. Muscle derived, cell based ex vivo gene therapy for treatment of full thickness articular cartilage defects. J Rheumatol 2002;29: 1920–30.
25. Kuroda R, Usas A, Kubo S, Corsi K, Peng H, Rose T, et al. Cartilage repair using bone morphogenetic protein 4 and muscle-derived stem cells. Arthritis Rheum 2006;54:433–42.
26. Crisostomo PR, Markel TA, Wang M, Lahm T, Lillemoe KD, Meldrum DR. In the adult mesenchymal stem cell population, source gender is a biologically relevant aspect of protective power. Surgery 2007;142:215–21.

27. Horner S, Pasternak G, Hehlmann R. A statistically significant sex difference in the number of colony-forming cells from human peripheral blood. Ann Hematol 1997;74:259–63.
28. Faiola B, Fuller ES, Wong VA, Pluta L, Abernethy DJ, Rose J, et al. Exposure of hematopoietic stem cells to benzene or 1,4-benzoquinone induces gender-specific gene expression. Stem Cells 2004;22:750–8.
29. Deasy BM, Lu A, Tebbets JC, Feduska JM, Schugar RC, Pollett JB, et al. A role for cell sex in stem cell-mediated skeletal muscle regeneration: female cells have higher muscle regeneration efficiency. J Cell Biol 2007;177:73–86.
30. Corsi KA, Pollett JB, Phillippi JA, Usas A, Li G, Huard J. Osteogenic potential of postnatal skeletal muscle-derived stem cells is influenced by donor sex. J Bone Miner Res 2007;22: 1592–602.
31. Gharaibeh B, Lu A, Tebbets J, Zheng B, Feduska J, Crisan M, et al. Isolation of a slowly adhering cell fraction containing stem cells from murine skeletal muscle by the preplate technique. Nat Protoc 2008;3:1501–9.
32. Peng H, Usas A, Gearhart B, Young B, Olshanski A, Huard J. Development of a self-inactivating tet-on retroviral vector expressing bone morphogenetic protein 4 to achieve regulated bone formation. Mol Ther 2004;9:885–94.
33. Peng H, Chen ST, Wergedal JE, Polo JM, Yee JK, Lau KH, et al. Development of an MFG-based retroviral vector system for secretion of high levels of functionally active human BMP4. Mol Ther 2001;4:95–104.
34. Johnstone B, Hering TM, Caplan AI, Goldberg VM, Yoo JU. In vitro chondrogenesis of bone marrow-derived mesenchymal progenitor cells. Exp Cell Res 1998;238:265–72.
35. Jadlowiec J, Koch H, Zhang X, Campbell PG, Seyedain M, Sfeir C. Phosphophoryn regulates the gene expression and differentiation of NIH3T3, MC3T3-E1, and human mesenchymal stem cells via the integrin/MAPK signaling pathway. J Biol Chem 2004;279: 53323–30.
36. Jadlowiec JA, Zhang X, Li J, Campbell PG, Sfeir C. Extracellular matrix-mediated signaling by dentin phosphophoryn involves activation of the Smad pathway independent of bone morphogenetic protein. J Biol Chem 2006;281:5341–7.
37. O'Driscoll SW, Keeley FW, Salter RB. Durability of regenerated articular cartilage produced by free autogenous periosteal grafts in major full-thickness defects in joint surfaces under the influence of continuous passive motion: a follow-up report at one year. J Bone Joint Surg Am 1988;70:595–606.
38. Hatakeyama Y, Tuan RS, Shum L. Distinct functions of BMP4 and GDF5 in the regulation of chondrogenesis. J Cell Biochem 2004;91:1204–17.
39. Hoffman LM, Garcha K, Karamboulas K, Cowan MF, Drysdale LM, Horton WA, et al. BMP action in skeletogenesis involves attenuation of retinoid signaling. J Cell Biol 2006;174:101–13.
40. Sekiya I, Larson BL, Vuoristo JT, Reger RL, Prockop DJ. Comparison of effect of BMP-2, -4, and -6 on in vitro cartilage formation of human adult stem cells from bone marrow stroma. Cell Tissue Res 2005;320:269–76.
41. Shirasawa S, Sekiya I, Sakaguchi Y, Yagishita K, Ichinose S, Muneta T. In vitro chondrogenesis of human synovium-derived mesenchymal stem cells: optimal condition and comparison with bone marrow-derived cells. J Cell Biochem 2006;97:84–97.
42. Semba I, Nonaka K, Takahashi I, Takahashi K, Dashner R, Shum L, et al. Positionally-dependent chondrogenesis induced by BMP4 is co-regulated by Sox9 and Msx2. Dev Dyn 2000;217:401–14.
43. Zheng B, Cao B, Li G, Huard J. Mouse adipose-derived stem cells undergo multilineage differentiation in vitro but primarily osteogenic and chondrogenic differentiation in vivo. Tissue Eng 2006; 12:1891–901.
44. Hachisuka H, Mochizuki Y, Yasunaga Y, Natsu K, Sharman P, Shinomiya R, et al. Flow cytometric discrimination of mesenchymal progenitor cells from bone marrow-adherent cell populations using CD34/44/45(−) and Sca-1(+) markers. J Orthop Sci 2007; 12:161–9.
45. Yoshida S, Shimmura S, Nagoshi N, Fukuda K, Matsuzaki Y, Okano H, et al. Isolation of multipotent neural crest-derived stem cells from the adult mouse cornea. Stem Cells 2006;24:2714–22.
46. Felson DT, Lawrence RC, Dieppe PA, Hirsch R, Helmick CG, Jordan JM, et al. Osteoarthritis: new insights. Part 1: the disease and its risk factors. Ann Intern Med 2000;133:635–46.
47. Ding C, Cicuttini F, Scott F, Glisson M, Jones G. Sex differences in knee cartilage volume in adults: role of body and bone size, age and physical activity. Rheumatology (Oxford) 2003;42:1317–23.
48. Jones G, Glisson M, Hynes K, Cicuttini F. Sex and site differences in cartilage development: a possible explanation for variations in knee osteoarthritis in later life. Arthritis Rheum 2000;43:2543–9.
49. Csintalan RP, Schulz MM, Woo J, McMahon PJ, Lee TQ. Gender differences in patellofemoral joint biomechanics. Clin Orthop Relat Res 2002:260–9.

ARTHRITIS & RHEUMATISM
Vol. 60, No. 1, January 2009, pp 155–165
DOI 10.1002/art.24153

Appendix 3

Blocking Vascular Endothelial Growth Factor With Soluble Flt-1 Improves the Chondrogenic Potential of Mouse Skeletal Muscle–Derived Stem Cells

Seiji Kubo,[1] Gregory M. Cooper,[1] Tomoyuki Matsumoto,[1] Julie A. Phillippi,[2] Karin A. Corsi,[2] Arvydas Usas,[2] Guangheng Li,[2] Freddie H. Fu,[3] and Johnny Huard[1]

Objective. **To investigate the effect of vascular endothelial growth factor (VEGF) stimulation and the effect of blocking VEGF with its antagonist, soluble Flt-1 (sFlt-1), on chondrogenesis, using muscle-derived stem cells (MDSCs) isolated from mouse skeletal muscle.**

Methods. **The direct effect of VEGF on the in vitro chondrogenic ability of mouse MDSCs was tested using a pellet culture system, followed by real-time quantitative polymerase chain reaction (PCR) and histologic analyses. Next, the effect of VEGF on chondrogenesis within the synovial joint was tested, using genetically engineered MDSCs implanted into rat osteochondral defects. In this model, MDSCs transduced with a retroviral vector to express bone morphogenetic protein 4 (BMP-4) were coimplanted with MDSCs transduced to express either VEGF or sFlt-1 (a VEGF antagonist) to provide a gain- and loss-of-function experimental design. Histologic scoring was used to compare cartilage formation among the treatment groups.**

Results. **Hyaline-like cartilage matrix production was observed in both VEGF-treated and VEGF-blocked (sFlt-1–treated) pellet cultures, but quantitative PCR revealed that sFlt-1 treatment improved the expression of chondrogenic genes in MDSCs that were stimulated to undergo chondrogenic differentiation with BMP-4 and transforming growth factor β3 (TGFβ3). In vivo testing of articular cartilage repair showed that VEGF-transduced MDSCs caused an arthritic change in the knee joint, and sFlt-1 improved the MDSC-mediated repair of articular cartilage, compared with BMP-4 alone.**

Conclusion. **Soluble Flt-1 gene therapy improved the BMP-4– and TGFβ3-induced chondrogenic gene expression of MDSCs in vitro and improved the persistence of articular cartilage repair by preventing vascularization and bone invasion into the repaired articular cartilage.**

Articular cartilage is an avascular tissue with a limited intrinsic capacity for regeneration. For this reason, tissue engineering techniques to repair articular cartilage have been extensively studied, and chondrocyte transplantation already has become a clinical reality (1–3).

For the repair of large cartilage defects caused by osteoarthritis or rheumatoid arthritis, stem cells are more attractive than primary chondrocytes because of their superior capacity for self renewal, proliferation, and resistance to stress (4–6). Several studies have suggested that stem-like cells can undergo chondrogenesis and repair articular cartilage in experimental cartilage-injury models, including studies using muscle-derived stem cells (MDSCs) (7–11). Stem cells have recently been used clinically for cartilage repair (12,13).

However, problems still surround the use of stem

Supported by the US Department of Defense (contract W81XWH-08-0076), the NIH (grant R01-DE-13420-06), and the Hirtzel Foundation. Dr. Huard's work was supported by the William F. and Jean W. Donaldson Chair at the Children's Hospital of Pittsburgh, and the Henry J. Mankin Endowed Chair for Orthopaedic Research at the University of Pittsburgh.

[1]Seiji Kubo, MD, PhD, Gregory M. Cooper, PhD, Tomoyuki Matsumoto, MD, PhD, Johnny Huard, PhD: Children's Hospital of Pittsburgh, and University of Pittsburgh, Pittsburgh, Pennsylvania; [2]Julie A. Phillippi, PhD, Karin A. Corsi, PhD, Arvydas Usas, MD, Guangheng Li, MD, PhD: Children's Hospital of Pittsburgh, Pittsburgh, Pennsylvania; [3]Freddie H. Fu, MD: University of Pittsburgh, Pittsburgh, Pennsylvania.

Dr. Huard has received consulting fees, speaking fees, and/or honoraria from Cook Myosite, Inc. (more than $10,000).

Address correspondence and reprint requests to Johnny Huard, PhD, Children's Hospital of Pittsburgh, 4100 Rangos Research Center, 3705 Fifth Avenue, Pittsburgh, PA 15213-2582. E-mail: jhuard@pitt.edu.

Submitted for publication October 1, 2007; accepted in revised form September 17, 2008.

cells to repair cartilage. One of the most important issues is the control of vascular endothelial growth factor (VEGF) signaling during the chondrogenic differentiation of stem cells. Previous research has shown that VEGF treatment prevents condensation of chondrogenic mesenchyme during early limb bud development, through abnormal vascularization (14). The expression of high levels of VEGF in the terminal stages of chondrogenesis leads to endochondral ossification through angiogenesis (15,16). Also, VEGF has been shown to enhance endochondral bone formation elicited by bone morphogenetic protein (BMP)–transduced MDSCs in a model of ectopic bone formation (17). VEGF expression by chondrocytes in osteoarthritic joints may be related to cartilage destruction (18–24). Furthermore, high doses of VEGF may induce the onset and progression of arthritis (25–27). This theory is supported by studies showing that treatment with soluble Flt-1 (sFlt-1), a VEGF antagonist, decreased the progression of arthritis in a mouse model (28,29). Taken together, these results suggest that VEGF may be a catabolic molecule for cartilage. Contrary to this interpretation, VEGF has been shown to be necessary for chondrocyte survival during cartilage development. In VEGF-deficient mouse models, massive cell death was observed in the joint and epiphyseal regions of cartilage during cartilage development (30,31).

Despite these paradoxic results, the effects of VEGF on stem cell–mediated chondrogenesis in vitro and on cartilage repair in vivo have not been rigorously investigated. Our current study used a gain- and loss-of-function approach based on gene therapy techniques to ascertain the role of VEGF in stem cell–mediated cartilage repair. MDSCs were genetically engineered to express human BMP-4, human $VEGF_{165}$, or the VEGF antagonist, sFlt-1. These cells were used to test the effect of VEGF on MDSC-mediated cartilage repair in the knee joint in an in vivo osteochondral defect model.

This study was designed to test the hypothesis that increased VEGF expression within a healing osteochondral defect will inhibit the persistence of cartilage repair, and that blocking VEGF signaling using sFlt-1 will improve the quality and persistence of MDSC-mediated cartilage regeneration. The effects on chondrogenesis of VEGF stimulation and blocking VEGF signaling with sFlt-1 were studied, not only with respect to the intrinsic chondrogenic capacity of stem cells, but also within the more complex in vivo environment that includes interactions with synovia, subchondral bone, and adjacent cartilage in the knee joint.

MATERIALS AND METHODS

Isolation of primary MDSCs. MDSCs were isolated from the hind limb skeletal muscle of 3-week-old male C57BL/10J mice (The Jackson Laboratory, Bar Harbor, ME) via a modified preplate technique that has been described previously (5).

Retroviral transduction. Retroviral vectors expressing human BMP-4 (retro–BMP-4), VEGF (retro-VEGF), or sFlt-1 (retro–sFlt-1) were generated by replacing the U3 region in the 5′ long terminal repeat with the human cytomegalovirus promoter, as previously described (8,17). MDSCs were transduced separately with these retroviral vectors at a multiplicity of infection of 5 in the presence of Polybrene (8 μg/ml). The transduced cells were expanded for 2 weeks before being used in experiments, and conditioned medium was sampled to determine transgene expression.

The level of BMP-4 secreted from the transduced cells was estimated with a BMP-4 bioassay, as previously described (32). The levels of VEGF or sFlt-1 secreted from the transduced cells were measured using enzyme-linked immunosorbent assay (ELISA) kits (R&D Systems, Minneapolis, MN).

In vitro chondrogenesis. Pellet culturing was performed as described previously (33). Cell pellets were made with the following: 1) 1.4×10^5 nontransduced MDSCs and 1.4×10^5 BMP-4–expressing MDSCs (B4 group), 2) 1.4×10^5 VEGF-expressing MDSCs and 1.4×10^5 BMP-4–expressing MDSCs (B4+VEGF group), 3) 1.4×10^5 sFlt-1–expressing MDSCs and 1.4×10^5 BMP-4–expressing MDSCs (B4+sFlt-1 group), and 4) 2.8×10^5 primary chondrocytes derived from the mouse knee (Chond group). Three more groups (groups 5, 6, and 7) were created using 2.8×10^5 nontransduced MDSCs. Pellets from groups 1–4 were cultured in 0.5 ml of chondrogenic medium that contained Dulbecco's modified Eagle's medium supplemented with 1% penicillin/streptomycin, $10^{-7}M$ dexamethasone, 50 μg/ml ascorbate-2-phosphate, 40 μg/ml proline, 100 μg/ml pyruvate, and 1% ITS+ Premix (Becton Dickinson, Franklin Lakes, NJ) with 10 ng/ml of transforming growth factor β3 (TGFβ3; R&D Systems). Group 5 pellets (made with nontransduced cells) were cultured in chondrogenic medium without the TGFβ3 supplement (C group). Group 6 pellets were fed with chondrogenic medium without TGFβ3 but with 50 ng/ml BMP-4 added (C+B4 group). Finally, group 7 pellets were fed with chondrogenic medium supplemented with 10 ng/ml of TGFβ3 (C+T group). All pellets were incubated at 37°C in 5% CO_2, and the medium was changed every 2–3 days. Pellets were harvested after 7, 14, and 28 days in culture.

Alcian blue staining. Pellets were fixed overnight in 10% neutral buffered formalin, dehydrated, embedded in paraffin, and sectioned in 5-μm–thick slices. Pellet sections were deparaffinized, placed in 3% acetic acid for 3 minutes, and transferred into Alcian blue solution for 30 minutes. The slides were then rinsed with running tap water for 10 minutes and counterstained with nuclear fast red.

Real-time quantitative polymerase chain reaction (PCR) analysis of pellet culture cells. Messenger RNA was isolated using the RNeasy Plus Kit (Qiagen, Valencia, CA), according to the manufacturer's instructions. After RNA extraction, real-time quantitative PCR analysis was carried out as described previously (34,35). Gene expression levels were

calculated based on the difference in threshold cycle (ΔC_t) method (separate tubes). All target genes were normalized to the reference housekeeping gene, *18S*. *18S* primers and probes were designed by and purchased from Applied Biosystems (Foster City, CA). Primers and probes were designed for type II collagen, SOX9, and type X collagen, according to the GenBank sequence. All target gene primers and probes were purchased from Integrated DNA Technologies Inc. (Coralville, IA).

Each experimental value is reported as the mean ± SEM results of triplicate treatments. For quantitative PCR assays, the coefficient of variation (CV) was calculated from 3 assay replicates. For all treatment groups and target genes analyzed, the CV did not exceed 3%. One-way analysis of variance, followed by Tukey-Kramer's post hoc test, was performed to determine significance among treatment groups. *P* values less than 0.05 were considered significant.

Repair of osteochondral defects. The policies and procedures of our animal laboratory are in accordance with those published by the US Department of Health and Human Services. The research techniques used for these experiments were approved by the Animal Research and Care Committee at Children's Hospital of Pittsburgh. Twenty-eight 10-week-old nude rats (NIH-*Whn* NIHRNU-M; Taconic, Germantown, NY) were used in this study. The rats were anesthetized via exposure to 3% isofluorane and O_2 gas (1.5 liter/minute) delivered through an inhalation mask. The knee joint was exposed by the medial parapatellar approach, and the trochlear groove was exposed by lateral dislocation of the patella. A 1.8-mm outer diameter trephine drill was used to create an osteochondral defect (1.8 × 2.0 mm) in the trochlear groove of each femur. MDSCs isolated from mouse skeletal muscle were mixed with fibrin glue (Tisseel VH; Baxter Healthcare, Glendale, CA) before transplantation.

The rats were divided into 7 treatment groups. The defects in group 1 rats (no-cell control) were treated with acellular fibrin glue, defects in group 2 rats (MDSC group) were treated with 500,000 MDSCs embedded in fibrin glue, defects in group 3 rats (VEGF group) were treated with 250,000 MDSC-VEGF cells plus 250,000 MDSCs embedded in fibrin glue, defects in group 4 rats (sFlt-1 group) were treated with 250,000 MDSC–sFlt-1 cells plus 250,000 MDSCs embedded in fibrin glue, defects in group 5 rats (B4 group) were treated with 250,000 MDSC-B4 cells plus 250,000 MDSCs embedded in fibrin glue, defects in group 6 rats (B4+VEGF group) were treated with 250,000 MDSC-B4 cells plus 250,000 MDSC-VEGF cells embedded in fibrin glue, and defects in group 7 rats (B4+sFlt-1 group) were treated with 250,000 MDSC-B4 cells plus 250,000 MDSC–sFlt-1 cells embedded in fibrin glue. Four defects (in 2 rats) were made for each group (n = 4 knees per group). The rats were allowed to move freely within their cages after surgery. Rats were killed 8 weeks or 16 weeks after surgery. Groups of rats that received VEGF treatment were killed 8 weeks after surgery because the deterioration of the knee joint impaired the ability of the rats to move freely.

Histologic evaluation of cartilage repair. After qualitative macroscopic examination, 4 distal femora per group per time point were dissected and fixed with 10% neutral buffered formalin for 48 hours, followed by decalcification with 10% EDTA for 2 weeks and paraffin embedding. Sagittal sections, 5 μm in thickness, were obtained from the center of each defect and stained with Safranin O–fast green. The histologic grading scale described by Sellers et al (36) was used to evaluate the quality of the repaired tissue. All data are expressed as the mean ± SD. Differences in each category and the total score were analyzed by Kruskal-Wallis and Mann-Whitney U tests, using SPSS software, version 12.0.1 (SPSS, Chicago, IL). *P* values less than 0.05 were considered significant.

RESULTS

Expression of BMP-4, VEGF, and sFlt-1 by transduced MDSCs. To ensure that we had successfully transduced the cells and induced protein secretion, we tested the supernatant collected from transduced or nontransduced cells, using either an activity bioassay (for BMP) or an ELISA (for VEGF and sFlt-1). MDSCs transduced with retro–BMP-4 secreted 327 ng/10^6 cells/24 hours, as detected by BMP-4 bioassay. MDSCs transduced with retro-VEGF secreted human VEGF at a mean ± SD rate of 1.14 ± 0.05 μg/10^6 cells/24 hours, compared with nontransduced MDSCs, which secreted mouse VEGF at a rate of 750 ± 12.2 pg/10^6 cells/24 hours. Retro–sFlt-1–transduced MDSCs secreted sFlt-1 at a level of 2.1 ± 0.004 ng/10^6 cells/24 hours.

In a separate set of experiments, 2.5 × 10^5 transduced or nontransduced cells were cultured in 3-dimensional micromass pellet culture for 48 hours, the medium was collected, and VEGF expression was tested using an ELISA. Medium from nontransduced MDSC pellets contained 409.0 ± 49.4 (mean ± SD) ng/ml of VEGF, which was significantly more than primary chondrocytes (226.7 ± 53.8 ng/ml) and significantly less than cells transduced to express BMP-4 (B4 cells; 592.9 ± 52 ng/ml).

Effect of VEGF and sFlt-1 on chondrogenic differentiation of MDSCs. Histologic analysis was used to determine whether the different mixtures of transduced and nontransduced cells were capable of undergoing chondrogenic differentiation in vitro. Histologic analysis of tissues stained with Alcian blue showed that all of the pellets from every group contained some well-differentiated, round chondrocytic cells and also showed some level of hyaline-like cartilage extracellular matrix (ECM) production, as evidenced by positive Alcian blue staining (Figure 1A). Nontransduced control MDSCs (group C; Figure 1A) showed the least intense staining, whereas primary chondrocytes (Chond group; Figure 1A) showed the largest amount of Alcian blue–positive ECM. Pellets from the B4+VEGF group showed evi-

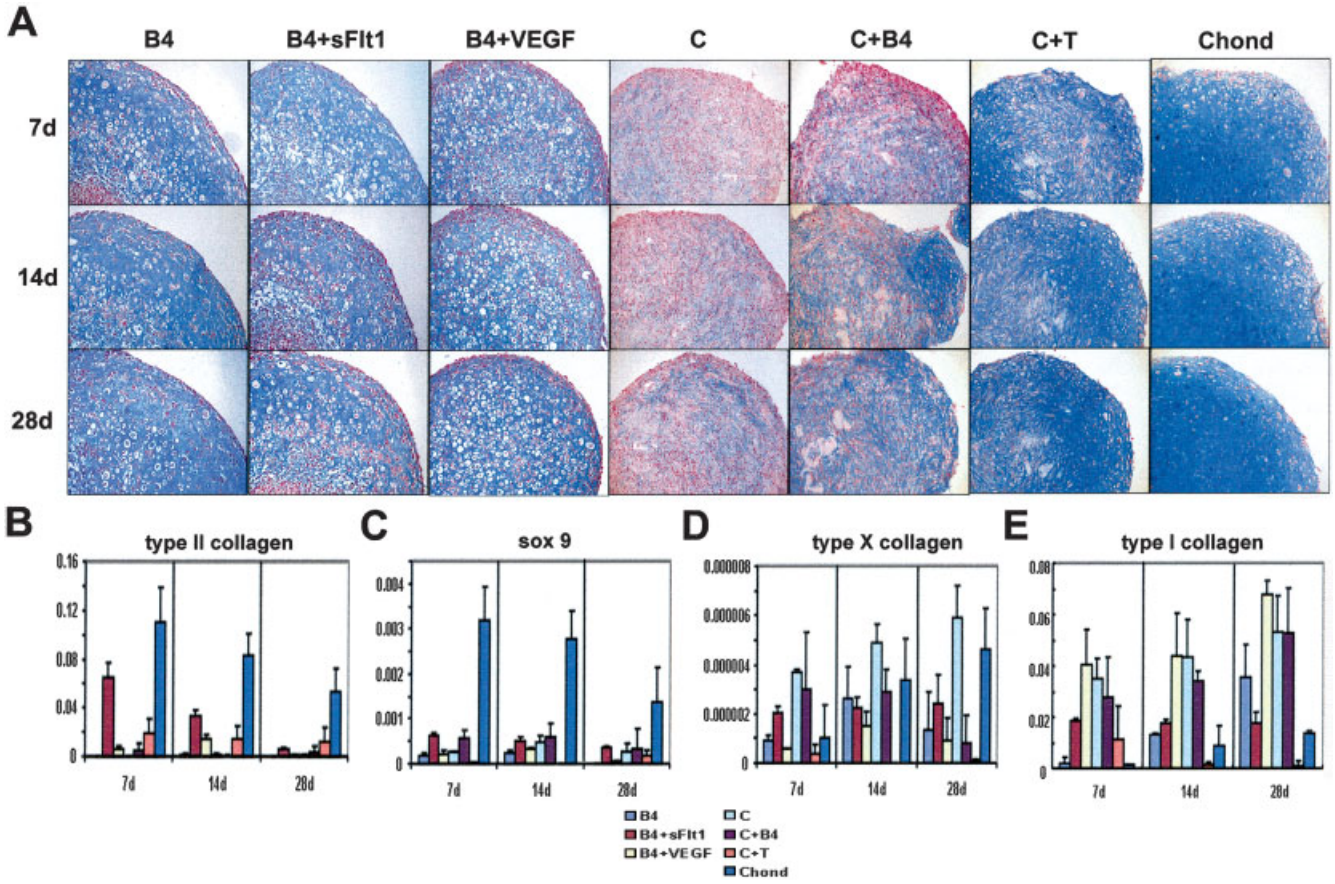

Figure 1. A, Alcian blue staining of pellets. Hyaline cartilage–like Alcian blue–positive matrix was observed in pellets created with chondrocytes (Chond) or with muscle-derived stem cells (MDSCs) transduced to express bone morphogenetic protein (BMP-4; B4), a mixture of cells expressing BMP-4 or vascular endothelial growth factor (VEGF; B4+VEGF), and in pellets with a mixture of cells expressing BMP-4 or soluble Flt-1 (sFlt-1; B4+sFlt-1). Nontransduced cells (C) with BMP-4 (C+B4) or transforming growth factor β3 (C+T) added to the medium did not show similar matrix formation. Chondrocyte-like round cells were observed in all groups in which cells were transduced (B4, B4+sFlt-1, B4+VEGF) and at all time points (days 7, 14, and 28) but not in control pellet cultures (C, C+B4, C+T). The pellets cultured with BMP-4 plus sFlt-1 contained more chondrocyte-like cells at all time points compared with the other groups. (Original magnification × 100.) **B–E,** Results of quantitative polymerase chain reaction performed on cells cultured in 3-dimensional micromass pellet culture. Pellets created with a mixture of MDSCs expressing BMP-4 or sFlt-1 (B4+sFlt-1) demonstrated significantly higher type II collagen and SOX9 gene expression than other groups at all time points in culture. Type X collagen expression was significantly higher in the B4+sFlt-1 group compared with the B4+VEGF group at 7 days and 28 days. Type I collagen expression was highest in the B4+VEGF group at all time points. Bars show the mean and SEM.

dence of chondrogenesis peripherally, with a region of fibrous, noncartilaginous tissue near the center of the pellet, especially after 28 days in culture (B4+VEGF group; Figure 1A). Together, these results suggest that neither VEGF nor sFlt-1 inhibits the intrinsic chondrogenic capacity of MDSCs.

In order to assess the expression of several chondrogenic marker genes under different in vitro experimental conditions, we performed quantitative PCR analysis. Pellets from the B4+sFlt-1 group showed significantly greater type II collagen and SOX9 gene expression than the groups treated with BMP-4 or BMP-4 plus VEGF at all time points, and showed higher type X collagen gene expression than the B4+VEGF group at 7 days and 28 days (Figures 1B–D). The B4+VEGF group showed significantly higher type II collagen gene expression than the B4 group at 14 days (Figure 1B). It was also observed that the expression of type II collagen decreased over time in the B4+sFlt-1 group; however, a similar trend was observed in the primary chondrocyte control pellets (Figure 1B). Type I collagen expression increased over time in the B4, B4+VEGF and Chond groups but remained constant in the group treated with B4+sFlt-1 (Figure 1E).

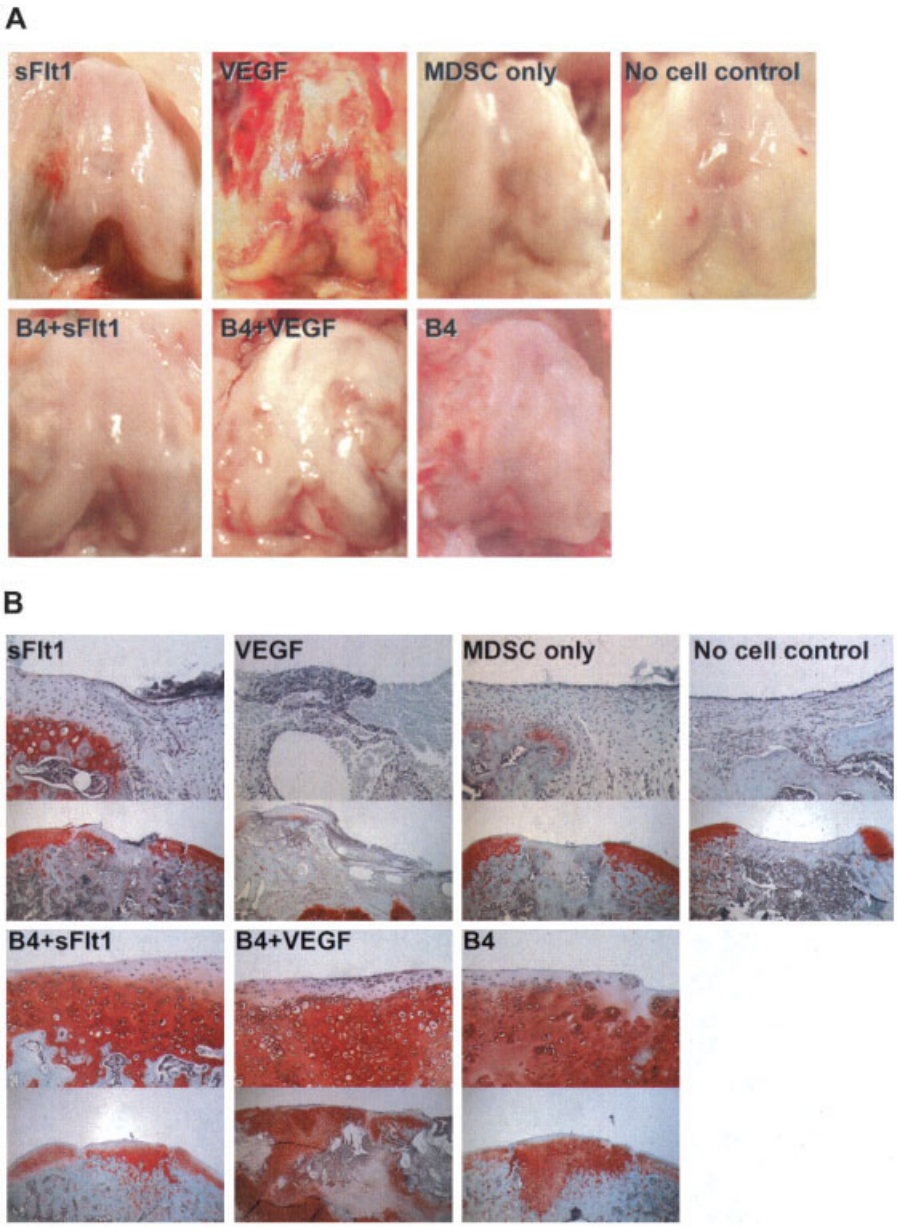

Figure 2. A, Macroscopic images of osteochondral defects 8 weeks after transplantation. Grossly, the defects treated with either BMP-4 or a mixture of BMP-4– and sFlt-1–expressing cells appeared more similar to the surrounding cartilage. Both groups treated with VEGF showed evidence of cartilage destruction. **B,** Photomicrographs showing Safranin O staining of defect areas 8 weeks postoperatively. Large areas of Safranin O–positive cartilage were noted in defects treated with BMP-4. Although the defects treated with VEGF plus BMP-4 showed Safranin O–positive cartilage, damage in other regions of the joint was observed. Each photomicrograph shows both a high-magnification view (original × 200; top) and a lower-magnification view (original × 50; bottom). See Figure 1 for definitions.

Effect of VEGF treatment on progression of arthritis in the knee joint. In order to generally assess the effects of our different treatments, we performed a qualitative gross analysis of the knee joint at 8 weeks or 16 weeks postoperatively. Eight weeks after surgery, the B4+VEGF group showed the appearance of arthritis

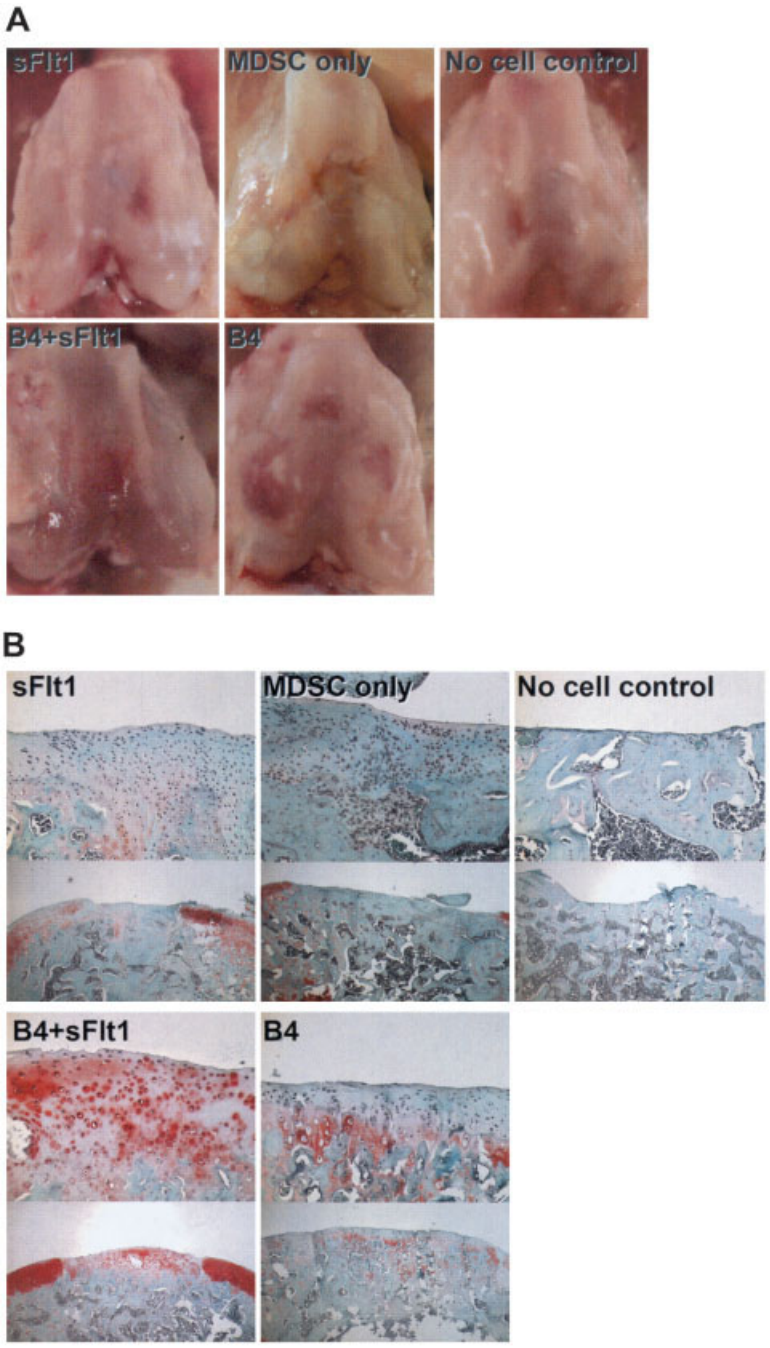

Figure 3. A, Macroscopic images of osteochondral defects 16 weeks after transplantation. Grossly, the defects treated with BMP-4 appeared to be healed with cartilaginous tissue that resembled the surrounding articular cartilage. **B,** Photomicrographs showing Safranin O staining of defect areas 16 weeks postoperatively. Both groups treated with BMP-4–expressing cells showed some Safranin O–positive tissue in the defect region. The defects treated with a mixture of cells expressing either BMP-4 or sFlt-1 (B4+sFlt-1) showed the best repair of tissue, based on histologic analysis. Each photomicrograph shows both a high-magnification view (original × 200; top) and a lower-magnification view (original × 50; bottom). See Figure 1 for definitions.

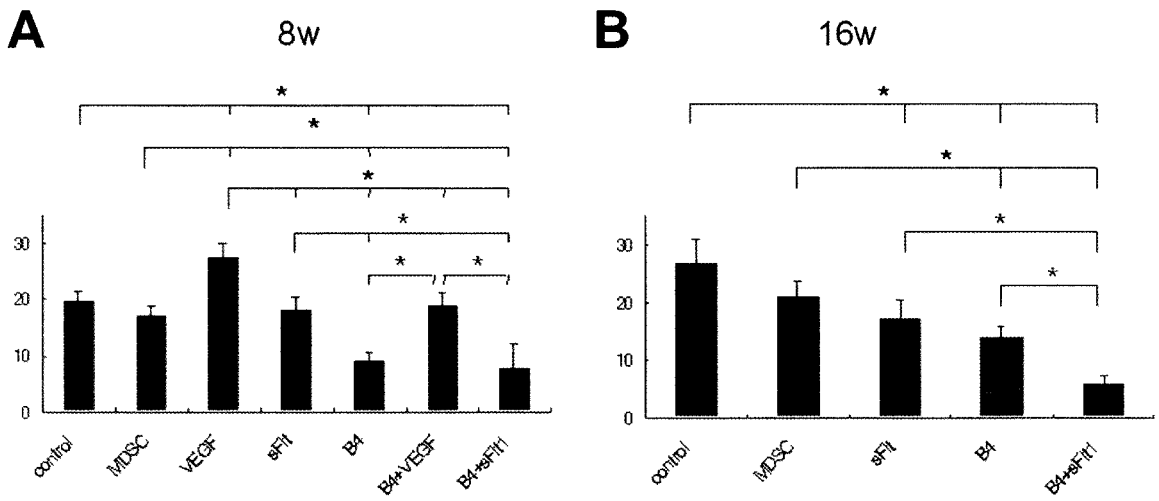

Figure 4. A, Total histologic scores for samples analyzed 8 weeks after surgery. Scores were significantly lower in the B4 and B4+sFlt-1 groups compared with all other treatment groups and were significantly higher in the B4+VEGF group compared with all other groups. **B,** Total histologic scores for samples analyzed 16 weeks after surgery. Statistical analysis of the total scores showed that the group treated with BMP-4 plus sFlt-1 had significantly lower scores than all other groups tested. Bars show the mean and SD. $* = P < 0.05$. See Figure 1 for definitions.

progression (Figure 2A). In the VEGF-treated group, similar arthritis progression was observed. Groups that were not treated with cells expressing VEGF showed no signs of arthritis 8 weeks after surgery (Figure 2A). Defects in the B4, B4+VEGF, or B4+sFlt-1 group showed good coverage by cartilaginous tissue that was well integrated with the surrounding cartilage. Defects in groups that were not treated with BMP-4–expressing cells were covered by connective tissue, and the surfaces of those defects were concave compared with surrounding normal convex cartilage (Figure 2A). Between 8 weeks and 16 weeks after surgery, the knees treated with cells expressing VEGF showed high levels of joint destruction, inhibiting normal movement of the rats. Therefore, rats in the VEGF or B4+VEGF group were removed from the study before the 16-week postoperative time point.

Sixteen weeks after transplantation, defects that were not treated with BMP-4–expressing cells appeared to be rough, and the margin between the defects and the surrounding cartilage could be clearly identified (Figure 3A). Defects in the B4 or B4+sFlt-1 group still contained smooth repaired tissue that was well integrated with the surrounding cartilage. However, the group treated with BMP-4 showed some mild cartilage erosion (Figure 3A).

Improved cartilage formation in the sFlt-1–treated group, by Safranin O staining. We used Safranin O staining to highlight the glycosaminoglycan content in the repaired region as an indicator of overall cartilage health. Eight weeks after transplantation, defects in the B4 or B4+sFlt-1 group contained Safranin O–positive hyaline cartilage, and the subchondral area was replaced by bone or cartilage. In contrast, defects in groups that were not treated with BMP-4–expressing cells (no cell control, MDSC only, VEGF, and sFlt-1 groups) were covered and filled with undifferentiated mesenchymal tissue or fibrous tissue (Figure 2B). Groups treated with VEGF-expressing cells showed evidence of mild destruction, including pannus invasion, osteolysis, and cyst formation in subchondral bone area, although the B4+VEGF group did show Safranin O–positive hyaline cartilage repair near the articular surface.

Sixteen weeks after transplantation, defects in the control group showed eburnated bone covered by thin fibrous tissue (Figure 3B). The MDSC-treated defects showed undifferentiated fibrous tissue, while the B4+sFlt-1 group showed the presence of cartilaginous tissue that stained slightly positive with Safranin O. The defects in the B4 and B4+sFlt-1 groups were covered by Safranin O–positive cartilage, although the B4 group showed less Safranin O–positive cartilage compared with the B4+sFlt-1 group.

Table 1. Histologic scores for cartilage repair at 8 weeks and 16 weeks after surgery*

Group	Filling of defect	Integration to adjacent tissue	Safranin O staining	Cellular morphology	Architecture within defect	Architecture of surface	Subchondral bone replacement	Tidemark formation	Total score
8 weeks									
Control	1.25 ± 0.5	0.50 ± 0.6	4.00 ± 0.0	5.00 ± 0.0	0.25 ± 0.5	1.75 ± 0.5	3.00 ± 0.8	4.00 ± 0.0	19.75 ± 1.7
MDSCs	0.75 ± 1.0	0.00 ± 0.0	3.25 ± 0.5	4.50 ± 0.6	0.25 ± 0.5	1.00 ± 0.8	3.50 ± 0.6	4.00 ± 0.0	17.25 ± 1.7
VEGF	2.50 ± 1.0	2.50 ± 0.6	4.00 ± 0.0	5.00 ± 0.0	3.00 ± 0.8	2.50 ± 1.0	4.00 ± 0.0	4.00 ± 0.0	27.50 ± 2.5
sFlt-1	1.50 ± 0.6	0.00 ± 0.0	3.25 ± 0.5	4.75 ± 0.5	0.75 ± 1.0	1.25 ± 0.5	3.00 ± 1.2	3.50 ± 0.6	18.00 ± 2.6
BMP-4	0.00 ± 0.0	0.00 ± 0.0	0.75 ± 0.5	2.00 ± 0.0	0.00 ± 0.0	1.00 ± 0.0	1.50 ± 1.3	3.75 ± 0.5	9.00 ± 1.6
BMP-4+VEGF	0.00 ± 0.0	1.25 ± 1.0	1.75 ± 1.0	2.50 ± 1.3	3.50 ± 1.0	2.50 ± 1.0	4.00 ± 0.0	3.50 ± 1.0	19.00 ± 2.2
BMP-4+sFlt-1	0.00 ± 0.0	0.00 ± 0.0	1.75 ± 1.3	1.50 ± 1.0	0.00 ± 0.0	0.75 ± 1.0	1.75 ± 1.3	2.00 ± 0.8	7.75 ± 4.4
16 weeks									
Control	3.25 ± 1.0	2.00 ± 1.2	4.00 ± 0.0	5.00 ± 0.0	3.00 ± 2.0	1.50 ± 0.6	4.00 ± 0.0	4.00 ± 0.0	26.75 ± 4.3
MDSCs	1.75 ± 1.0	0.00 ± 0.0	3.50 ± 0.6	5.00 ± 0.0	1.25 ± 1.9	1.50 ± 0.6	4.00 ± 0.0	4.00 ± 0.0	21.00 ± 2.7
sFlt-1	0.75 ± 0.5	0.00 ± 0.0	3.00 ± 0.8	4.75 ± 0.5	0.00 ± 0.0	1.25 ± 1.0	3.75 ± 0.5	3.50 ± 0.6	17.00 ± 3.4
BMP-4	0.50 ± 1.0	0.50 ± 0.6	2.50 ± 0.6	3.00 ± 0.8	0.00 ± 0.0	1.25 ± 0.5	3.00 ± 0.0	3.00 ± 0.8	13.75 ± 1.9
BMP-4+sFlt-1	0.00 ± 0.0	0.00 ± 0.0	1.50 ± 0.6	0.50 ± 0.6	0.00 ± 0.0	1.00 ± 0.0	1.25 ± 1.0	1.50 ± 0.6	5.75 ± 1.7

* Values are the mean ± SD. The histologic grading scale described by Sellers et al (36) was used to evaluate the quality of the repaired tissue. The total score ranges from 0 (normal articular cartilage) to 31 (no repair). MDSCs = muscle-derived stem cells; VEGF = vascular endothelial growth factor; sFlt-1 = soluble Flt-1; BMP-4 = bone morphogenetic protein 4.

Usefulness of blocking VEGF in cartilage repair, as supported by histologic scoring. We evaluated articular cartilage repair semiquantitatively, using a previously described histologic grading system, in order to better characterize the types of tissue that formed within the defects. In this system, 7 histologic categories (filling of defect, integration to adjacent tissue, Safranin O staining, cellular morphology, architecture within defect, architecture of surface, subchondral bone replacement, and tidemark formation) are evaluated and scored. The total score ranges from 0 (normal articular cartilage) to 31 (no repair) (36).

In general, 8 weeks after implantation, defects treated with BMP-4 showed improved healing compared with defects that were not treated with BMP-4 (Figure 4A and Table 1). Among the groups treated with BMP-4, defects that were also treated with cells expressing sFlt-1 (B4+sFlt-1) showed the lowest scores, suggesting that the repaired cartilage was most histologically normal in this group.

The total score for the B4+sFlt-1 group was significantly lower (histologically more similar to normal, undamaged cartilage) than that for all other groups (Figures 4A and B and Table 1). The total score for the B4 group was lower than that for the control group, the MDSC group, and the sFlt-1–only group. Also, the total score for the sFlt-1 group was lower than that for the control group.

DISCUSSION

VEGF signaling has been shown to play important roles during endochondral bone formation, apoptosis, osteophyte formation, and cartilage destruction in the osteoarthritic joint (15,16,18–24). Furthermore, VEGF has been shown to be one of the most important factors that can cause arthritis (25–27). These data support the idea that VEGF is related to cartilage destruction. However, it also has been shown that VEGF is important for stem cell and chondrocyte survival during limb bud development (30,31), and that blocking VEGF signaling can suppress BMP-4–induced endochondral bone formation by MDSCs (17). Therefore, the role of VEGF during stem cell–mediated chondrogenesis needs to be better understood.

To gain insight into the paradoxic effects of VEGF, in the current study, we first tested the in vitro chondrogenic ability of MDSCs, using a 3-dimensional pellet culture system in chondrogenic medium with 10 ng/ml of TGFβ3. Using this system, it was possible to determine the direct effect of VEGF on the intrinsic capacity of MDSCs to undergo chondrogenic differentiation. Specifically, the system enabled the determination of whether VEGF secretion by differentiated chondrocytes can cause intrinsic cartilage resorption, and whether inhibition of VEGF signaling by sFlt-1 could prevent chondrogenic differentiation of MDSCs. Hyaline cartilage–like matrix production was observed by histologic evaluation of pellets from the group treated with BMP-4 plus VEGF, as evidenced by Alcian blue–positive staining after 7, 14, and 28 days in culture (Figure 1A). Also, it was observed that coculture of VEGF-expressing cells with BMP-4–expressing cells did not alter the expression of chondrogenic genes (type II

collagen, type X collagen, and SOX9) compared with culture with BMP-4 alone (Figures 1B and C).

These results suggest that VEGF does not prevent the chondrogenic differentiation of BMP-4–transduced MDSCs in pellet culture after stimulation with chondrogenic medium containing 10 ng/ml of TGFβ3. These results seem to be in agreement with previous studies of the effect of VEGF on micromass culture of mesenchymal cells from the chicken limb bud (14). More importantly, it was observed that the presence of sFlt-1–expressing cells within the pellets further enhanced the chondrogenic differentiation of BMP-4–expressing MDSCs at all time points, as shown both histologically (Figure 1A) and by gene expression (Figures 1B and C). These results suggest that blocking VEGF with sFlt-1 does not prevent in vitro chondrogenesis of BMP-4–transduced MDSCs in pellet culture but, in fact, improves the expression of chondrogenic marker genes by MDSCs induced to undergo chondrogenic differentiation. Although sFlt-1 does not block the expression of VEGF by MDSCs, it blocks VEGF activity after it is secreted, suggesting either a potential beneficial effect of blocking VEGF activity on chondrogenesis or that sFlt-1 influences chondrogenesis through an unknown mechanism independent of VEGF.

In addition, this study used an in vivo transplantation experiment to provide information about the effect of VEGF on the BMP-4–induced chondrogenic ability of MDSCs, using a gain- and loss-of-function experimental design. MDSCs were exposed to the more stressful environment of the synovial joint, where matrix production is normally strongly suppressed. Furthermore, a complete assessment of healing can be obtained in this model, because the local environment in which cartilage regeneration must be elicited was preserved.

Eight weeks after surgery, the BMP-4–treated groups, regardless of the presence or absence of VEGF activity, showed better cartilage repair macroscopically on the surface of the defect than groups not treated with BMP-4 (Figure 2A). By Safranin O staining, the repaired tissue seemed to resemble hyaline cartilage (Figure 2B). The difference in the histologic scores between the 3 BMP-4–treated groups was mostly attributable to pannus invasion into the subchondral region and osteolysis of the subchondral bone, which affected the histologic scores for "architecture within defect" and "subchondral bone formation" (Figure 2B and Table 1). This result suggests that even in the synovial joint, VEGF will not prevent the BMP-4–induced chondrogenesis mediated by MDSCs, but that VEGF can cause osteolysis and pannus invasion through the activation of cells related to osteolysis and synovial hypertrophy. However, the VEGF-treated groups were given markedly worse total scores than groups that had no VEGF treatment or received sFlt-1 treatment (Table 1). Interestingly, when comparing the group treated with BMP-4 plus VEGF with the VEGF group, osteophyte formation was seen only in the group that received BMP-4 plus VEGF, although both groups commonly showed arthritis development, including an increased amount of joint fluid, synovial hypertrophy, and pannus invasion into cartilage and bone (Figures 2A and B). Regardless of the presence or absence of BMP-4 treatment, the results suggest that treatments for articular cartilage repair that involve VEGF should be avoided.

Sixteen weeks after surgery, the BMP-4–treated groups showed improved healing, both macroscopically and microscopically, compared with the groups that were not treated with BMP-4 (Figure 3B and Table 1). This result supports a previous report by our group (8). In addition, the group treated with BMP-4 plus sFlt-1 showed significantly better histologic scores compared with the group treated with BMP-4 only, which resulted from improved scores in the "cellular morphology," "subchondral bone formation," and "tidemark formation" categories. These scores were affected by the invasion of bone into regions that were cartilaginous 8 weeks after surgery (Figures 3A and B). The improved, but suboptimal, repair of cartilage through the addition of BMP-expressing cells has been suggested in previous reports (37). The inhibition of vascular invasion by sFlt-1 could be a factor that led to improved scores in these categories. Moderate osteophyte formation was observed only in the BMP-4 group. It is possible that endogenous VEGF expression combined with BMP-4 treatment might play a role in the formation of osteophytes as time progresses.

The results of the current study are consistent with those of previous studies demonstrating that VEGF triggers cartilage destruction (18–24). Furthermore, this study suggests that the destruction observed following the implantation of VEGF-expressing cells was caused by extrinsic environmental changes rather than via direct effects on chondrogenic differentiation of the implanted MDSCs. This hypothesis is supported by the observation that the addition of VEGF did not inhibit MDSCs from undergoing chondrogenic differentiation in vitro (Figure 1).

In contrast, sFlt-1 improves BMP-4– and TGFβ3-induced chondrogenic gene expression of MDSCs in vitro and improves the persistence of articular cartilage repair by preventing angiogenesis that can lead to the

invasion of bone into cartilage. However, in this study, no differences were observed between any of the groups in the histologic score for "architecture of surface." This result suggests that growth factors other than BMP or VEGF are needed to fully repair cartilage at the articular surface. In conclusion, sFlt-1 treatment combined with BMP-4 treatment of MDSCs is a potential therapy for cartilage repair that may improve the quality and persistence of articular cartilage repair.

ACKNOWLEDGMENTS

We thank Dr. Ryosuke Kuroda for animal experiment guidance and Mr. David Humiston for editing the manuscript.

AUTHOR CONTRIBUTIONS

Dr. Huard had full access to all of the data in the study and takes responsibility for the integrity of the data and the accuracy of the data analysis.

Study design. Kubo, Cooper, Phillippi, Usas, Li, Fu, Huard.
Acquisition of data. Kubo, Matsumoto, Corsi, Li.
Analysis and interpretation of data. Kubo, Cooper, Matsumoto, Phillippi, Corsi, Usas, Li, Huard.
Manuscript preparation. Kubo, Cooper, Corsi, Usas, Li, Fu, Huard.
Statistical analysis. Kubo, Cooper, Matsumoto, Huard.

REFERENCES

1. Brittberg M, Lindahl A, Nilsson A, Ohlsson C, Isaksson O, Peterson L. Treatment of deep cartilage defects in the knee with autologous chondrocyte transplantation. N Engl J Med 1994;331: 889–95.
2. Ochi M, Uchio Y, Kawasaki K, Wakitani S, Iwasa J. Transplantation of cartilage-like tissue made by tissue engineering in the treatment of cartilage defects of the knee. J Bone Joint Surg Br 2002;84:571–8.
3. Visna P, Pasa L, Cizmar I, Hart R, Hoch J. Treatment of deep cartilage defects of the knee using autologous chondrograft transplantation and by abrasive techniques: a randomized controlled study. Acta Chir Belg 2004;104:709–14.
4. Oshima H, Payne TR, Urish KL, Sakai T, Ling Y, Gharaibeh B, et al. Differential myocardial infarct repair with muscle stem cells compared to myoblasts. Mol Ther 2005;12:1130–41.
5. Qu-Petersen Z, Deasy B, Jankowski R, Ikezawa M, Cummins J, Pruchnic R, et al. Identification of a novel population of muscle stem cells in mice: potential for muscle regeneration. J Cell Biol 2002;157:851–64.
6. Deasy BM, Gharaibeh BM, Pollett JB, Jones MM, Lucas MA, Kanda Y, et al. Long-term self-renewal of postnatal muscle-derived stem cells. Mol Biol Cell 2005;16(7):3323–33.
7. Adachi N, Sato K, Usas A, Fu FH, Ochi M, Han CW, et al. Muscle derived, cell based ex vivo gene therapy for treatment of full thickness articular cartilage defects. J Rheumatol 2002;29: 1920–30.
8. Kuroda R, Usas A, Kubo S, Corsi K, Peng H, Rose T, et al. Cartilage repair using bone morphogenetic protein 4 and muscle-derived stem cells. Arthritis Rheum 2006;54:433–42.
9. Wakitani S, Yamamoto T. Response of the donor and recipient cells in mesenchymal cell transplantation to cartilage defect. Microsc Res Tech 2002;58:14–8.
10. Koga H, Muneta T, Ju YJ, Nagase T, Nimura A, Mochizuki T, et al. Synovial stem cells are regionally specified according to local microenvironments after implantation for cartilage regeneration. Stem Cells 2007;25:689–96.
11. Wakitani S, Goto T, Pineda SJ, Young RG, Mansour JM, Caplan AI, et al. Mesenchymal cell-based repair of large, full-thickness defects of articular cartilage. J Bone Joint Surg Am 1994;76: 579–92.
12. Kuroda R, Ishida K, Matsumoto T, Akisue T, Fujioka H, Mizuno K, et al. Treatment of a full-thickness articular cartilage defect in the femoral condyle of an athlete with autologous bone-marrow stromal cells. Osteoarthritis Cartilage 2007;15:226–31.
13. Wakitani S, Mitsuoka T, Nakamura N, Toritsuka Y, Nakamura Y, Horibe S. Autologous bone marrow stromal cell transplantation for repair of full-thickness articular cartilage defects in human patellae: two case reports. Cell Transplant 2004;13:595–600.
14. Yin M, Pacifici M. Vascular regression is required for mesenchymal condensation and chondrogenesis in the developing limb. Dev Dyn 2001;222:522–33.
15. Gerber HP, Vu TH, Ryan AM, Kowalski J, Werb Z, Ferrara N. VEGF couples hypertrophic cartilage remodeling, ossification and angiogenesis during endochondral bone formation. Nat Med 1999;5:623–8.
16. Carlevaro MF, Cermelli S, Cancedda R, Descalzi Cancedda F. Vascular endothelial growth factor (VEGF) in cartilage neovascularization and chondrocyte differentiation: auto-paracrine role during endochondral bone formation. J Cell Sci 2000;113(Pt 1):59–69.
17. Peng H, Wright V, Usas A, Gearhart B, Shen HC, Cummins J, et al. Synergistic enhancement of bone formation and healing by stem cell-expressed VEGF and bone morphogenetic protein-4. J Clin Invest 2002;110:751–9.
18. Hashimoto S, Ochs RL, Komiya S, Lotz M. Linkage of chondrocyte apoptosis and cartilage degradation in human osteoarthritis. Arthritis Rheum 1998;41:1632–8.
19. Hashimoto S, Creighton-Achermann L, Takahashi K, Amiel D, Coutts RD, Lotz M. Development and regulation of osteophyte formation during experimental osteoarthritis. Osteoarthritis Cartilage 2002;10:180–7.
20. Enomoto H, Inoki I, Komiya K, Shiomi T, Ikeda E, Obata K, et al. Vascular endothelial growth factor isoforms and their receptors are expressed in human osteoarthritic cartilage. Am J Pathol 2003;162:171–81.
21. Tanaka E, Aoyama J, Miyauchi M, Takata T, Hanaoka K, Iwabe T, et al. Vascular endothelial growth factor plays an important autocrine/paracrine role in the progression of osteoarthritis. Histochem Cell Biol 2005;123:275–81.
22. Pufe T, Petersen W, Tillmann B, Mentlein R. The splice variants $VEGF_{121}$ and $VEGF_{189}$ of the angiogenic peptide vascular endothelial growth factor are expressed in osteoarthritic cartilage. Arthritis Rheum 2001;44:1082–8.
23. Pufe T, Harde V, Petersen W, Goldring MB, Tillmann B, Mentlein R. Vascular endothelial growth factor (VEGF) induces matrix metalloproteinase expression in immortalized chondrocytes. J Pathol 2004;202:367–74.
24. Pufe T, Lemke A, Kurz B, Petersen W, Tillmann B, Grodzinsky AJ, et al. Mechanical overload induces VEGF in cartilage discs via hypoxia-inducible factor. Am J Pathol 2004;164:185–92.
25. Murakami M, Iwai S, Hiratsuka S, Yamauchi M, Nakamura K, Iwakura Y, et al. Signaling of vascular endothelial growth factor receptor-1 tyrosine kinase promotes rheumatoid arthritis through activation of monocytes/macrophages. Blood 2006;108:1849–56.
26. Afuwape AO, Kiriakidis S, Paleolog EM. The role of the angiogenic molecule VEGF in the pathogenesis of rheumatoid arthritis. Histol Histopathol 2002;17:961–72.

27. Matsumoto Y, Tanaka K, Hirata G, Hanada M, Matsuda S, Shuto T, et al. Possible involvement of the vascular endothelial growth factor-Flt-1-focal adhesion kinase pathway in chemotaxis and the cell proliferation of osteoclast precursor cells in arthritic joints. J Immunol 2002;168:5824–31.
28. De Bandt M, Ben Mahdi MH, Ollivier V, Grossin M, Dupuis M, Gaudry M, et al. Blockade of vascular endothelial growth factor receptor I (VEGF-RI), but not VEGF-RII, suppresses joint destruction in the K/BxN model of rheumatoid arthritis. J Immunol 2003;171:4853–9.
29. Afuwape AO, Feldmann M, Paleolog EM. Adenoviral delivery of soluble VEGF receptor 1 (sFlt-1) abrogates disease activity in murine collagen-induced arthritis. Gene Ther 2003;10:1950–60.
30. Zelzer E, Mamluk R, Ferrara N, Johnson RS, Schipani E, Olsen BR. VEGFA is necessary for chondrocyte survival during bone development. Development 2004;131:2161–71.
31. Haigh JJ, Gerber HP, Ferrara N, Wagner EF. Conditional inactivation of VEGF-A in areas of collagen2a1 expression results in embryonic lethality in the heterozygous state. Development 2000; 127:1445–53.
32. Peng H, Chen ST, Wergedal JE, Polo JM, Yee JK, Lau KH, et al. Development of an MFG-based retroviral vector system for secretion of high levels of functionally active human BMP4. Mol Ther 2001;4:95–104.
33. Johnstone B, Hering TM, Caplan AI, Goldberg VM, Yoo JU. In vitro chondrogenesis of bone marrow-derived mesenchymal progenitor cells. Exp Cell Res 1998;238:265–72.
34. Jadlowiec J, Koch H, Zhang X, Campbell PG, Seyedain M, Sfeir C. Phosphophoryn regulates the gene expression and differentiation of NIH3T3, MC3T3-E1, and human mesenchymal stem cells via the integrin/MAPK signaling pathway. J Biol Chem 2004;279: 53323–30.
35. Jadlowiec JA, Zhang X, Li J, Campbell PG, Sfeir C. Extracellular matrix-mediated signaling by dentin phosphophoryn involves activation of the Smad pathway independent of bone morphogenetic protein. J Biol Chem 2006;281:5341–7.
36. Sellers RS, Peluso D, Morris EA. The effect of recombinant human bone morphogenetic protein-2 (rhBMP-2) on the healing of full-thickness defects of articular cartilage. J Bone Joint Surg Am 1997;79:1452–63.
37. Gelse K, von der Mark K, Aigner T, Park J, Schneider H. Articular cartilage repair by gene therapy using growth factor–producing mesenchymal cells. Arthritis Rheum 2003;48:430–41.

Cartilage Repair after Osteoarthritis through Intra-articular Injection of Muscle Stem Cells Expressing BMP4 and sFlt1

*#† Matsumoto, T ; *Cooper, GM; *Gharaibeh, B; *Meszaros, L; *Li G; *Usas A; # Fu, FH; * # Huard, J;
* Stem Cell Research Center, Children's Hospital of Pittsburgh of UPMC, Pittsburgh PA. + # Department of Orthopaedic Surgery, University of Pittsburgh, Pittsburgh, PA. + † Department of Orthopaedic Surgery, Kobe University Graduate School of Medicine, Kobe, Japan.
Senior author jhuard@pitt.edu

Introduction:

Osteoarthritis (OA), a chronic degenerative joint disorder worldwide and characterized by articular cartilage destruction and osteophyte formation, affects over 40 million individuals in the United States alone. Stem cells are attractive because of their superior capacity for self renewal, proliferation, and survival post-implantation. Several studies have suggested that stem cells can undergo chondrogenesis and repair articular cartilage in experimental cartilage injury models, including studies using muscle derived stem cells (MDSCs). We have already reported that bone morphogenic protein 4 (BMP4) transduced MDSCs improve cartilage regeneration in the *in vitro* pellet culture and the *in vivo* cartilage defect model [1]. The control of angiogenesis such as using sFlt1, vascular endothelial growth factor (VEGF) antagonist, during the chondrogenic differentiation of stem cells is also an important issue to consider especially for the persistence of the regenerate cartilage.

Based on these backgrounds, the series of experiments is designed to clarify the therapeutic efficacy of BMP4 and sFlt1 transduced MDSCs for the repair of articular cartilage after OA.

Methods:

The animal experiments of this study were approved by the Animal Research and Care Committee at Children's Hospital of Pittsburgh. *Isolation of MDSCs*: MDSCs were isolated from the hind-limb skeletal muscle of 3-week-old male C57-BL10J mice, via a modified preplate technique that has been previously described [2]. *Retroviral transduction*: MDSCs used were retrovirally transduced with green fluorescence protein (GFP), BMP4-GFP, sFlt1-LacZ, or VEGF-LacZ. *Repair of mono-iodoacetic acid (MIA)-induced arthritis*: Transduced MDSCs were injected into the joint capsule 2 weeks after MIA injection (30 nude rats, 60 OA knees). The animals were divided into 5 treatment groups (Table. 1a). *Macroscopic and histological evaluation of cartilage repair*: After macroscopic assessment, we evaluated OA repair semi-quantitatively using a grading and staging system [3]. In this system, there are six histological grades and four histological stages. The total score (score= grade x stage) ranges from 1 point (normal articular cartilage) to 24 points (no repair). *Contribution of transduced MDSCs to cartilage healing*:To histologically assess the contribution of the different types of transduced MDSCs to OA healing in these models, double immunohistochemistry (IHC) for type 2 collagen (Col2) and GFP or β-galactosidase (β-gal) was performed using tissue samples obtained 4 weeks after cell injection. *Chondrocyte apoptosis and proliferation analysis*: To analyze chondrocytes apoptosis and proliferation histologically, TUNEL staining and BrdU incorporation assay was performed using tissue samples obtained 4 weeks after cell infusion (n=6 in each group). *Mixed pellet culture*: To assess the chondrogenic differentiation of MDSCs and their effects on OA chondrocytes, we performed mixed pellet co-culture (Table 1b). Pellets were made in standard chondrogenic medium with 10ng/ml of transforming growth factor-beta3. Pellets were harvested after 14 days in culture and assessed by size, alcian blue staining, quantitative (q) PCR of Col2, Sox9, and Col10, double IHC of Col2 and GFP or β-gal, and fluorescent in situ hybridization (FISH) using mouse Y chromosomes (from the male mouse MDSCs) and rat X chromosomes (from the rat OA chondrocytes).*Separated pellet culture*: To assess the chondrogenesis of OA chondrocytes cultured in the presence of factors released by MDSCs, we performed separated pellet co-culture (Table 1c). Pellets were harvested after 14 days in culture and assessed by size and alcian blue staining.

Results:

Macroscopic and histological evaluation of the joint: *In vivo* testing of articular cartilage regeneration showed macroscpically and histologically that VEGF transduced MDSCs prevented but sFlt1 improved the B4-mediated MDSC regeneration of articular cartilage compared to the B4 alone, as confirmed by histological scores (Fig. 1a). *Contribution of MDSCs in cartilage regeneration and repair*: Double IHC of Col2 and GFP or β-gal demonstrated that VEGF transduced MDSCs prevented but sFlt1 improved chongenic differentiation of MDSC (Fig. 1b) and intrinsic chondrogenesis (Fig. 1c), compared to BMP4 alone. *Chondrocyte apoptosis and proliferation analyses*: TUNEL stain and BrdU assay demonstrated that sFlt1-transduced MDSCs, unlike VEGF expressing cells, lead to less apoptosis and more proliferation compared to B4 alone (Fig. 1d, e). *Mixed pellet culture*: In vitro mixed co-culture showed BMP4 treated group produced significantly larger pellets with hyaline cartilage-like matrix production than all other groups, confirmed by the chondrogenic differentiation capacity of MDSCs using qPCR and qIHC of Col2 and GFP or β-gal. FISH showed no fusion between OA chondrocytes and MDSCs and higher intrinsic chondrogenesis in BMP4 treated group. *Separated pellet culture*: In vitro separated co-culture showed BMP4 treated group produced significantly larger pellets with hyaline cartilage-like matrix production than all other groups.

Table1

a

Group	Cell type	Cell number (cells)
sFlt1/B4-MDSC	sFlt1-MDSC/BMP4-MDSC	$2.5x10^5/2.5x10^5$
VEGF/B4-MDSC	VEGF-MDSC/BMP4-MDSC	$2.5x10^5/2.5x10^5$
B4-MDSC	BMP4-MDSC	$5.0x10^5$
MDSC	MDSCs	$5.0x10^5$
PBS	No cells	0

b

Group	Cell type	Cell number (cells)
sFlt1/B4-MDSC+C	sFlt1-MDSC/BMP4-MDSC +OA chondrocyte	$0.5x10^5/0.5x10^5 + 1.0x10^5$
VEGF/B4-MDSC+C	VEGF-MDSC/BMP4-MDSC+OA chondrocyte	$0.5x10^5/0.5x10^5 + 1.0x10^5$
B4-MDSC+C	BMP4-MDSC+OA chondrocyte	$1.0x10^5 + 1.0x10^5$
MDSC+C	MDSCs+OA chondrocyte	$1.0x10^5 + 1.0x10^5$
C	OA chondrocyte	$2.0x10^5$

c

Group	Cell type (bottom; OA chondrocyte)	Cell number (cells)
sFlt1/B4-MDSC+C	sFlt1-MDSC/BMP4-MDSC +OA chondrocyte	$1.0x10^5/1.0x10^5 + 2.0x10^5$
VEGF/B4-MDSC+C	VEGF-MDSC/BMP4-MDSC+OA chondrocyte	$1.0x10^5/1.0x10^5 + 2.0x10^5$
B4-MDSC+C	BMP4-MDSC+OA chondrocyte	$2.0x10^5 + 2.0x10^5$
MDSC+C	MDSCs+OA chondrocyte	$2.0x10^5 + 2.0x10^5$
C	OA chondrocyte	$2.0x10^5$

Figure 1

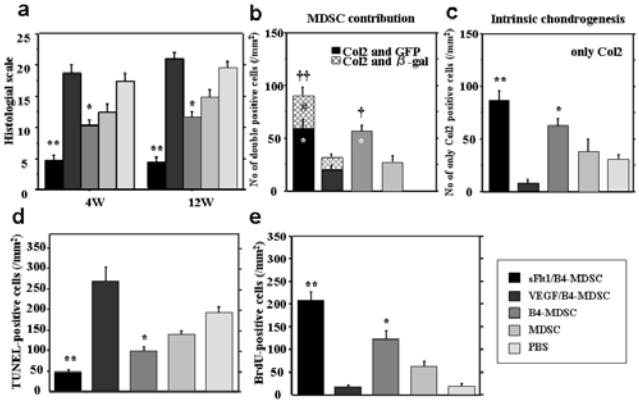

**, ††: p< 0.05 vs the other groups; *, †: p<0.05 vs VEGF/B4-MDSC, MDSC, and PBS groups ; #: p< 0.05 vs VEGF/B4-MDSC group.

Conclusions:

In conclusion, our results suggest that MDSC-based gene/cell therapy involving sFlt1 and BMP4 repaired articular cartilage after OA mainly by having a beneficial effect on chondrogenesis by the donor and host cells as well as by preventing angiogenesis which eventually prevent cartilage resorption, resulting in a persistent cartilage regeneration and repair.

References:

[1] Kuroda R, et al. *Arthritis Rheum.* 2006;54(2):433-42.
[2] Qu Z, et al. *J Cell Biol.* 2002; 27;157(5):851-64.

Appendix 5

ARTHRITIS & RHEUMATISM
Vol. 60, No. 5, May 2009, pp 1390–1405
DOI 10.1002/art.24443

Cartilage Repair in a Rat Model of Osteoarthritis Through Intraarticular Transplantation of Muscle-Derived Stem Cells Expressing Bone Morphogenetic Protein 4 and Soluble Flt-1

Tomoyuki Matsumoto,[1] Gregory M. Cooper,[1] Burhan Gharaibeh,[1] Laura B. Meszaros,[1] Guangheng Li,[2] Arvydas Usas,[2] Freddie H. Fu,[3] and Johnny Huard[1]

Objective. **The control of angiogenesis during chondrogenic differentiation is an important issue affecting the use of stem cells in cartilage repair, especially with regard to the persistence of regenerated cartilage. This study was undertaken to investigate the effect of vascular endothelial growth factor (VEGF) stimulation and the blocking of VEGF with its antagonist, soluble Flt-1 (sFlt-1), on the chondrogenesis of skeletal muscle-derived stem cells (MDSCs) in a rat model of osteoarthritis (OA).**

Methods. **We investigated the effect of VEGF on cartilage repair in an immunodeficiency rat model of OA after intraarticular injection of murine MDSCs expressing bone morphogenetic protein 4 (BMP-4) in combination with MDSCs expressing VEGF or sFlt-1.**

Results. **In vivo, a combination of sFlt-1– and BMP-4–transduced MDSCs demonstrated better repair without osteophyte formation macroscopically and histologically following OA induction, when compared with the other groups. Higher differentiation/proliferation and lower levels of chondrocyte apoptosis were also observed in sFlt-1– and BMP-4–transduced MDSCs compared with a combination of VEGF- and BMP-4–transduced MDSCs or with BMP-4–transduced MDSCs alone. In vitro experiments with mixed pellet coculture of MDSCs and OA chondrocytes revealed that BMP-4–transduced MDSCs produced the largest pellets, which had the highest gene expression of not only type II collagen and SOX9 but also type X collagen, suggesting formation of hypertrophic chondrocytes.**

Conclusion. **Our results demonstrate that MDSC-based therapy involving sFlt-1 and BMP-4 repairs articular cartilage in OA mainly by having a beneficial effect on chondrogenesis by the donor and host cells as well as by preventing angiogenesis, which eventually prevents cartilage resorption, resulting in persistent cartilage regeneration and repair.**

Osteoarthritis (OA), a chronic degenerative joint disorder with worldwide impact, is characterized by articular cartilage destruction and osteophyte formation. OA affects >40 million individuals in the US alone and influences more lives than any other musculoskeletal condition (1). Since articular cartilage is a tissue type that is poorly supplied by blood vessels, nerves, and the lymphatic system, it has a very limited capacity for repair after injury. Although several therapies have been used for OA, no widely accepted treatments have been established, with the exception of arthroplasty. For this reason, tissue engineering techniques aimed at repairing articular cartilage have been extensively studied, and chondrocyte transplantation has already been performed (2–4).

Currently, the most effective treatment for OA, besides arthroplasty, is autologous chondrocyte transplantation. However, this treatment has several limitations, including the need to use neighboring healthy

Supported by the US Department of Defense (contract (W81XWH-08-0076). Dr. Huard's work was supported by the William F. and Jean W. Donaldson Chair at the Children's Hospital of Pittsburgh, and the Henry J. Mankin Endowed Chair for Orthopaedic Research at the University of Pittsburgh.

[1]Tomoyuki Matsumoto, MD, PhD, Gregory M. Cooper, PhD, Burhan Gharaibeh, PhD, Laura B. Meszaros, BS, Johnny Huard, PhD: Children's Hospital of Pittsburgh, and University of Pittsburgh, Pittsburgh, Pennsylvania; [2]Guangheng Li, MD, PhD, Arvydas Usas, MD: Children's Hospital of Pittsburgh, Pittsburgh, Pennsylvania; [3]Freddie H. Fu, MD: University of Pittsburgh, Pittsburgh, Pennsylvania.

Dr. Huard has received consulting fees from Cook Myosite, Inc. (more than $10,000) and receives royalties from Cook Myosite, Inc. for the licensing through the University of Pittsburgh of patented technology for the preplate technique for isolation of muscle-derived stem cells.

Address correspondence and reprint requests to Johnny Huard, PhD, Stem Cell Research Center, Children's Hospital of Pittsburgh, 4100 Rangos Research Center, 3705 Fifth Avenue, Pittsburgh, PA 15213-2582. E-mail: jhuard@pitt.edu.

Submitted for publication September 3, 2008; accepted in revised form January 19, 2009.

donor cartilage, difficulty in treating large-scale defects, limited expansion capacity of primary chondrocytes, and the need for a periosteal patch to maintain engineered cartilage. In addition, in most cases only 30–40% of the defect regenerates articular cartilage, with the remaining defect being filled with fibrocartilage (5,6).

In light of these limitations, it is important to find other sources of cells that are abundant and capable of chondrogenic differentiation. Muscle stem cells are more attractive than primary chondrocytes because of their superior capacity for self-renewal, proliferation, and survival following environmental stress (7–9). Recently, stem cell–based therapies have been used clinically for cartilage repair (10,11). The results of several previous studies, including those using muscle-derived stem cells (MDSCs), have indicated that stem cells can undergo chondrogenesis and repair articular cartilage in experimental cartilage injury models (12–15). We previously demonstrated that bone morphogenetic protein 4 (BMP-4)–transduced MDSCs improved cartilage formation in an in vitro pellet culture and regeneration in an in vivo cartilage defect model (13). Based on those results, the present study was designed to clarify the therapeutic efficacy of BMP-4–transduced MDSCs in OA.

The control of angiogenesis during chondrogenic differentiation is one of the most important issues affecting the application of stem cells for cartilage repair. Among angiogenesis-modulating factors, including antiangiogenic factors such as troponin 1 (16) and chondromodulin 1 (17), vascular endothelial growth factor (VEGF) is an important mediator of angiogenesis (18). VEGF stimulates capillary formation in vivo and exerts direct mitogenic actions on various cells in vitro (19). In the growth plate, VEGF has been reported to play an essential role in cartilage vascularization and absorption of hypertrophic chondrocytes, which together lead to ossification (20,21). Similar to this endochondral ossification, osteophyte formation during OA development has been reported to involve VEGF signaling (22).

Similarly, recent data reveal the expression of VEGF and its receptors (Flt-1 and Flk-1) in OA cartilage and reflect the ability of VEGF to enhance catabolic pathways in chondrocytes by stimulating matrix metalloproteinase (MMP) activity and reducing tissue inhibitors of MMPs (TIMPs) (23–25). These data suggest that, apart from the effect of VEGF on cartilage vascularization and proliferation of cells in the synovial membrane, chondrocyte-derived VEGF promotes catabolic pathways in the cartilage itself, thereby leading to a progressive breakdown of the extracellular matrix (ECM) of articular cartilage.

In the current study, we used a gain- and loss-of-function approach based on tissue engineering techniques to assess the role of VEGF in MDSC-mediated cartilage repair. We demonstrated that genetically modified MDSCs expressing a VEGF antagonist and BMP-4 and transplanted intracapsularly in a rat model of OA enhanced chondrogenesis, repaired cartilage via the autocrine/paracrine effects of BMP-4, and contributed to an appropriate environment that prevented chondrocyte apoptosis by blocking both the intrinsic VEGF catabolic pathway and extrinsic VEGF-induced vascular invasion. This is the first report to describe the effects of VEGF on MDSC-mediated chondrogenesis and OA repair in vitro and in vivo.

MATERIALS AND METHODS

Isolation of MDSCs. MDSCs were isolated from the hind limb skeletal muscle of 3-week-old male C57BL/10J mice (The Jackson Laboratory, Bar Harbor, ME) via a previously described modified preplate technique (7).

Retroviral transduction. Retroviral vectors encoding for green fluorescent protein (GFP), BMP-4 and GFP (BMP-4–GFP), human $VEGF_{165}$ and bacterial nuclear-localized LacZ (VEGF-LacZ), or human soluble Flt-1 (sFlt-1), a VEGF antagonist, and LacZ (sFlt-1–LacZ) expression were generated as previously described (26). Transduction efficiency was ~80% for each retroviral vector. MDSCs were transduced separately with these retroviral vectors at a multiplicity of infection of 5 in the presence of 8 μg/ml of Polybrene. The transduced cells were expanded for 2 weeks before being used in experiments, and the conditioned media were sampled to determine transgene expression. The level of BMP-4 secreted from the transduced cells was estimated with a BMP-4 bioassay, as previously described (27). The levels of VEGF or sFlt-1 secreted by the transduced cells were confirmed by enzyme-linked immunosorbent assay (ELISA) as previously described (28).

Repair of mono-iodoacetate (MIA)–induced arthritis. The animal experiments conducted as a part of this study were approved by the Animal Research and Care Committee at Children's Hospital of Pittsburgh. Sixty 10-week-old female nude rats (NIH-*Whn* NIHRNU-M; Taconic, Germantown, NY) were used. The animals were anesthetized with 3% isoflurane and O_2 gas (1.5 liters/minute) delivered through an inhalation mask. OA-like arthritis was induced by a single intraarticular injection of MIA (Aldrich Chemical, Milwaukee, WI) (0.3 mg per 150 mg body weight) into both knee joints of the rats.

Rats were divided into 2 groups based on OA model (n = 30 rats [60 knees] per group) and further divided into 5 groups based on treatment type (n = 6 rats [12 knees] per group). The 2 models of OA were a chronic disease model in which rats were intraarticularly injected with cells after OA had progressed significantly (2 weeks after MIA injection) and a subacute disease model in which rats were treated with cells before significant OA progression (1 week after MIA injection). Rats in treatment group 1 received 2.5×10^5 sFlt-1–transduced MDSCs combined with 2.5×10^5 BMP-4–transduced MDSCs in phosphate buffered saline (PBS) (sFlt-

1/BMP-4–MDSC group). Group 2 rats were treated with 2.5×10^5 VEGF-transduced MDSCs combined with 2.5×10^5 BMP-4–transduced MDSCs in PBS (VEGF/BMP-4–MDSC group). Group 3 rats were treated with 5.0×10^5 BMP-4–transduced MDSCs in PBS (BMP-4–MDSC group). Group 4 rats were treated with 5×10^5 MDSCs in PBS (MDSC group), and group 5 rats were treated with PBS alone (PBS group). Rats were allowed to move freely within their cages after cell injection. Rats were killed 4 weeks (both chronic OA and subacute OA models), 12 weeks (chronic OA model), or 16 weeks (subacute OA model) after cell transplantation (n = 6 OA knees for each time point).

Tissue harvest. After macroscopic examination, 6 distal femora per group per time point were dissected for histologic and histochemical staining and fixed with 10% neutral buffered formalin for 48 hours, followed by decalcification with 10% EDTA for 2 weeks and paraffin embedding. For immunohistochemical staining, 6 distal femora per group at week 4 were harvested and quickly embedded in OCT compound (Miles, Elkhart, IN), snap-frozen in liquid nitrogen, and stored at −80°C until used.

Histologic evaluation of cartilage repair. Sagittal sections (5 μm thick) were obtained and stained with Safranin O–fast green. We evaluated OA repair semiquantitatively using a grading and staging system (29). This system included 6 histologic grades and 4 histologic stages. The total score (grade multiplied by stage) ranged from 1 point (normal articular cartilage) to 24 points (no repair).

Contribution of transduced MDSCs to cartilage healing. Rat femurs in OCT-embedded blocks were sectioned, and 5-μm serial sections were mounted on silane-coated glass slides and air dried for 1 hour before being fixed with 4.0% paraformaldehyde at 4°C for 5 minutes and stained immediately. To detect transplanted mouse cells in the articular cartilage of the femoral condyle, immunohistochemistry was performed at week 4 (in 6 additional rats in each group) with the following antibodies: rabbit anti–rat type II collagen (Col2) (Sigma, St. Louis, MO) to detect rat and mouse chondrocytes (mouse via cross-reactivity of the antibody with mouse Col2 [13]), Alexa Fluor 488–conjugated rabbit anti-GFP (Molecular Probes, Eugene, OR) for detection of BMP-4 and GFP–transduced MDSCs and GFP-transduced MDSCs, and biotin-conjugated anti–β-galactosidase (anti–β-gal) for detection of sFlt-1 and LacZ–transduced MDSCs and VEGF and LacZ–transduced MDSCs.

GFP or LacZ genes were used to distinguish the contributions of BMP-4–transduced MDSCs from those of nontransduced MDSCs and of sFlt-1–transduced MDSCs from those of VEGF-transduced MDSCs. In addition, due to green autofluorescence in GFP, red fluorescence was applied for LacZ staining to avoid false-positive staining. Double immunohistochemistry with GFP or β-gal and Col2 was performed to detect the contribution of transduced MDSCs to cartilage healing. To assess the contribution of intracapsular-injected MDSCs, the number of double-positive or Col2-positive cells was morphometrically counted as the average value in 5 randomly selected articular cartilage areas in the femoral condyle. The following secondary antibodies were used for each immunostaining: Cy3-conjugated or fluorescein isothiocyanate (FITC)–conjugated anti-rabbit antibody (Molecular Probes) for Col2 staining, and Cy3-conjugated streptavidin (Molecular Probes) for β-gal staining. For nuclear staining, 4′,6-diamidino-2-phenylindole (DAPI) solution was applied for 5 minutes.

Analysis of chondrocyte apoptosis and proliferation. Sagittal paraffin-embedded sections (5 μm thick) were obtained, and the TUNEL assay was performed at week 4 using an Apop Tag Plus Peroxidase In Situ Apoptosis Detection kit according to the recommendations of the manufacturer (Chemicon, Temecula, CA). Briefly, sections were incubated with 15 μg/ml of proteinase K for 15 minutes at room temperature, and then washed in PBS. Endogenous peroxidase was quenched with 3% H_2O_2 for 5 minutes at room temperature. After washing in PBS, sections were immersed in buffer containing terminal deoxynucleotidyl transferase enzyme and incubated for 90 minutes at 37°C in a humid atmosphere. After washing again in PBS, sections were incubated with antidigoxigenin conjugate for 30 minutes at room temperature. After washing in PBS and developing color in peroxidase substrate with diaminobenzidine, signals were examined by microscopy (n = 6 rats from each treatment group).

To measure cell proliferation, immunohistochemistry was performed, using additional animals at week 4, on formalin-fixed, bromodeoxyuridine (BrdU)–incorporated, paraffin-embedded sections, as previously described (20). BrdU was administered intraperitoneally to rats, at 50 mg/kg, 1 and 24 hours before the rats were killed in order to incorporate enough BrdU. After a 20-minute treatment with 0.05% trypsin at 37°C and a 45-minute treatment with 95% formamide in 0.15*M* trisodium citrate at 70°C for denaturing, tissues were stained overnight at 4°C with mouse biotin-conjugated anti-BrdU (Zymed, San Diego, CA) at a dilution of 1:1,000. Signals were then detected using the Vectastain ABC Standard Elite kit (Vector, Burlingame, CA) (n = 6 rats from each treatment group). Labeled nuclei were counted in 5 independent, randomly selected fields.

Isolation of rat OA chondrocytes and normal mouse chondrocytes. Articular cartilage was removed from the femoral condyles of rats 2 weeks after injection of MIA under sterile conditions. The tissue fragments were cut into 1-mm slices and washed 4 times with PBS containing 100 units/ml of penicillin and 100 μg/ml of streptomycin. Slices were cut into small pieces and incubated for 16–24 hours with 1.5 mg/ml of collagenase B (Roche, Mannheim, Germany) and 1 m*M* cysteine in Dulbecco's modified Eagle's medium (DMEM). The cell suspension was filtered through a 20-μm nylon mesh to remove debris and washed 3 times with calcium-free DMEM. The cells were seeded at a density of 100,000 cells/cm^2 overnight at 37°C in a humidified atmosphere containing 5% CO_2 and used for each experiment. Similarly, normal mouse chondrocytes were isolated from mouse articular cartilage and used as controls.

Mixed pellet culture. Pellet culture was performed as described previously (30). Mixed pellet cultures consisted of the following: 1) 0.5×10^5 sFlt-1–transduced MDSCs, 0.5×10^5 BMP-4–transduced MDSCs, and 1.0×10^5 OA chondrocytes (sFlt-1/BMP-4–MDSC plus chondrocytes group), 2) 0.5×10^5 VEGF-transduced MDSCs, 0.5×10^5 BMP-4–transduced MDSCs, and 1.0×10^5 OA chondrocytes (VEGF/BMP-4–MDSC plus chondrocytes group), 3) 1.0×10^5 BMP-4–transduced MDSCs and 1.0×10^5 OA chondrocytes (BMP-4–MDSC plus chondrocytes group), 4) 1.0×10^5 nontransduced MDSCs and 1.0×10^5 OA chondrocytes (MDSC plus chondrocytes group), and 5) 2.0×10^5 OA chondrocytes

(chondrocytes group). Pellets were made in 0.5 ml of chondrogenic medium that contained DMEM supplemented with 1% penicillin/streptomycin, $10^{-7}M$ dexamethasone, 50 μg/ml of ascorbate 2-phosphate, 40 μg/ml of proline, 100 μg/ml of pyruvate, and 1% BD ITS+ (insulin–transferrin–selenium) premix (Becton Dickinson, Franklin Lakes, NJ) with 10 ng/ml of transforming growth factor β3 (R&D Systems, Minneapolis, MN). The pellets were incubated at 37°C in 5% CO_2, and the medium was changed every 2 to 3 days. Pellets were harvested after 14 days in culture.

Separated pellet culture. MDSCs and OA chondrocytes were separated by sterilized culture plate insert (Millicell; Millipore, Bedford, MA). Pellets of OA chondrocytes were made in the medium at the bottom of a 15-ml tube, as previously described (31). The membrane plate was inserted into the 15-ml tube so that the MDSC pellets were placed within the membrane plate. Separated pellets were made with 1) 1.0×10^5 sFlt-1–transduced MDSCs, 1.0×10^5 BMP-4–transduced MDSCs, and 2.0×10^5 OA chondrocytes (sFlt-1/BMP-4–MDSC plus chondrocytes group), 2) 1.0×10^5 VEGF-transduced MDSCs, 1.0×10^5 BMP-4–transduced MDSCs, and 2.0×10^5 OA chondrocytes (VEGF/BMP-4–MDSC plus chondrocytes group), 3) 2.0×10^5 BMP-4–transduced MDSCs and 2.0×10^5 OA chondrocytes (BMP-4–MDSC plus chondrocytes group), 4) 2.0×10^5 nontransduced MDSCs and 2.0×10^5 OA chondrocytes (MDSC plus chondrocytes group), and 5) 2.0×10^5 OA chondrocytes (chondrocytes group). Pellets were made in 0.5 ml of chondrogenic medium. The pellets were incubated at 37°C in 5% CO_2, and the medium was changed every 2–3 days. Pellets were harvested after 14 days in culture.

ELISA assessment of VEGF levels. VEGF levels in the medium were measured 48 hours after pellet culture in both mixed pellet culture and pellet coculture using an ELISA kit according to the recommendations of the manufacturer (R&D Systems) (n = 3 in each group).

Alcian blue staining. Paraffin sections of the pellets were deparaffinized, placed in 3% acetic acid for 3 minutes, and transferred into Alcian blue solution (pH 2.5) for 30 minutes. The slides were rinsed with running tap water for 10 minutes and counterstained with nuclear fast red.

Differentiation of MDSCs into chondrocytes. Pellets in OCT blocks were sectioned and prepared for staining as described above. To detect mouse cells in the pellets, double immunohistochemistry (n = 3) was performed as described above. To assess the contribution of each MDSC, the number of double-positive cells and Col2-positive cells was determined in 5 randomly selected soft tissue fields in the pellets, and the average value was calculated.

Quantitative real-time reverse transcriptase–polymerase chain reaction (PCR) analysis of pellet cultured cells. Messenger RNA was isolated using the RNeasy Plus kit, according to the recommendations of the manufacturer (Qiagen, Valencia, CA). After RNA extraction, quantitative PCR analysis of pellets was carried out as described previously (32). Gene expression levels were calculated based on the ΔC_t method. All target genes were normalized to the housekeeping gene *18S*; *18S* primers and probes were designed by and purchased from Applied Biosystems (Foster City, CA). Primers and probes were designed for Col2, SOX9, and type X collagen (Col10) according to GenBank sequence. All target gene primers and probes were purchased from Integrated DNA Technologies (Coralville, IA). For quantitative PCR assays, the coefficients of variation calculated from triplicate assays were within 3%.

The following primer sequences and probes were used: for mouse Col2, forward AAG-TCA-CTG-AAC-AAC-CAG-ATT-GAG-A, reverse AAG-TGC-GAG-CAG-GGT-TCT-TG, and TaqMan probe ATC-CGC-AGC-CCC-GAC-GGC-T; for mouse SOX9, forward CGG-CTC-CAG-CAA-GAA-CAA-G, reverse TGC-GCC-CAC-ACC-ATG-A, and TaqMan probe ACG-TCA-AGC-GAC-CCA-TGA-ACG-C; and for mouse Col10, forward TAC-TTA-CAC-GGA-TGG-AGA-CCA-TGT-T, reverse ATC-CAG-TTG-ACT-ACT-GGT-GCA-ATT-T, and TaqMan probe AAC-CCT-CTT-TTC-GGA-TTA-ACC-CTG-CGA-GTT.

Fluorescence in situ hybridization (FISH). Slides from frozen sections were fixed with 4% paraformaldehyde, air dried, and then dehydrated in a series of successive concentrations of 70%, 80%, 95%, and 100% ethanol for 3 minutes each. Slides were incubated in pepsin solution for 5 minutes, then washed in 2× sodium chloride–sodium citrate (SSC), and dehydrated. FITC-conjugated mouse Y chromosome probe and rhodamine-conjugated rat X chromosome were mixed with hybridization buffer according to the recommendations of the manufacturer (IDLabs Biotechnology, London, Ontario, Canada) and were applied to the target area on the slide, covered with a coverslip, and sealed with rubber cement. After the cement had dried (~10 minutes at room temperature), the slides and probe were codenatured by placing on a heating block (Fisher, Kalamazoo, MI) set at 68.5°C for 5 minutes followed by hybridization overnight in a prewarmed, opaque humidified chamber at 37°C. On day 2, the rubber cement and coverslips were removed by soaking briefly in 2× SSC solution (pH 7.0) at 45°C. Excess probe was rinsed with 50% formamide–2× SSC for 12 minutes; followed by 20 minutes in 2× SSC at 45°C. Nuclei were counterstained with DAPI.

Statistical analysis. All values are expressed as the mean ± SEM. Paired *t*-tests were performed for comparison of data before and after treatment. The comparisons among the 5 groups were made using one-way analysis of variance. Post hoc analysis was performed using Fisher's protected least significant difference test. Histologic scores were compared using the Kruskal-Wallis test. *P* values less than 0.05 were considered significant.

RESULTS

Macroscopic and histologic findings in the joints. Transduced MDSCs were injected into the joint capsule 2 weeks after MIA injection (n = 30 rats [60 OA knees]). The animals were divided into 5 treatment groups (sFlt-1/BMP-4–MDSC, VEGF/BMP-4–MDSC, BMP-4–MDSC, nontransduced MDSC, and PBS groups). MDSCs used were retrovirally transduced with GFP, BMP-4–GFP, sFlt-1–LacZ, or VEGF-LacZ. There was no gross evidence of any side effects such as infection or tumor formation throughout the observation period.

Four weeks after MDSC transplantation into the OA model (2 weeks of induction), macroscopic evaluation of the sFlt-1/BMP-4–transduced MDSC group re-

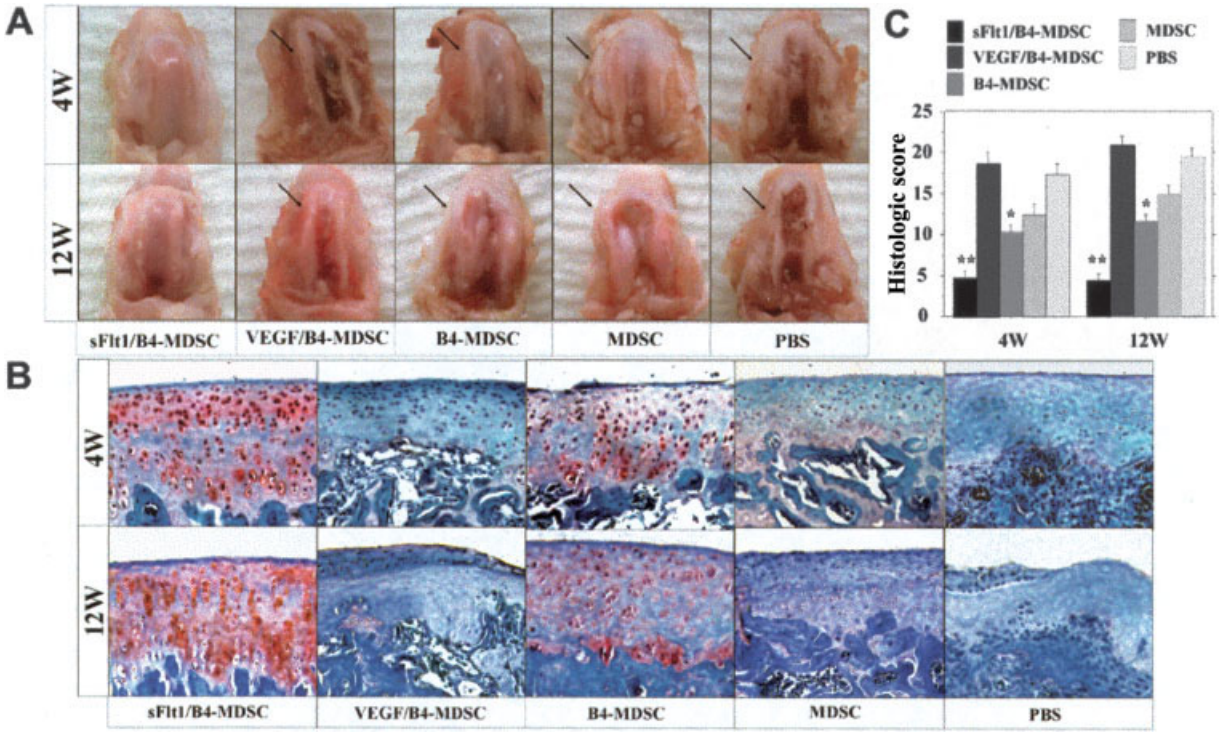

Figure 1. **A** and **B**, Macroscopic (**A**) and histologic (**B**) evaluation of representative joints from rats injected with muscle-derived stem cells (MDSCs) transduced with soluble Flt-1 (sFlt-1) and bone morphogenetic protein 4 (BMP-4 [B4]) (sFlt-1/BMP-4–MDSC), MDSCs transduced with vascular endothelial growth factor (VEGF) and BMP-4 (VEGF/BMP-4–MDSC), MDSCs transduced with BMP-4 alone (BMP-4–MDSC), nontransduced MDSCs (MDSC), or phosphate buffered saline (PBS) alone, 4 and 12 weeks after transplantation. Four weeks after transplantation, the sFlt-1/BMP-4–MDSC and BMP-4–MDSC groups macroscopically and histologically showed smooth joint surface with well-repaired articular cartilage and Safranin O–positive hyaline-like cartilage (red staining in **B**). However, the other groups showed marked arthritic progression, synovial hypertrophy, and osteophyte formation (**arrows**). Twelve weeks after transplantation, although the sFlt-1/BMP-4–MDSC group still showed well-repaired articular cartilage, the other groups exhibited more severe arthritis compared with 4 weeks. (Original magnification × 100.) **C**, Semiquantitative histologic scores for all groups, 4 and 12 weeks following transplantation. The sFlt-1/BMP-4–MDSC group had the lowest (best) scores of all groups. Bars show the mean and SEM. ** = $P < 0.05$ versus all other groups; * = $P < 0.05$ versus the VEGF/BMP-4–MDSC, MDSC, and PBS groups.

vealed smooth joint surfaces of articular cartilage and no osteophyte formation (Figure 1A). Although the BMP-4–transduced MDSC group also showed well-healed articular surfaces, some parts of the joints included osteophyte formation (Figure 1A). However, the VEGF/BMP-4–MDSC, nontransduced MDSC, and PBS groups showed marked arthritis including synovial hypertrophy and osteophyte formation (Figure 1A).

Histologic assessment demonstrated that Safranin O–positive hyaline-like cartilage was present in the sFlt-1/BMP-4–MDSC and BMP-4–MDSC groups only, and the BMP-4—MDSC group had much less Safranin O staining than did the sFlt-1/BMP-4–MDSC group (Figure 1B). However, Safranin O–positive hyaline-like cartilage was less prominent in the nontransduced MDSC group and was completely absent in both the VEGF/BMP-4–MDSC and PBS groups (Figure 1B).

Twelve weeks after transplantation, rat knees treated with sFlt-1/BMP-4–MDSCs still showed smooth joint surfaces in most regions of the articular condyles (Figure 1A). In the BMP-4–MDSC group, although the articular cartilage surfaces tended to be smooth, osteophyte formation was more advanced than at 4 weeks (Figure 1A). The VEGF/BMP-4–MDSC, nontransduced MDSC, and PBS groups showed marked progression of arthritis (Figure 1A). Histologic assessment also demonstrated that more Safranin O–positive tissue and fewer clusters of chondrocytes near necrotic tissue were found in the sFlt-1/BMP-4–MDSC and BMP-4–MDSC groups compared with the other groups (Figure 1B). Destructive events, including pannus invasion, osteolysis, cyst formation within the subchondral bone area, and cartilage tissue lacking Safranin O–positive staining were observed in the VEGF/BMP-4–MDSC and PBS groups (Figure 1B).

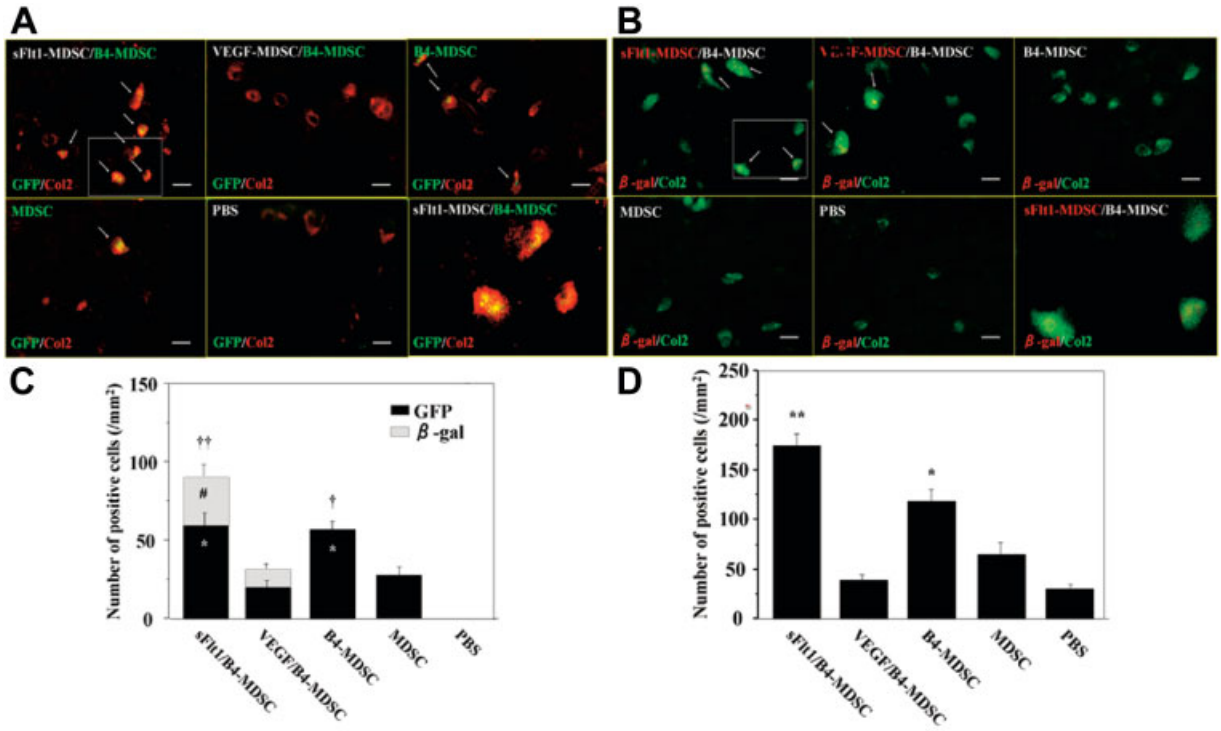

Figure 2. Contribution of MDSCs to cartilage regeneration and repair. **A,** Double immunohistochemical staining for type II collagen (Col2) and green fluorescent protein (GFP). The sFlt-1/BMP-4–MDSC and BMP-4–MDSC groups showed significantly higher levels of chondrogenic differentiation than did the other groups. **B,** Double immunohistochemical staining for Col2 and β-galactosidase (β-gal). The sFlt-1/BMP-4–MDSC group showed higher levels of chondrogenic differentiation than did the VEGF/BMP-4–MDSC group. In **A** and **B,** the last panel shows a higher-magnification view of the boxed area in the first panel. **Arrows** show double-positive cells. Bars = 20 μm. **C,** Numbers of GFP-positive and β-gal–positive cells in each group. The total chondrogenic differentiation of MDSCs was significantly greater in the sFlt-1/BMP-4–MDSC group than in the other groups. Bars show the mean and SEM. ∗ = $P < 0.05$ versus the VEGF/BMP-4–MDSC and MDSC groups; †† = $P < 0.05$ versus all other groups; † = $P < 0.05$ versus the VEGF/BMP-4–MDSC, MDSC, and PBS groups; # = $P < 0.05$ versus the VEGF/BMP-4–MDSC group. **D,** Total number of Col2-positive cells in each group. The sFlt-1/BMP-4–MDSC group had a significantly greater number of chondrocytes than did the other groups. Bars show the mean and SEM. ∗∗ = $P < 0.05$ versus all other groups; ∗ = $P < 0.05$ versus the VEGF/BMP-4–MDSC, MDSC, and PBS groups. See Figure 1 for other definitions.

A previously described histologic grading scale (28) was used to evaluate the quality of the repaired tissue. Four weeks after transplantation, the total score in the sFlt-1/BMP-4–MDSC group was significantly lower than that in all of the other groups. The score in the BMP-4–MDSC group was significantly lower than the scores in the VEGF/BMP-4–MDSC, nontransduced MDSC, and PBS groups (mean ± SEM score 4.7 ± 0.8 in sFlt-1/BMP-4–MDSC, 18.7 ± 1.3 in VEGF/BMP-4–MDSC, 10.0 ± 1.3 in BMP-4–MDSC, 12.3 ± 1.3 in nontransduced MDSC, and 17.3 ± 0.8 in the PBS group) ($P < 0.01$ for sFlt-1/BMP-4–MDSC versus VEGF/BMP-4–MDSC, nontransduced MDSC, and PBS groups, and for BMP-4–MDSC versus VEGF/BMP-4–MDSC and PBS groups; $P < 0.05$ for sFlt-1/BMP-4–MDSC versus BMP-4–MDSC group, and for BMP-4–MDSC versus nontransduced MDSC group) (Figure 1C).

Twelve weeks after transplantation, the total score in the sFlt-1/BMP-4–MDSC group was also significantly lower than that in all other groups. The score in the BMP-4–MDSC group was significantly lower than the scores in the VEGF/BMP-4–MDSC, nontransduced MDSC, and PBS groups (mean ± SEM score 4.3 ± 0.8 in sFlt-1/BMP-4–MDSC, 20.7 ± 1.3 in VEGF/BMP-4–MDSC, 11.5 ± 0.5 in BMP-4–MDSC, 14.7 ± 0.8 in nontransduced MDSC, and 19.3 ± 1.3 in the PBS group) ($P < 0.01$ for sFlt-1/BMP-4–MDSC versus VEGF/BMP-4–MDSC, nontransduced MDSC, and PBS groups, and for BMP-4–MDSC versus VEGF/BMP-4–MDSC and PBS groups; $P < 0.05$ for sFlt-1/BMP-4–MDSC versus BMP-4–MDSC group, and for BMP-4–MDSC versus nontransduced MDSC group) (Figure 1C). Notably, although the scores in the sFlt-1/BMP-4–MDSC group at 12 weeks were similar to the scores at the 4-week time

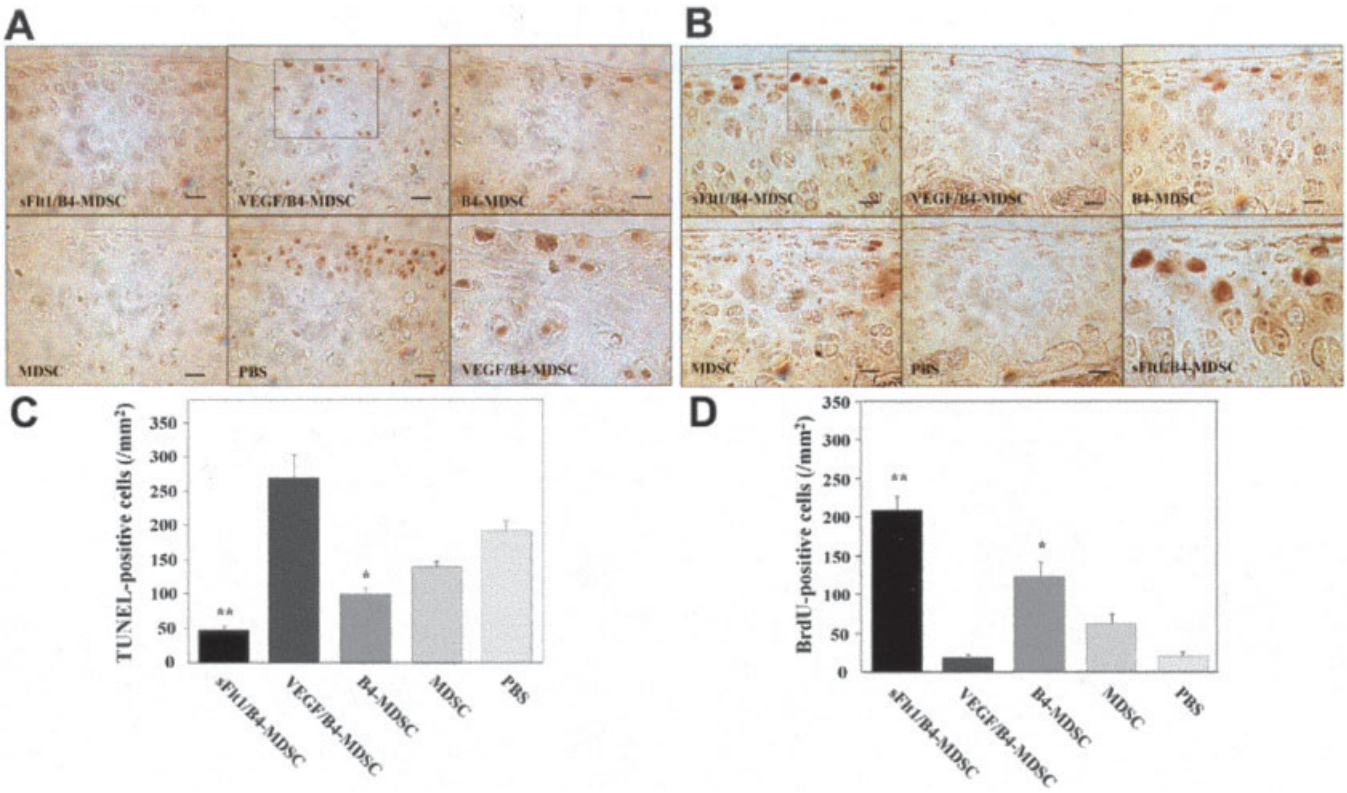

Figure 3. Chondrocyte apoptosis and proliferation. **A,** TUNEL staining in all groups 4 weeks after transplantation. The sFlt-1/BMP-4–MDSC group had significantly fewer apoptotic cells, and the VEGF/BMP-4–MDSC group had a greater number of apoptotic cells, compared with the other groups. **B,** Bromodeoxyuridine (BrdU) assay in all groups 4 weeks after transplantation. The sFlt-1/BMP-4–MDSC group had a significantly greater number of proliferative cells, and the VEGF/BMP-4–MDSC group had fewer proliferative cells, compared with the other groups. In **A** and **B,** the last panel shows a higher-magnification view of the boxed area in the first panel. Bars = 50 μm. **C,** Number of TUNEL-positive cells in each group. **D,** Number of BrdU-positive cells in each group. Bars in **C** and **D** show the mean and SEM. ** = $P < 0.05$ versus all other groups; * = $P < 0.05$ versus the VEGF/BMP-4–MDSC, MDSC, and PBS groups. See Figure 1 for other definitions.

point, all other treatment groups showed variable levels of disease progression.

Contribution of MDSCs to cartilage regeneration and repair. To histologically assess the contribution of the different types of transduced MDSCs to OA healing in these models, double immunohistochemical staining for Col2 and GFP or β-gal was performed using tissue samples obtained 4 weeks after cell injection. Differentiated chondrocytes derived from transduced MDSCs were detected in the superficial and mid-zones of the articular cartilage of the femoral condyle, by double-positive staining for Col2 and either GFP or β-gal, depending on the cell type used. All cells that were transduced to express BMP-4 were also transduced to express GFP. Also, the control MDSCs used for the MDSC group were transduced to express GFP. GFP-positive cells expressing Col2 were found in the femoral condyles in all groups except the PBS control group, which received no GFP-labeled MDSCs (Figure 2A). Cells that were transduced to express VEGF or sFlt-1 were also transduced to express β-gal using the LacZ gene. Within the knee, cells that coexpressed Col2 and β-gal were identified (Figure 2B).

Quantification of the number of cells that were double positive for Col2 and GFP demonstrated that the sFlt-1/BMP-4–MDSC and BMP-4–MDSC groups showed significantly higher numbers of GFP-labeled cells differentiated into Col2-expressing cells (chondrocytes) compared with the VEGF/BMP-4–MDSC and nontransduced MDSC groups (mean ± SEM cells/mm^2 58.7 ± 7.9 in sFlt-1/BMP-4–MDSC, 18.7 ± 4.9 in VEGF/BMP-4–MDSC, 56.0 ± 5.5 in BMP-4–MDSC, and 26.7 ± 5.3 in MDSC) ($P < 0.01$ for sFlt-1/BMP-4–MDSC and BMP-4–MDSC groups versus VEGF/BMP-4–MDSC and nontransduced MDSC groups) (Figure 2C).

Colocalization of Col2 and β-gal demonstrated that the sFlt-1/BMP-4–MDSC group had significantly more β-gal–positive chondrocytes than did the VEGF/BMP-4–MDSC group (mean ± SEM cells/mm^2 29.3 ± 6.4 in sFlt-1/BMP-4–MDSC and 10.7 ± 3.4 in VEGF/

BMP-4–MDSC) ($P < 0.01$) (Figure 2C). Total counts of cells that were double positive for Col2 and either GFP or β-gal indicated that the sFlt-1/BMP-4–MDSC group contained significantly more double-positive cells than did the BMP-4–MDSC, VEGF/BMP-4–MDSC, and nontransduced MDSC groups (mean ± SEM cells/mm^2 88.0 ± 3.6 in sFlt-1/BMP-4–MDSC, 29.3 ± 4.9 in VEGF/BMP-4–MDSC, 56.0 ± 5.5 in BMP-4–MDSC, and 26.7 ± 5.3 in nontransduced MDSC) ($P < 0.01$ for sFlt-1/BMP-4–MDSC versus BMP-4–MDSC, VEGF/BMP-4–MDSC, and MDSC groups, and for BMP-4–MDSC versus VEGF/BMP-4–MDSC and MDSC groups) (Figure 2C).

The total number of Col2-positive cells (chondrocytes from MDSCs and host chondrocytes) was also significantly higher in the sFlt-1/BMP-4–MDSC group than in the other groups (mean ± SEM cells/mm^2 173.3 ± 12.0 in sFlt-1/BMP-4–MDSC, 37.3 ± 3.4 in VEGF/BMP-4–MDSC, 117.3 ± 8.9 in BMP-4–MDSC, 64.0 ± 8.3 in MDSC, and 29.3 ± 2.7 in the PBS group) ($P < 0.01$ for sFlt-1/BMP-4–MDSC versus all other groups; $P < 0.05$ for BMP-4–MDSC versus VEGF/BMP-4–MDSC, MDSC, and PBS groups) (Figure 2D).

Results of chondrocyte apoptosis and proliferation analyses. To analyze chondrocyte apoptosis histologically, TUNEL staining was performed using tissue samples obtained 4 weeks after cell infusion. Chondrocyte apoptosis was less abundant in the superficial and mid-zones of the articular cartilage of the femoral condyle, especially in the sFlt-1/BMP-4–MDSC and BMP-4–MDSC groups compared with the VEGF/BMP-4–MDSC group (Figure 3A). Quantification of TUNEL staining showed that the sFlt-1/BMP-4–MDSC group had significantly fewer apoptotic chondrocytes compared with other treatment groups (mean ± SEM cells/mm^2 46.5 ± 7.1 in sFlt-1/BMP-4–MDSC, 268.5 ± 30.2 in VEGF/BMP-4–MDSC, 99.0 ± 7.3 in BMP-4–MDSC, 138.0 ± 11.3 in MDSC, and 190.5 ± 15.3 in the PBS group) ($P < 0.01$ for sFlt-1/BMP-4–MDSC versus VEGF/BMP-4–MDSC, MDSC, and PBS groups, and for BMP-4–MDSC versus VEGF/BMP-4–MDSC and PBS groups; $P < 0.05$ for sFlt-1/BMP-4–MDSC versus BMP-4–MDSC, and for BMP-4–MDSC versus MDSC) (Figure 3C).

A BrdU incorporation assay was performed on tissue samples from 4-week postoperative animals in order to assess cell proliferation in the knee joint. Proliferating cells were identified primarily in the superficial and mid-zones of the femoral articular cartilage, especially in the sFlt-1/BMP-4–MDSC and BMP-4–MDSC groups (Figure 3B). The number of BrdU-positive chondrocytes was significantly higher in the sFlt-1/BMP-4–MDSC group compared with all other groups (mean ± SEM cells/mm^2 207.0 ± 16.1 in sFlt-1/BMP-4–MDSC, 16.2 ± 3.4 in VEGF/BMP-4–MDSC, 122.4 ± 11.9 in BMP-4–MDSC, 61.2 ± 11.5 in MDSC, and 19.8 ± 1.8 in the PBS group) ($P < 0.01$ for sFlt-1/BMP-4–MDSC versus all other groups, and for BMP-4–MDSC versus VEGF/BMP-4–MDSC and PBS groups; $P < 0.05$ for BMP-4–MDSC versus MDSC) (Figure 3D).

Results of mixed pellet culture. To assess the chondrogenic differentiation of MDSCs and their effects on OA chondrocytes, we performed mixed-cell micromass pellet culture (Figure 4A). ELISA for VEGF levels in the control medium of unmixed pellet culture and in mixed pellet culture showed that VEGF action in MDSCs was blocked by sFlt-1 and significantly enhanced by BMP-4 (mean ± SEM pg/ml per 48 hours 426.7 ± 8.8 in sFlt-1/BMP-4–MDSC plus chondrocytes, 872.0 ± 5.7 in VEGF/BMP-4–MDSC plus chondrocytes, 759.2 ± 15.5 in BMP-4–MDSC plus chondrocytes, 724.9 ± 4.0 in MDSC plus chondrocytes, 270.4 ± 14.8 in chondrocytes alone, 524.9 ± 4.0 in MDSC, 84.3 ± 29.1 in sFlt-1–MDSC, 806.2 ± 7.6 in VEGF-MDSC, and 637.6 ± 19.7 in BMP-4–MDSC) ($P < 0.01$ for all paired comparisons except for BMP-4–MDSC plus chondrocytes versus MDSC plus chondrocytes) (Figure 4B).

Pellets formed using BMP-4–MDSCs and OA chondrocytes were significantly larger than the pellets formed with the other cell types. Also, the pellets formed by mixing cells expressing sFlt-1 were larger than the other mixed-cell combinations, with the exception of the BMP-4–MDSC plus chondrocytes group (mean ± SEM mm 1.40 ± 0.05 in sFlt-1/BMP-4–MDSC plus chondrocytes, 1.13 ± 0.05 in VEGF/BMP-4–MDSC plus chondrocytes, 1.62 ± 0.07 in BMP-4–MDSC plus chondrocytes, 1.22 ± 0.09 in MDSC plus chondrocytes, and 0.93 ± 0.06 in chondrocytes alone) ($P < 0.01$ for BMP-4–MDSC plus chondrocytes versus VEGF/BMP-4–MDSC plus chondrocytes, MDSC plus chondrocytes, and chondrocytes alone, and for sFlt-1/BMP-4–MDSC plus chondrocytes versus chondrocytes alone; $P < 0.05$ for BMP-4–MDSC plus chondrocytes versus sFlt-1/BMP-4–MDSC plus chondrocytes, and for sFlt-1/BMP-4–MDSC plus chondrocytes versus VEGF/BMP-4–MDSC plus chondrocytes and MDSC plus chondrocytes) (Figure 4C).

All of the pellets from every group showed hyaline cartilage–like ECM that stained positively for Alcian blue and contained well-differentiated, round chondrocyte-like cells (Figure 4D). Double immunohistochemical staining for Col2 and either GFP or β-gal showed that chondrocyte-like cells within the pellets

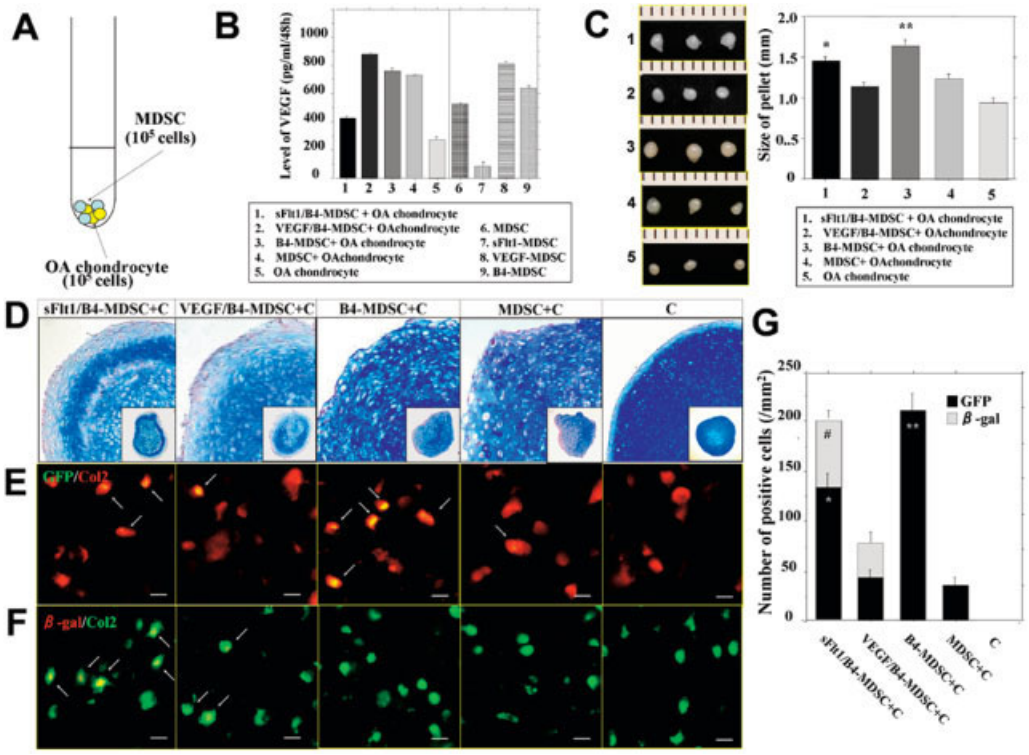

Figure 4. **A,** Mixed pellet coculture of MDSCs and osteoarthritic (OA) chondrocytes. **B,** Levels of VEGF in the medium of mixed pellet coculture in each group. VEGF activity in MDSCs was blocked by sFlt-1 and enhanced by BMP-4. Bars show the mean and SEM. **C,** Size of pellets in mixed pellet coculture in each group. The BMP-4–MDSC plus chondrocytes group formed significantly larger pellets compared with the other groups. Bars show the mean and SEM. $* = P < 0.05$ versus the VEGF/BMP-4–MDSC plus chondrocytes and MDSC plus chondrocytes groups; $** = P < 0.05$ versus all other groups. **D,** Alcian blue staining in each group. C = OA chondrocytes. **E,** Double immunohistochemical staining for type II collagen (Col2) and green fluorescent protein (GFP). The BMP-4–MDSC plus chondrocytes group formed a significantly greater number of chondrocytes than did the sFlt-1/BMP-4–MDSC plus chondrocytes, VEGF/BMP-4–MDSC plus chondrocytes, and MDSC plus chondrocytes groups. **F,** Double immunohistochemical staining for Col2 and β-galactosidase (β-gal). The sFlt-1/BMP-4–MDSC plus chondrocytes group formed a significantly greater number of chondrocytes than did the VEGF/BMP-4–MDSC plus chondrocytes group. **Arrows** show double-positive cells. Bars = 20 μm. **G,** Numbers of GFP-positive and β-gal–positive cells in each group. Bars show the mean and SEM. $** = P < 0.05$ versus all other groups; $*$ and $\# = P < 0.05$ versus the VEGF/BMP-4–MDSC plus chondrocytes and MDSC plus chondrocytes groups. See Figure 1 for other definitions.

were derived from BMP-4/GFP–MDSCs and GFP-MDSCs in the sFlt-1/BMP-4–MDSC plus chondrocytes, VEGF/BMP-4–MDSC plus chondrocytes, BMP-4–MDSC plus chondrocytes, and MDSC plus chondrocytes groups (Figure 4E) and from the sFlt-1/LacZ–MDSCs and VEGF/LacZ–MDSCs in the sFlt-1/BMP-4–MDSC plus chondrocytes and VEGF/BMP-4–MDSC plus chondrocytes groups (Figure 4F).

The number of double-positive cells was significantly higher in the BMP-4–MDSC plus chondrocytes group compared with sFlt-1/BMP-4–MDSC plus chondrocytes, VEGF/BMP-4–MDSC plus chondrocytes, and MDSC plus chondrocytes groups (mean ± SEM 133.3 ± 16.7 in sFlt-1/BMP-4–MDSC plus chondrocytes, 41.7 ± 8.3 in VEGF/BMP-4–MDSC plus chondrocytes, 208.3 ± 16.7 in BMP-4–MDSC plus chondrocytes, 33.3 ± 8.3 in MDSC plus chondrocytes) ($P < 0.01$ for BMP-4–MDSC plus chondrocytes versus all other groups; sFlt-1/BMP-4–MDSC versus VEGF/BMP-4–MDSC and MDSC groups) (Figure 4G).

Double staining for Col2 and β-gal demonstrated that the number of double-positive cells was significantly higher in the sFlt-1/BMP-4–MDSC plus chondrocytes group compared with the VEGF/BMP-4–MDSC plus chondrocytes group (mean ± SEM mm^2 66.7 ± 8.3 in sFlt-1/BMP-4–MDSC plus chondrocytes and 33.3 ± 8.3

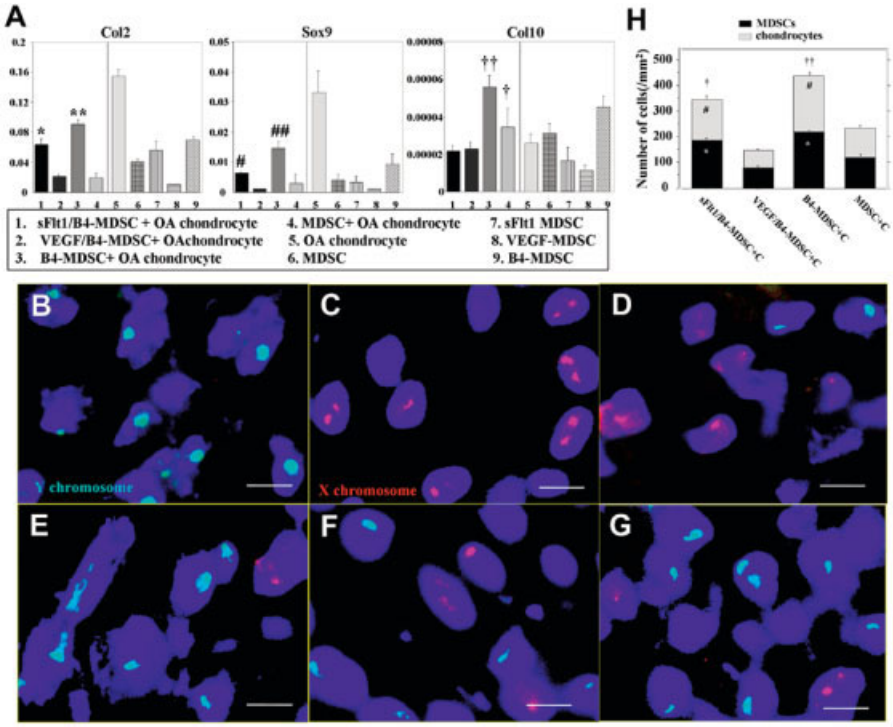

Figure 5. Quantitative polymerase chain reaction (PCR) and fluorescence in situ hybridization (FISH) analysis. **A,** Gene expression of type II collagen (Col2), SOX9, and type X collagen (Col10) in each group, as assessed by quantitative PCR analysis. Pellets from the BMP-4–MDSC plus osteoarthritic (OA) chondrocytes group showed significantly higher gene expression of Col2 and SOX9 than did the other groups; the sFlt-1/BMP-4–MDSC plus chondrocytes group had higher Col2 and SOX9 expression than did the VEGF/BMP-4–MDSC plus chondrocytes and MDSC plus chondrocytes groups. Pellets from the BMP-4–MDSC plus chondrocytes group showed significantly higher gene expression of Col10 than did the other groups; the MDSC plus chondrocytes group had higher Col10 expression than did the sFlt-1/BMP-4–MDSC plus chondrocytes and VEGF/BMP-4–MDSC plus chondrocytes groups. Bars show the mean and SEM. **, ##, and †† = $P < 0.05$ versus all other groups; *, #, and † = $P < 0.05$ versus the sFlt-1/BMP-4–MDSC plus chondrocytes and VEGF/BMP-4–MDSC plus chondrocytes groups. **B–G,** FISH analysis of mixed pellets of normal rat chondrocytes (**B**), mouse MDSCs (**C**), sFlt-1/BMP-4–MDSC plus chondrocytes (**D**), VEGF/BMP-4–MDSC plus chondrocytes (**E**), BMP-4–MDSC plus chondrocytes (**F**), and MDSC plus chondrocytes (**G**), demonstrating that chondrogenic differentiation of mouse MDSCs did not occur through cell fusion (complex of rat X chromosome [red] and mouse Y chromosome [green]). Bars = 20 μm. **H,** Quantification of chondrocytes derived from mouse MDSCs and of rat chondrocytes in each group. The sFlt-1/BMP-4–MDSC plus chondrocytes (C) and BMP-4–MDSC plus chondrocytes groups formed significantly more rat chondrocytes and mouse MDSC–derived chondrocytes than did the other groups. The total number of chondrocytes was significantly higher in the BMP-4–MDSC plus chondrocytes group. Bars show the mean and SEM. * and # = $P < 0.05$ versus the VEGF/BMP-4–MDSC plus chondrocytes and MDSC plus chondrocytes groups; †† = $P < 0.05$ versus all other groups; †= $P < 0.05$ versus the VEGF/BMP-4–MDSC plus chondrocytes and MDSC plus chondrocytes groups. See Figure 1 for other definitions.

in VEGF/BMP-4–MDSC plus chondrocytes) ($P < 0.05$) (Figure 4G).

Quantitative PCR and FISH. Quantitative PCR analysis demonstrated that pellets from the BMP-4–MDSC plus chondrocytes group showed significantly higher gene expression of Col2 than did the sFlt-1/BMP-4–MDSC plus chondrocytes, VEGF/BMP-4–MDSC plus chondrocytes, and MDSC plus chondrocytes groups; Col2 gene expression in the sFlt-1/BMP-4–MDSC plus chondrocytes group was higher than that in the VEGF/BMP-4–MDSC plus chondrocytes and MDSC plus chondrocytes groups (mean ± SEM 0.063 ±

0.0087 in sFlt-1/BMP-4–MDSC plus chondrocytes, 0.022 ± 0.0018 in VEGF/BMP-4–MDSC plus chondrocytes, 0.091 ± 0.0058 in BMP-4–MDSC plus chondrocytes, 0.020 ± 0.0051 in MDSC plus chondrocytes, 0.154 ± 0.0090 in chondrocytes alone, 0.041 ± 0.0020 in MDSC, 0.057 ± 0.012 in sFlt-1–MDSC, 0.011 ± 0.00030 in VEGF-MDSC, and 0.069 ± 0.0043 in BMP-4–MDSC) ($P < 0.01$ for BMP-4–MDSC plus chondrocytes versus sFlt-1/BMP-4–MDSC plus chondrocytes, VEGF/BMP-4–MDSC plus chondrocytes, and MDSC plus chondrocytes, and for sFlt-1/BMP-4–MDSC plus chondrocytes versus VEGF/BMP-4–MDSC plus chondrocytes and MDSC plus chondrocytes) (Figure 5A).

Pellets from the BMP-4–MDSC plus chondrocytes group showed significantly higher gene expression of SOX9 than did those from the sFlt-1/BMP-4–MDSC plus chondrocytes, VEGF/BMP-4–MDSC plus chondrocytes, and MDSC plus chondrocytes groups; SOX9 gene expression was higher in the sFlt-1/BMP-4–MDSC plus chondrocytes group than in the VEGF/BMP-4–MDSC plus chondrocytes and MDSC plus chondrocytes groups (mean ± SEM 0.0064 ± 0.00044 in sFlt-1/BMP-4–MDSC plus chondrocytes, 0.0010 ± 0.00019 in VEGF/BMP-4–MDSC plus chondrocytes, 0.015 ± 0.0021 in BMP-4–MDSC plus chondrocytes, 0.0031 ± 0.0030 in MDSC plus chondrocytes, 0.033 ± 0.0070 in chondrocytes alone, 0.0043 ± 0.0018 in MDSC, 0.0033 ± 0.0021 in sFlt-1–MDSC, 0.0011 ± 0.00014 in VEGF-MDSC, and 0.0092 ± 0.0034 in BMP-4–MDSC) ($P < 0.01$ for BMP-4–MDSC plus chondrocytes versus sFlt-1/BMP-4–MDSC plus chondrocytes, VEGF/BMP-4–MDSC plus chondrocytes, and MDSC plus chondrocytes; $P < 0.01$ for sFlt-1/BMP-4–MDSC plus chondrocytes versus VEGF/BMP-4–MDSC plus chondrocytes and MDSC plus chondrocytes) (Figure 5A).

Additionally, pellets from the BMP-4–MDSC plus chondrocytes group showed significantly higher gene expression of Col10 than did those from the other groups; Col10 gene expression was higher in the MDSC plus chondrocytes group than in the sFlt-1/BMP-4–MDSC plus chondrocytes and VEGF/BMP-4–MDSC plus chondrocytes groups (mean ± SEM 0.000022 ± 0.0000031 in sFlt-1/BMP-4–MDSC plus chondrocytes, 0.000023 ± 0.0000036 in VEGF/BMP-4–MDSC plus chondrocytes, 0.000056 ± 0.0000056 in BMP-4–MDSC plus chondrocytes, 0.000034 ± 0.000011 in MDSC plus chondrocytes, 0.000026 ± 0.0000072 in chondrocytes alone, 0.000031 ± 0.0000049 in MDSC, 0.000016 ± 0.0000072 in sFlt-1–MDSC, 0.000012 ± 0.0000022 in VEGF-MDSC, and 0.000045 ± 0.0000057 in BMP-4–MDSC) ($P < 0.01$ for BMP-4–MDSC plus chondrocytes versus sFlt-1/BMP-4–MDSC plus chondrocytes, VEGF/BMP-4–MDSC plus chondrocytes, and MDSC plus chondrocytes, and for MDSC plus chondrocytes versus sFlt-1/BMP-4–MDSC plus chondrocytes and VEGF/BMP-4–MDSC plus chondrocytes) (Figure 5A).

To determine whether the chondrogenic differentiation of MDSCs occurred through fusion of MDSCs with chondrocytes or through direct differentiation of the MDSCs, we performed FISH with mouse Y chromosomes (from male mouse MDSCs) and rat X chromosomes (from rat OA chondrocytes). The specificity of the probes was tested in pellets of normal rat chondrocytes (Figure 5B) and mouse MDSCs (Figure 5C). The FISH analysis revealed no nuclei in which the mouse Y chromosome colocalized with the rat X chromosome (Figures 5D–G), suggesting that cellular fusion between MDSCs and OA chondrocytes was unlikely in this experiment (Figures 5D–G).

The FISH analysis also demonstrated that the number of MDSCs was significantly higher in the sFlt-1/BMP-4–MDSC plus chondrocytes (Figure 5D) and BMP-4–MDSC plus chondrocytes groups (Figure 5F) than in the VEGF/BMP-4–MDSC plus chondrocytes (Figure 5E) and MDSC plus chondrocytes groups (Figure 5G) (mean ± SEM number/mm^2 182.7 ± 6.8 in sFlt-1/BMP-4–MDSC plus chondrocytes, 78.7 ± 8.7 in VEGF/BMP-4–MDSC plus chondrocytes, 217.3 ± 9.0 in BMP-4–MDSC plus chondrocytes, and 118.0 ± 7.6 in MDSC plus chondrocytes) ($P < 0.01$ for BMP-4–MDSC plus chondrocytes versus all other groups and for sFlt-1/BMP-4–MDSC plus chondrocytes versus VEGF/BMP-4–MDSC plus chondrocytes and MDSC plus chondrocytes groups) (Figure 5H).

Notably, the number of rat chondrocytes was also significantly higher in the sFlt-1/BMP-4–MDSC plus chondrocytes and BMP-4–MDSC plus chondrocytes groups than in the VEGF/BMP-4–MDSC plus chondrocytes and MDSC plus chondrocytes groups (mean ± SEM number/mm^2 158.7 ± 16.7 in sFlt-1/BMP-4–MDSC plus chondrocytes, 66.0 ± 4.2 in VEGF/BMP-4–MDSC plus chondrocytes, 218.0 ± 12.1 in BMP-4–MDSC plus chondrocytes, and 115.3 ± 5.9 in MDSC plus chondrocytes) ($P < 0.01$ for BMP-4–MDSC plus chondrocytes versus all other groups, and for sFlt-1/BMP-4–MDSC plus chondrocytes versus VEGF/BMP-4–MDSC plus chondrocytes and MDSC plus chondrocytes groups) (Figure 5H).

The total number of rat chondrocytes and MDSCs was significantly higher in the BMP-4–MDSC plus chondrocytes group than in all other groups (mean ± SEM number/mm^2 341.3 ± 23.5 in sFlt-1/BMP-4–MDSC plus chondrocytes, 144.7 ± 4.7 in VEGF/BMP-4–MDSC plus chondrocytes, 435.3 ± 19.8

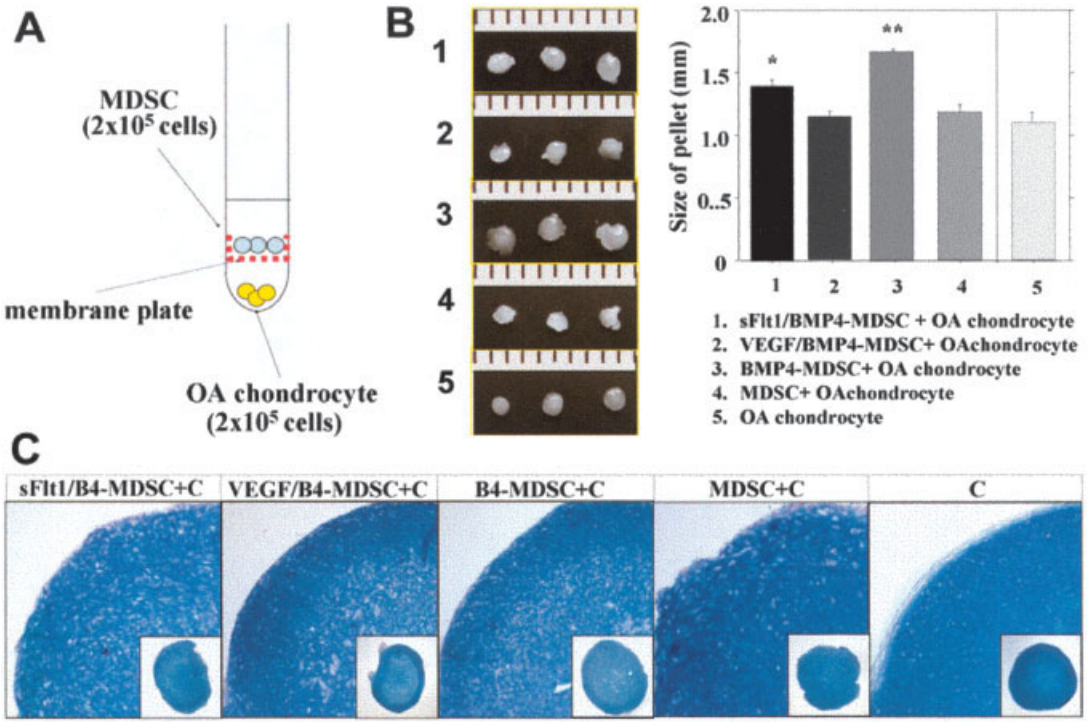

Figure 6. A, Separated pellet coculture of MDSCs and osteoarthritic (OA) chondrocytes. **B,** Size of pellets in each group. OA chondrocytes in the BMP-4–MDSC plus chondrocytes group formed significantly larger pellets compared with the other groups. Bars show the mean and SEM. ** = $P < 0.05$ versus all other groups; * = $P < 0.05$ versus the VEGF/BMP-4–MDSC plus chondrocytes, MDSC plus chondrocytes, and chondrocytes alone groups. **C,** Alcian blue staining in each group. C = OA chrondrocytes (see Figure 1 for other definitions).

in BMP-4–MDSC plus chondrocytes, and 233.3 ± 10.3 in MDSC plus chondrocytes) ($P < 0.01$ for BMP-4–MDSC plus chondrocytes versus all other groups and for sFlt-1/BMP-4–MDSC plus chondrocytes versus VEGF/BMP-4–MDSC plus chondrocytes and MDSC plus chondrocytes groups) (Figure 5H).

Results of separated pellet culture. To assess the chondrogenesis of OA chondrocytes cultured in the presence of factors released by MDSCs, we performed micromass pellet coculture (Figure 6A). Pellet size analysis showed that OA chondrocytes cocultured with BMP-4–MDSCs formed significantly larger pellets compared with all other groups (mean ± SEM mm 1.39 ± 0.04 in sFlt-1/BMP-4–MDSC plus chondrocytes, 1.12 ± 0.07 in VEGF/BMP-4–MDSC plus chondrocytes, 1.65 ± 0.04 in BMP-4–MDSC plus chondrocytes, 1.16 ± 0.03 in MDSC plus chondrocytes, and 1.09 ± 0.07 in chondrocytes alone) ($P < 0.01$ for BMP-4–MDSC plus chondrocytes versus all other groups, and for sFlt-1/BMP-4–MDSC plus chondrocytes versus VEGF/BMP-4–MDSC plus chondrocytes, MDSC plus chondrocytes, and chondrocytes alone) (Figure 6B). All of the pellets from every group showed hyaline cartilage–like ECM that stained positively for Alcian blue and contained well-differentiated, round chondrocytic cells (Figure 6C).

DISCUSSION

Researchers use different rat models of OA to confirm the effectiveness of different treatments. OA-like arthritis is primarily induced by surgical procedures or chemical adjuvants, such as MIA (32–36). Surgically induced OA models may be more clinically relevant than chemically induced models with regard to the pathophysiology of OA. However, there are several drawbacks to surgically induced OA models, including the need for surgical manipulation to induce OA and the difficulty in achieving reproducible levels of severity of arthritis. Therefore, we used an MIA-induced OA model and confirmed the reproducibility of the grade and stage of OA in immunodeficient rats, which was consistent with previous reports of OA in other rat strains (32–34) (Additional information is available upon request from the corresponding author.)

Our in vivo macroscopic and histologic evaluations showed that sFlt-1/BMP-4–transduced MDSCs

had the greatest potential for cartilage repair in the chemically induced OA model. In contrast, the mixture of BMP-4–expressing cells and VEGF-expressing cells led to marked arthritis progression, including synovial hypertrophy, pannus invasion, and osteophyte formation (Figure 1). In a previous study, we found that BMP-4–transduced MDSCs had a higher potential for cartilage regeneration and repair than did nontransduced MDSCs in an osteochondral defect model in the nude rat (13). In the gain- and loss-of-function experiments conducted in the present study, we demonstrated that sFlt-1 improved, and VEGF delayed, cartilage repair with BMP-4–transduced MDSCs in the chemically induced OA model.

Interestingly, in the model of subacute OA the regenerative effects in the sFlt-1/BMP-4–MDSC group were observed up to 16 weeks. (Results in the subacute group are available upon request from the corresponding author.) This same treatment was less effective at the same time in the model in which OA was induced for 2 weeks (chronic OA model). These findings suggest that, to obtain long-term beneficial results, a combined treatment consisting of sFlt-1 (antiangiogenic factor) and BMP-4 with MDSCs is more beneficial in subacute OA than in chronic OA.

In the present study, even when transplanted within the joint space (intraarticularly), MDSCs were found to undergo chondrogenic differentiation, as evidenced by double-positive staining for the GFP or β-gal transgenes and the chondrocyte marker Col2. This showed that both chondrogenic differentiation of transduced MDSCs and intrinsic chondrogenesis were most frequently found in the sFlt-1/BMP-4–treated group, although similar results were found in the BMP-4–transduced MDSC group (Figure 2). In a previous study, we demonstrated that BMP-4 secretion by transduced MDSCs influences the differentiation of multipotent MDSCs toward the chondrogenic lineage in vitro and in vivo (13). Additionally, the present study showed that sFlt-1 improved, while VEGF inhibited, the chondrogenic differentiation of these BMP-4–transduced MDSCs in an OA model.

Furthermore, the intrinsic chondrogenic potential of BMP-4–transduced MDSCs was found to be higher than that of nontransduced MDSCs both in vitro and in vivo. In this study, sFlt-1 enhanced the chondrogenic potential of BMP-4–expressing cells, while VEGF reduced this potential (Figure 2). We reason that the in vivo results that were observed were due to an improvement in chondrogenic differentiation of both the host OA chondrocytes and the implanted MDSCs through the activity of BMP-4, and due to the prevention of vascularization and bone invasion into the regenerated cartilage tissue through the activity of sFlt-1 (23,25).

To attempt to better delineate the mechanism behind the beneficial effects of sFlt-1 and BMP-4 treatment, we performed apoptosis and proliferation assays in vivo (Figure 3). TUNEL assay (apoptosis) results suggested that VEGF induced higher levels of chondrocyte apoptosis and reduced levels of cellular proliferation in the OA knee. In contrast, sFlt-1–treated OA knees showed the lowest level of chondrocyte apoptosis and the highest level of cell proliferation. There are 2 plausible mechanisms by which VEGF may affect cartilage degeneration in OA. VEGF may directly increase catabolic pathways in cartilage tissue through the stimulation of MMP activity and the reduction of TIMPs (23,25). Additionally, VEGF may indirectly cause cartilage destruction by enhancing angiogenesis and vascular invasion, leading to replacement of cartilage by bone. Although the in vivo results presented here support the assertion that VEGF is detrimental to cartilage, we decided to examine whether VEGF worked directly or indirectly on the OA-derived chondrocytes.

In an attempt to establish conditions similar to those in the in vivo experiment, we used in vitro mixed and separated coculture systems to investigate the interaction between transduced MDSCs and OA-derived chondrocytes. The mixed-cell pellet culture showed that, although sFlt-1–transduced and VEGF-transduced MDSCs themselves did not alter chondrogenic potential in an autocrine manner, secreted sFlt-1 enhanced, and VEGF prevented, the chondrogenic differentiation of BMP-4–transduced MDSCs in a paracrine manner. However, BMP-4–transduced MDSCs formed the largest pellets and showed the highest rate of differentiation into chondrocytes (Figure 4). These results indicate that blocking and enhancing VEGF may partially affect the chondrogenic differentiation of BMP-4–transduced MDSCs in vitro, but that BMP-4 itself plays an important role in enhancing the chondrogenic differentiation of MDSCs in an autocrine/paracrine manner, as previously described by our group (13).

In addition, quantitative PCR analysis demonstrated that BMP-4–transduced MDSCs (double dose compared with sFlt-1/BMP-4–MDSCs and VEGF/BMP-4–MDSCs) showed higher gene expression not only of Col2 and SOX9 but also of Col10 (Figure 5A), suggesting that the higher dose of BMP-4 caused differentiation toward hypertrophic chondrocytes. These findings may indicate that a high dose of BMP-4 leads to overproliferation of chondrocytes. In this assay, however, ELISA showed up-regulated VEGF secretion of MDSCs by BMP-4 (Figure 4).

In another previous study, we showed that the beneficial effect of VEGF on bone healing elicited by BMP-4 depended critically on the ratio of VEGF to BMP-4, with an improper ratio leading to detrimental effects on bone healing (26). These findings may indicate that VEGF in moderate concentrations, as opposed to overexpression, maintains chondrocyte survival and control cell differentiation and proliferation in vitro, as previously described (20,37–39). The results of the mixed pellet coculture system indicate that sFlt-1 and BMP-4–expressing MDSCs offer the best balanced combination therapy, despite the fact that the largest pellets in BMP-4–expressing MDSCs also contained the highest gene expression of Col10 (Figures 4 and 5A).

We also tested the separated cell coculture system to investigate the intrinsic effects of sFlt-1, VEGF, and BMP-4 secreted from transduced MDSCs on OA chondrocytes. The results suggest that BMP-4 secreted by MDSCs produced the largest pellets, whereas sFlt-1 enhanced, and VEGF inhibited, the chondrogenic potential of OA chondrocytes to various degrees (Figure 6). These results suggest that BMP-4 mainly affects the redifferentiation or proliferation of OA chondrocytes in vitro. These in vitro mixed and separated pellet coculture experiments suggest the following mechanism: BMP-transduced MDSCs act through an autocrine/paracrine system by releasing BMP-4 that affects the MDSCs themselves, nearby MDSCs, and nearby OA chondrocytes, up-regulating chondrogenesis in vitro. In contrast, VEGF and sFlt-1 secreted by MDSCs have little effect on the chondrogenic differentiation of MDSCs themselves. However, both VEGF and sFlt-1 have some effects on the chondrogenic differentiation of BMP-4–transduced MDSCs and nearby OA chondrocytes.

Stem cells have been reported to undergo multilineage differentiation, but this capacity has recently been a subject of controversy because of possible fusion of stem cells with target-differentiated/lineage-committed cells in the target tissue (39,40). Following these first reports, many researchers reported differentiation of stem cells through fusion with target mature cells, such as hepatocytes with hematopoietic stem cells (41,42), cardiomyocytes with hematopoietic/endothelial progenitor cells (43,44), and neural cells with neural stem cells (45,46). Whether MDSCs undergo chondrogenic differentiation through fusion needed to be addressed.

In addition to characterizing the autocrine/paracrine effect of MDSCs, the present study investigated whether fusion of MDSCs and OA chondrocytes occurred during chondrogenic differentiation. FISH analysis using mixed-cell pellet culture of MDSCs and OA chondrocytes demonstrated no chondrocytes in which the mouse Y chromosome (from the MDSCs) was colocalized with rat X chromosome (from rat OA chondrocytes) (Figures 5B–G), suggesting that there was a lack of fusion between the 2 different cell types. These findings suggest that MDSCs adopted the chondrocyte-like phenotype through potential differentiation without fusion with previously existing chondrocytes. However, the Y chromosome probe is not 100% efficient. This inefficiency may have resulted in an underestimation of the numbers of mouse cells and the possibility that some cell fusion events may have occurred, but were not detected.

In addition, FISH analysis demonstrated the contribution of mouse MDSCs and rat OA chondrocytes. Quantification of the nuclei from cells surrounded by Alcian blue–positive tissue (Figure 4) demonstrated that the total contribution of MDSCs and OA chondrocytes was significantly greater in the BMP-4–MDSC group than in the sFlt-1/BMP-4–MDSC group, consistent with the larger pellet size in the groups that included BMP-4–expressing cells. Taken together, these findings indicate that sFlt-1 may enhance, and VEGF may inhibit, the chondrogenic differentiation of BMP-4–transduced MDSCs and the proliferation of OA chondrocytes; however, these effects are significantly lower than the potential of BMP-4–transduced MDSCs in vitro.

The results of this study support the published data that suggest that VEGF triggers cartilage destruction (23,25,47,48), since we observed that the addition of VEGF inhibited cartilage repair and regeneration or accelerated degeneration in the in vivo OA model. Also, the best histologically assessed regeneration of cartilage in vivo was found in knees treated with both MDSCs expressing BMP-4 and MDSCs expressing sFlt-1, when VEGF signaling was blocked. However, our in vitro results from mixed and separated cell pellet cultures, which were designed to simulate the in vivo situation, showed that the BMP-4–MDSC group had the greatest chondrogenic potential, rather than the sFlt-1/BMP-4–MDSC group. These results suggest that sFlt-1 has more of an enhancing effect in vivo.

With cell markers and flow cytometry, investigators at our laboratory have recently identified and purified a distinct cell population that is developmentally and anatomically related to blood vessels or blood vessel walls within human tissue (49,50). The myoendothelial cells are found in skeletal muscle and coexpress markers of endothelial and myogenic cells (CD34 and CD56) (50). The pericytes are found in multiple human organs including skeletal muscle, pancreas, adipose tis-

sue, and placenta and are isolated based on CD146, nerve/glial antigen 2, and platelet-derived growth factor receptor β expression and absence of hematopoietic, endothelial, and myogenic cell markers (49). These cell populations exhibit multilineage differentiation potential and can, in culture and in vivo, differentiate into myogenic, osteogenic, chondrogenic, and adipogenic cells. In the near future, based on the present findings, we should confirm the potential of this human cell population for cartilage healing and repair in OA.

In conclusion, sFlt-1/BMP-4–transduced MDSCs, VEGF-blocking treatment, which were transplanted intraarticularly in a rat model of OA, enhanced chondrogenesis and chondrogenic regeneration via the autocrine/paracrine effects of BMP-4, and contributed to an appropriate environment that prevented chondrocyte apoptosis by blocking the intrinsic VEGF catabolic pathway and extrinsic VEGF-induced vascular invasion. Blocking VEGF, combined with BMP-4 treatment, of MDSCs is a potentially effective therapy for OA repair that may improve the quality and persistence of regenerated articular cartilage.

ACKNOWLEDGMENTS

The authors are grateful to Jessica Tebbets and Michele Keller for excellent technical help.

AUTHOR CONTRIBUTIONS

Dr. Huard had full access to all of the data in the study and takes responsibility for the integrity of the data and the accuracy of the data analysis.

Study design. Matsumoto, Cooper, Li, Huard.
Acquisition of data. Matsumoto, Gharaibeh, Li, Usas.
Analysis and interpretation of data. Cooper, Gharaibeh, Meszaros, Li, Usas, Fu, Huard.
Manuscript preparation. Matsumoto, Cooper, Gharaibeh, Meszaros, Li, Usas, Fu, Huard.
Statistical analysis. Cooper, Meszaros.
Study oversight and direction. Fu, Huard.

REFERENCES

1. Buckwalter JA, Stanish WD, Rosier RN, Schenck RC Jr, Dennis DA, Coutts RD. The increasing need for nonoperative treatment of patients with osteoarthritis. Clin Orthop Relat Res 2001:36–45.
2. Brittberg M, Lindahl A, Nilsson A, Ohlsson C, Isaksson O, Peterson L. Treatment of deep cartilage defects in the knee with autologous chondrocyte transplantation. N Engl J Med 1994;331: 889–95.
3. Ochi M, Uchio Y, Kawasaki K, Wakitani S, Iwasa J. Transplantation of cartilage-like tissue made by tissue engineering in the treatment of cartilage defects of the knee. J Bone Joint Surg Br 2002;84:571–8.
4. Visna P, Pasa L, Cizmar I, Hart R, Hoch J. Treatment of deep cartilage defects of the knee using autologous chondrograft transplantation and by abrasive techniques—a randomized controlled study. Acta Chir Belg 2004;104:709–14.
5. O'Driscoll SW. The healing and regeneration of articular cartilage. J Bone Joint Surg Am 1998;80:1795–812.
6. Bentley G, Biant LC, Carrington RW, Akmal M, Goldberg A, Williams AM, et al. A prospective, randomised comparison of autologous chondrocyte implantation versus mosaicplasty for osteochondral defects in the knee. J Bone Joint Surg Br 2003;85: 223–30.
7. Qu-Petersen Z, Deasy B, Jankowski R, Ikezawa M, Cummins J, Pruchnic R, et al. Identification of a novel population of muscle stem cells in mice: potential for muscle regeneration. J Cell Biol 2002;157:851–64.
8. Deasy BM, Gharaibeh BM, Pollett JB, Jones MM, Lucas MA, Kanda Y, et al. Long-term self-renewal of postnatal muscle-derived stem cells. Mol Biol Cell 2005;16:3323–33.
9. Oshima H, Payne TR, Urish KL, Sakai T, Ling Y, Gharaibeh B, et al. Differential myocardial infarct repair with muscle stem cells compared to myoblasts. Mol Ther 2005;12:1130–41.
10. Wakitani S, Mitsuoka T, Nakamura N, Toritsuka Y, Nakamura Y, Horibe S. Autologous bone marrow stromal cell transplantation for repair of full-thickness articular cartilage defects in human patellae: two case reports. Cell Transplant 2004;13:595–600.
11. Kuroda R, Ishida K, Matsumoto T, Akisue T, Fujioka H, Mizuno K, et al. Treatment of a full-thickness articular cartilage defect in the femoral condyle of an athlete with autologous bone-marrow stromal cells. Osteoarthritis Cartilage 2007;15:226–31.
12. Adachi N, Sato K, Usas A, Fu FH, Ochi M, Han CW, et al. Muscle derived, cell based ex vivo gene therapy for treatment of full thickness articular cartilage defects. J Rheumatol 2002;29: 1920–30.
13. Kuroda R, Usas A, Kubo S, Corsi K, Peng H, Rose T, et al. Cartilage repair using bone morphogenetic protein 4 and muscle-derived stem cells. Arthritis Rheum 2006;54:433–42.
14. Wakitani S, Goto T, Pineda SJ, Young RG, Mansour JM, Caplan AI, et al. Mesenchymal cell-based repair of large, full-thickness defects of articular cartilage. J Bone Joint Surg Am 1994;76: 579–92.
15. Koga H, Muneta T, Ju YJ, Nagase T, Nimura A, Mochizuki T, et al. Synovial stem cells are regionally specified according to local microenvironments after implantation for cartilage regeneration. Stem Cells 2007;25:689–96.
16. Moses MA, Wiederschain D, Wu I, Fernandez CA, Ghazizadeh V, Lane WS, et al. Troponin I is present in human cartilage and inhibits angiogenesis. Proc Natl Acad Sci U S A 1999;96:2645–50.
17. Shukunami C, Oshima Y, Hiraki Y. Chondromodulin-I and tenomodulin: a new class of tissue-specific angiogenesis inhibitors found in hypovascular connective tissues. Biochem Biophys Res Commun 2005;333:299–307.
18. Robinson CJ, Stringer SE. The splice variants of vascular endothelial growth factor (VEGF) and their receptors. J Cell Sci 2001;114(Pt 5):853–65.
19. Thomas KA. Vascular endothelial growth factor, a potent and selective angiogenic agent. J Biol Chem 1996;271:603–6.
20. Maes C, Stockmans I, Moermans K, van Looveren R, Smets N, Carmeliet P, et al. Soluble VEGF isoforms are essential for establishing epiphyseal vascularization and regulating chondrocyte development and survival. J Clin Invest 2004;113:188–99.
21. Gerber HP, Vu TH, Ryan AM, Kowalski J, Werb Z, Ferrara N. VEGF couples hypertrophic cartilage remodeling, ossification and angiogenesis during endochondral bone formation. Nat Med 1999;5:623–8.
22. Hashimoto S, Creighton-Achermann L, Takahashi K, Amiel D, Coutts RD, Lotz M. Development and regulation of osteophyte formation during experimental osteoarthritis. Osteoarthritis Cartilage 2002;10:180–7.
23. Pufe T, Harde V, Petersen W, Goldring MB, Tillmann B, Mentlein R. Vascular endothelial growth factor (VEGF) induces matrix metalloproteinase expression in immortalized chondrocytes. J Pathol 2004;202:367–74.
24. Pfander D, Kortje D, Zimmermann R, Weseloh G, Kirsch T,

Gesslein M, et al. Vascular endothelial growth factor in articular cartilage of healthy and osteoarthritic human knee joints. Ann Rheum Dis 2001;60:1070–3.
25. Enomoto H, Inoki I, Komiya K, Shiomi T, Ikeda E, Obata K, et al. Vascular endothelial growth factor isoforms and their receptors are expressed in human osteoarthritic cartilage. Am J Pathol 2003;162:171–81.
26. Peng H, Wright V, Usas A, Gearhart B, Shen HC, Cummins J, et al. Synergistic enhancement of bone formation and healing by stem cell-expressed VEGF and bone morphogenetic protein-4. J Clin Invest 2002;110:751–9.
27. Peng H, Chen ST, Wergedal JE, Polo JM, Yee JK, Lau KH, et al. Development of an MFG-based retroviral vector system for secretion of high levels of functionally active human BMP4. Mol Ther 2001;4:95–104.
28. Peng H, Usas A, Olshanski A, Ho AM, Gearhart B, Cooper GM, et al. VEGF improves, whereas sFlt1 inhibits, BMP2-induced bone formation and bone healing through modulation of angiogenesis. J Bone Miner Res 2005;20:2017–27.
29. Pritzker KP, Gay S, Jimenez SA, Ostergaard K, Pelletier JP, Revell PA, et al. Osteoarthritis cartilage histopathology: grading and staging. Osteoarthritis Cartilage 2006;14:13–29.
30. Johnstone B, Hering TM, Caplan AI, Goldberg VM, Yoo JU. In vitro chondrogenesis of bone marrow-derived mesenchymal progenitor cells. Exp Cell Res 1998;238:265–72.
31. Jadlowiec J, Koch H, Zhang X, Campbell PG, Seyedain M, Sfeir C. Phosphophoryn regulates the gene expression and differentiation of NIH3T3, MC3T3-E1, and human mesenchymal stem cells via the integrin/MAPK signaling pathway. J Biol Chem 2004;279: 53323–30.
32. Van der Kraan PM, Vitters EL, van de Putte LB, van den Berg WB. Development of osteoarthritic lesions in mice by "metabolic" and "mechanical" alterations in the knee joints. Am J Pathol 1989;135:1001–14.
33. Guingamp C, Gegout-Pottie P, Philippe L, Terlain B, Netter P, Gillet P. Mono-iodoacetate–induced experimental osteoarthritis: a dose–response study of loss of mobility, morphology, and biochemistry. Arthritis Rheum 1997;40:1670–9.
34. Janusz MJ, Hookfin EB, Heitmeyer SA, Woessner JF, Freemont AJ, Hoyland JA, et al. Moderation of iodoacetate-induced experimental osteoarthritis in rats by matrix metalloproteinase inhibitors. Osteoarthritis Cartilage 2001;9:751–60.
35. Stoop R, Buma P, van der Kraan PM, Hollander AP, Billinghurst RC, Meijers TH, et al. Type II collagen degradation in articular cartilage fibrillation after anterior cruciate ligament transection in rats. Osteoarthritis Cartilage 2001;9:308–15.
36. Janusz MJ, Bendele AM, Brown KK, Taiwo YO, Hsieh L, Heitmeyer SA. Induction of osteoarthritis in the rat by surgical tear of the meniscus: inhibition of joint damage by a matrix metalloproteinase inhibitor. Osteoarthritis Cartilage 2002;10: 785–91.
37. Zelzer E, Mamluk R, Ferrara N, Johnson RS, Schipani E, Olsen BR. VEGFA is necessary for chondrocyte survival during bone development. Development 2004;131:2161–71.
38. Zelzer E, Olsen BR. Multiple roles of vascular endothelial growth factor (VEGF) in skeletal development, growth, and repair. Curr Top Dev Biol 2005;65:169–87.
39. Terada N, Hamazaki T, Oka M, Hoki M, Mastalerz DM, Nakano Y, et al. Bone marrow cells adopt the phenotype of other cells by spontaneous cell fusion. Nature 2002;416:542–5.
40. Ying QL, Nichols J, Evans EP, Smith AG. Changing potency by spontaneous fusion. Nature 2002;416:545–8.
41. Camargo FD, Finegold M, Goodell MA. Hematopoietic myelomonocytic cells are the major source of hepatocyte fusion partners. J Clin Invest 2004;113:1266–70.
42. Willenbring H, Bailey AS, Foster M, Akkari Y, Dorrell C, Olson S, et al. Myelomonocytic cells are sufficient for therapeutic cell fusion in liver. Nat Med 2004;10:744–8.
43. Zhang S, Wang D, Estrov Z, Raj S, Willerson JT, Yeh ET. Both cell fusion and transdifferentiation account for the transformation of human peripheral blood CD34-positive cells into cardiomyocytes in vivo. Circulation 2004;110:3803–7.
44. Nygren JM, Jovinge S, Breitbach M, Sawen P, Roll W, Hescheler J, et al. Bone marrow-derived hematopoietic cells generate cardiomyocytes at a low frequency through cell fusion, but not transdifferentiation. Nat Med 2004;10:494–501.
45. Alvarez-Dolado M, Pardal R, Garcia-Verdugo JM, Fike JR, Lee HO, Pfeffer K, et al. Fusion of bone-marrow-derived cells with Purkinje neurons, cardiomyocytes and hepatocytes. Nature 2003; 425:968–73.
46. Chen KA, Laywell ED, Marshall G, Walton N, Zheng T, Steindler DA. Fusion of neural stem cells in culture. Exp Neurol 2006;198: 129–35.
47. Hashimoto S, Ochs RL, Komiya S, Lotz M. Linkage of chondrocyte apoptosis and cartilage degradation in human osteoarthritis. Arthritis Rheum 1998;41:1632–8.
48. Tanaka E, Aoyama J, Miyauchi M, Takata T, Hanaoka K, Iwabe T, et al. Vascular endothelial growth factor plays an important autocrine/paracrine role in the progression of osteoarthritis. Histochem Cell Biol 2005;123:275–81.
49. Crisan M, Yap S, Casteilla L, Chen CW, Corselli M, Park TS, et al. A perivascular origin for mesenchymal stem cells in multiple human organs. Cell Stem Cell 2008;3:301–13.
50. Zheng B, Cao B, Crisan M, Sun B, Li G, Logar A, et al. Prospective identification of myogenic endothelial cells in human skeletal muscle. Nat Biotechnol 2007;25:1025–34.

Running title*:* Chondrogenic progenitor cells in adult skeletal muscle

Identification and characterization of chondrogenic progenitor cells in the fascia of postnatal skeletal muscle

Guangheng Li[1,2], Bo Zheng[1], Laura B Meszaros[1,3], Joseph B Vella[1,3], Arvydas Usas[1], Tomoyuki Matsumoto[1] and Johnny Huard[1,3,4]

[1]*Stem Cell Research Center, Children's Hospital of Pittsburgh, Department of Orthopaedic Surgery, University of Pittsburgh;*

[2]*Pediatric Cancer Biological Program, Department of Pediatrics, Oregon Health & Science University, Portland, Oregon;*

[3]*Department of Bioengineering, University of Pittsburgh;*

[4]*Department of Molecular Genetics and Biochemistry, University of Pittsburgh, Pittsburgh, Pennsylvania, USA*

Correspondence to: Dr. Johnny Huard, Stem Cell Research Center, Children's Hospital of Pittsburgh, 450 Technology Drive Suite 206, Pittsburgh, PA 15219 Tel. 412-648-2798; Fax 412-648-4066; E-mail: jhuard@pitt.edu; www.pitt.edu/~huardlab

Research Support: This work was also supported by the William F. and Jean W. Donaldson Chair at the Children's Hospital of Pittsburgh and by the Henry J. Mankin Endowed Chair in Orthopaedic Surgery at the University of Pittsburgh. This investigation was conducted in a facility constructed with support from Research Facilities Improvement Program Grant Number C06 RR-14489 from the National Center for Research Resources, the National Institutes of Health.

Keywords: skeletal muscle, fascia, chondrocyte, cartilage

Abstract

Intramuscular injection of bone morphogenetic protein (BMP) has been shown to induce ectopic bone formation. As in ectopic bone formation, a chondrogenic phase is typically observed in this process, which suggests that there may exist a chondrogenic sub-population of cells residing in skeletal muscle. Identification and isolation of this population could yield an important cell source for cartilage tissue engineering. Two prospective cell populations were isolated from rat skeletal muscle: fascia-derived cells (FDCs), extracted from gluteus maximus muscle fascia, and muscle-derived cells (MDCs), isolated from the muscle body. Both populations were investigated for their cell surface marker profile (flowcytometry analysis), proliferation rates, as well as their myogenic and chondrogenic potentials. The majority of FDCs expressed mesenchymal stromal cell markers (CD29, CD59, and CD90) but not endothelial cell markers (CD34, CD31, CD144, vWF, Flk-1 and CD146). FDCs underwent chondrogenic differentiation after BMP-4 treatment in vitro, but not myogenic differentiation when cultured in myogenic differentiation medium. Sorting on the basis of CD29 and CD146 expression demonstrated that chondrogenic potential correlated poorly with CD29 and CD146 expression. In fact, the unsorted FDCs demonstrated a significantly higher chondrogenic potential and proliferation rate compared to all the other sub-populations studied. Although MDCs were similar to the FDCs in terms of their cell surface marker profile and chondrogenic potential, they expressed the myogenic cell marker desmin and readily underwent myogenic differentiation in vitro; however, the chondrogenic potential of the MDCs is confounded by the presence of FDC-like cells (fibroblasts) residing in the muscle peri- and endomysium. To clarify the role of the muscle derived myogenic cells in chondrogenesis, mixed pellets with varying ratios of FDCs and L6 myoblasts were formed and studied for chondrogenic potential. Our results indicated that the chondrogenic potential of the FDCs decreased with the increased ratio of myogenic to FDCs supporting the role of FDCs in chondrogenesis. Additonal studies of human FDCs also demonstrated the presence of similar cells displaying a high chondrogenic potential with a low myogenic potential. Taken together, our results suggest that non-myogenic cells residing in the fascia of skeletal muscle have a strong chondrogenic potential and may represent a novel donor cell source for cartilage regeneration and repair.

Introduction:

The injection of BMPs into skeletal muscle has been shown to induce ectopic endochondral bone formation (Kawai, Hattori et al. 1994; Peng, Usas et al. 2005). This process is comprised of several sequential phases: inflammation, cartilage formation and resorption, and bone formation. However, it has not yet been determined whether the cells which reside in the muscle, and can undergo chondrogenic and osteogenic differentiation, are the same or represent different cell populations. If chondrogenic and osteogenic progenitors are distinct, identifying the cell population that undergoes cartilaginous cellular differentiation during this process and isolating them from skeletal muscle could provide an alternative cell source for cartilage repair.

It has been reported that skeletal muscle contains stem cells which have multi-lineage differentiation potentials including osteogenic, myogenic, and chondrogenic potentials (Qu-Petersen, Deasy et al. 2002; Zheng, Cao et al. 2007; Crisan, Yap et al. 2008; Gharaibeh, Lu et al. 2008). However, endochondral bone formation, induced by BMPs, occurring in skeletal muscle appears to involve different cell types including fibroblasts, which contribute to the intermediated chondrogenic phase, and myogenic cells, which contribute to the osteogenic phase (Li, Peng et al. 2005). An analogous paradigm of distinct chondrogenic and myogenic cell populations residing in the same skeletal structures is observed in embryonic limb-bud development (Sasse, Horwitz et al. 1984; Swalla and Solursh 1986; Kosher and Rodgers 1987; Stringa, Love et al. 1997). That is, a population of chondrogenic cells isolated from the limb-bud can be induced to differentiate into chondrocytes, but not in the myogenic lineage in vitro. Conversely, a population of myogenic cells isolated from the limb-bud can differentiate into myotubes (immature muscle fibers), but not chondrocytes (Swalla and Solursh 1986). These results have been verified in clonal studies of these distinct populations, and mixed clones of definitive chondrogenic and myogenic cells have not been observed (Dienstman, Biehl et al. 1974). Hence, it is reasonable to postulate that distinct populations of chondrogenic and myogenic progenitors are maintained throughout development and may be isolated from the mature limb.

Based on one of our previous study's (Li, Peng et al. 2005) and the latter studies performed on the embryonic limb-bud cells, we hypothesized that non-myogenic cells

residing in the fascia of skeletal muscle may contain a population of cells with chondrogenic potential. By definition, the fascia of skeletal muscle represents fibrous connective tissue that comprises the outermost sheath of the skeletal muscle. In the present study, fascia derived cells (FDCs) were isolated from the fascia of a Fischer 344 rat gluteus maximus muscle and investigated for their chondrogenic potential. FDCs are a heterogeneous population of cells including fibroblasts, endothelial cells from the vasculature, and various putative progenitor populations. In order to characterize the chondrogenic populations, FDCs were sorted into three subpopulations by FACS using two cell surface markers (CD29 and CD146). CD29 has been reported to be a cell surface marker of both mesenchymal stromal cells and chondrogenic progenitor cells (Wang, Hung et al. 2004; Wulf, Viereck et al. 2004; Gimeno, Maneiro et al. 2005; Crisan, Yap et al. 2008); therefore $CD29^+$ FDCs were expected to represent the cell fraction with the greatest chondrogenic potential. Furthermore, multiple studies have shown that there exist multipotent vasculature related cells residing in skeletal muscle (Dellavalle, Sampaolesi et al. 2007; Zheng, Cao et al. 2007; Crisan, Yap et al. 2008) . Since CD146 has been reported as a marker of vasculature related cells (endothelial cells, smooth muscle cells and pericytes) (Bardin, Anfosso et al. 2001; Li, Yu et al. 2003; Middleton, Americh et al. 2005; Duda, Cohen et al. 2006; Erdbruegger, Haubitz et al. 2006; Figarella-Branger, Schleinitz et al. 2006), it was also selected in the present study to determine whether CD146 expression correlated with chondrogenic potential. This sorting process yields four experimental groups: Unsorted FDCs, $CD29^+CD146^-$ FDCs, $CD29^+CD146^+$ FDCs, and $CD29^-CD146^-$ FDCs ($CD29^-CD146^+$ FDCs were not detected). Each population was investigated for their in vitro chondrogenic potential following treatment with BMP4 and TGF-β3.

Skeletal muscle perimysium and endomysium are sheaths of connective tissue that segregate skeletal muscle fascicles and fibers, respectively, and have a similar histology, structure and function to fascia, only at a different scale of muscle structure (Kragh, Svoboda et al. 2005; Kurose, Asai et al. 2006). It was further hypothesized that non-myogenic cells within skeletal muscle, likely associated with endomysium and perimysium, may possess chondrogenic potential. However there is no known physical method to isolate these tissues from skeletal muscle given skeletal muscle's super-

structural complexity. Therefore the presence of chondrogenic cells in skeletal muscle of a Fischer 344 rat gluteus maximus muscle was also investigated by isolating a heterogeneous population of muscle derived cells (MDCs), which then were examined for the presence of cells with chondrogenic potential.

Finally, human FDCs were isolated from a gluteus maximus muscle fascia biopsy. It was hypothesized that, like rat muscle fascia, there exists non-myogenic progenitors with chondrogenic potential residing in the human skeletal muscle fascia. Given the limited effectiveness of current cartilage repair modalities, this study could lead to the identification of chondrogenic progenitor cells that could be harvested from skeletal muscle fascia and used for cartilage regeneration.

Materials and Methods:

Histological and immunohistochemical staining of skeletal muscle

Skeletal muscle was harvested from the gluteus maximus of Fischer 344 rats, embedded in CRYO-GEL (Cancer Diagnostics), rapidly frozen in pre-cooled 2-methylbutane and stored at -80°C. Muscle sections were fixed in 10% formalin at room temperature (RT) for 15 minutes and were either stained with hematoxylin and eosin (H&E) or immunostained for vimentin, CD29 or CD146. For vimentin staining, sections were incubated at RT for 45 minutes with a Cy3 conjugated vimentin antibody (1:200 in PBS; Sigma, C9080, St. Louis, MO). For CD29 and CD146 staining, sections were immersed in biotinylated anti-CD29 (1:200 in 5% horse serum (HS), BD Pharmingen, 555004) and biotinylated anti-CD146 (1:200 in 5% HS, R&D system, BAF3250) for 2 hours at room temperature (RT), followed by streptavidin-Cy3 (1:500 in PBS, Sigma, S-6402) for 45 minutes at RT. Sections were then incubated for 10 minutes in 4',6-Diamidino-2-Phenylindole (DAPI) solution (1:1000 in PBS, Sigma, D9542), and examined under a fluorescent microscope.

Isolation and flow cytometry analysis of FDCs and MDCs

FDCs were isolated from the fascia of the left gluteus maximus of Fisher 344 rats, which was carefully detached from the muscle using surgical scissors. Both FDCs and MDCs were enzymatically isolated from their extra cellular matrix using a method previously described (Qu-Petersen, Deasy et al. 2002). They were resuspended in Dulbecco's modified Eagle's medium (DMEM) (Sigma) supplemented with 10% fetal bovine serum (FBS) and 1% penicillin/streptomycin (P/S), triturated, and passed through a 40-μm filter to obtain a single cell suspension. FDCs and MDCs were divided into ten equal aliquots (1×10^5 cells) and resuspended in mouse serum (Sigma) (1:10 in PBS) in 12x75mm polystyrene flow tubes for 10 minutes on ice. Primary antibodies for the surface markers of interest (1:200) were added to the tubes. Each tube was treated with one primary antibody. These antibodies included fluorescein isothiocyanate (FITC)-conjugated mouse anti-CD34 (Santa Cruz Biotechnology, Inc., Santa Cruz, CA), Phycoerythrin (PE)-conjugated mouse anti-rat CD45 and CD31, and FITC-conjugated mouse anti-rat CD59

and CD90 (all from BD Pharmingen) for 30 minutes. Biotin-conjugated hamster anti-rat CD29 (BD Pharmingen, San Jose, CA), biotinylated goat anti-rat CD146 (R&D Systems, Inc., Minneapolis, MN) and biotinylated rabbit anti-CD144 (VE-cadherin, Alexis Biochemicals, San Diego, CA) were added to tube for 30 minutes and followed by streptavidin-APC (BD Pharmingen) on ice for another 30 minutes. Purified rabbit anti-Flk1 (Santa Cruz Biotechnology) and rabbit anti-vWF (Chemicon, Billerica, MA) were then added to tubes for 30 minutes followed by goat anti-rabbit FITC (Vector, Burlingame, CA) on ice for another 30 minutes. To exclude dead cells, 7-amino-actinomycin D (BD Pharmingen) was added to each tube. Live cells were analyzed with a FACS Calibur flow cytometer (Becton Dickinson, Franklin Lakes, NJ) and CellQuest software (Becton Dickinson). The control samples obtained for each individual cell population received equivalent amounts of isotype antibody and were used to set the dot-plot intercepts used for analysis.

Cell sorting of FDCs and cell culture

For cell sorting, FDCs were suspended in DMEM supplemented with 10% FBS, incubated with Pacific Blue anti-mouse/rat CD29 (Biolegend, San Diego, CA) and PE-conjugated mouse anti-rat CD45 (BD Pharmingen) and biotinylated anti-rat CD146 (R&D Systems) on ice for 30 minutes. Cells were washed with phosphate buffered saline (PBS) supplemented with 2% fetal bovine serum (FBS) and incubated in streptavidin-APC (1:300, BD Pharmingen) on ice for 30 minutes. Isotype control antibodies used were Pacific Blue Armenian hamster IgG (Biolegend) and PE-conjugated mouse IgG1 (BD Pharmingen), Streptavidin-APC (BD Pharmingen). 7-amino-actinomycin D (BD Pharmingen) was added to each tube for dead cell exclusion. Cell sorting was performed on a fluorescence activated cell sorting (FACS) multiple laser fluorescence cell sorter that was equipped with 488, 633 and 407nm excitation wavelengths (Becton Dickinson). Sorted cells were re-analyzed in all experiments. All cells were grown in 24-well plate in proliferation medium (PM) (DMEM supplemented with 10% FBS, 10% HS, 0.5% chick embryo extract and 1% P/S) and were incubated at 37 °C in humidified air mixed with 5% CO_2.

Immunocytochemical staining and myogenic assay of FDCs and MDCs.

FDCs and MDCs were cultured in PM in 6-well plates and fixed in cold methanol (-20°C) for 20 minutes. The cells were washed in PBS and blocked with 5% HS for 30 minutes. For desmin staining, a desmin antibody (1:200 in 5% HS; Sigma; D1033) was added to the cells for 2 hours at RT. Following a PBS wash (3 times for 5 minutes), anti-mouse IgG with a Cy3 conjugate (1:200; Sigma; C2181) was then added to the cells for 1 hour at RT. For vimentin staining, cells were incubated for 45 minutes with a Cy3 labeled vimentin antibody (1:200 in PBS; Sigma, C9080) at RT, then washed in PBS and incubated for 10 minutes with DAPI solution (1:1000 in PBS). For the myogenic potential assay, FDCs or MDCs were cultured in PM until confluence and switched to a myogenic differentiation medium (DMEM with 2% HS) for 3 days. Cells were immunostained with MyoD according to the above protocol using an anti-MyoD primary antibody (1:200 in 5% HS; BD Pharmingen; 554130) for 2 hours at RT, followed by a PBS wash and addition of a biotinylated goat anti-mouse (1:200 in PBS; Vector; BA9200) for 1 hour at RT. Finally, streptavidin-Cy3 (1:500 in PBS; Sigma; S6402) was added to the cells for 45 minutes, as well as DAPI (1:1000 in PBS) solution for 10 minutes at RT. Cells were washed in PBS and examined under an inverted fluorescent microscope (Leica DM IRB, Leica Microsystems Inc. Bannockburn, IL), digitally recorded using a charge-coupled device (CCD) camera (Qimaging Retiga, Surrey, BC), and analyzed using image analysis software (Northern Exposure, St. Paul, MN).

Proliferation assay of sorted FDCs

Proliferation rates were measured for unsorted FDCs, $CD29^{+}CD146^{-}$ FDCs, $CD29^{+}CD146^{+}$ FDCs and $CD29^{-}CD146^{-}$ FDCs using a colorimetric absorbance assay. Briefly, to determine short term proliferation potential, cells were plated in 96-well plates (6000 cells/well) and cultured in DMEM supplemented with two different fetal bovine serum concentrations (1% and 10%, the lower concentration will increase sensitivity of proliferation potential assay) and BMP4 (500ng/ml, R&D Systems). After 2 days, 20µl of CellTiter 96 AQ_{UEOUS} One Reagent (Promega, Fitchberg Center, WI) was added to each well. The plate was incubated in 5% CO_2 at 37ºC for 2 hours. A 96-well plate reader was used to measure the absorbance at 490 nm.

Four populations of cells (unsorted FDCs, CD29+CD146- FDCs, CD29+CD146+ FDCs and CD29-CD146- FDCs) were cultured up to 14 days in either PM or endothelial growth medium-2 (EGM2) to test their proliferation potentials. 6.5×10^4 cells of each population were plated in T-25 flasks and cultured. They were counted and passaged into T-25 flasks where they grew to 60% confluence.

Chondrogenic differentiation of different FDCs and MDCs populations in vitro

Using a method described previously (Johnstone, Hering et al. 1998), $2.5x10^5$ cells of each cell group (passage 5) were centrifuged at 500*g* in 15-ml polypropylene conical tubes and the resulting pellets were cultured for up to 28 days in chondrogenic medium (Cambrex, East Rutherford, NJ) supplemented with BMP4 (500ng/ml, R&D Systems) and TGF-β3 (10ng/ml, R&D Systems). The medium was changed every 2 to 3d. The pellets were harvested on day 14, 21 and 28, embedded in paraffin, sectioned, and stained with Safranin O (Sigma, S-8884) and Alcian blue/ nuclear fast red (Sigma A-5268/ Sigma N-8002) to determine the presence of proteoglycans (PGs) and gylcosaminoglycans (GAGs), indicated by the color red and positive reaction of sulfated proteoglycans indicated by a blue color respectively.

Chondrogenic assay for mixed pellets of FDCs and rat L6 myoblasts in vitro

The rat L6 myoblast cell line (ATCC CRL 1458: American Type Culture Collection, Rockville, MD) was grown in T-75 cm^2 flasks in DMEM supplemented with 10% FBS and 1% penicillin-streptomycin at sub-confluence to prevent differentiation or myotube formation. FDCs and rat L6 myoblast cells were mixed and centrifuged to make pellets with different ratios (1:0, 4:1, 1:1, 1:4, 0:1 of FDCs to L6 cells) with each pellet having the same total number of cells (2.5×10^5). These mixed pellets were generated to mimic the possible presence of the MDC population with FDCs (chondrogenic progenitors) and to study the effect of myoblasts on the chondrogenic potential of FDCs. The five groups of pellets were cultured in chondrogenic medium supplemented with BMP4 and TGF-β3 for 21d. Pellets were embedded in paraffin, sectioned and stained with Safranin O and Alcian blue.

Collagen type II staining

Pellets were deparaffinized and processed for Collagen type II immunostaining according to the manufacturer's protocol (Vecstastain ABC kit; Alkaline phosphatase universal AK-5200; Vector laboratories, Burlingame, CA). Pepsin solution (Thermo Scientific; AP-9007-005, Waltham, MA) was used for enzyme-induced epitope retrieval from paraffin embedded sections. Collagen type II antibody (1:100; Thermo Scientific; MS-235-P1) was used for immunostaining. The Vector blue substrate kit (SK-5300, Vector) was used to reveal positive signal.

Isolation and analysis of human FDCs

Human FDCs were isolated from a fresh gluteus maximus muscle fascia biopsy, from a recently deceased cadaver, using the same method used to isolate rat FDCs (protocol approved by IRB). Human fascia was carefully removed from the attached gluteus maximus muscle and minced into a coarse slurry. The fascia tissue was then enzymatically dissociated at 37°C in 0.2% collagenase-type XI (Sigma-Aldrich) for 1 h and then centrifuged at 3,500 rpm for 5 min. The pelleted cells were next incubated in 2.4 units dispase/ml Hank's balanced salt solution (HBSS) (GIBCO BRL) for 45 min, and then incubated for 30 min in 0.1% trypsin-EDTA (GIBCO BRL) diluted in HBSS. After enzymatic dissociation, the human fascia cells were centrifuged and resuspended in PM. FDCs were immunostained for desmin and vimentin and their chondrogenic potential was evaluated after BMP4 treatment.

Statistical Analysis

Data are expressed as a mean ± standard deviation, except where noted. Direct comparisons between two cell populations were made using an ANOVA analysis. Statistical significance was assigned if $p<0.05$.

Results:

Staining of fascia tissue of gluteus maximus muscle and characterization of FDCs

H&E staining showed that fascia tissue is composed of fibrous and highly cellular connective tissue enveloping the skeletal muscle. Immunohistochemical staining of fascia tissue revealed that all fascia cells were vimentin (fibroblast marker) positive, a smaller fraction was CD29 positive or CD146 positive (Fig.1a). Freshly isolated FDCs were immunostained for a hematopoietic cell marker (CD45), endothelial cell markers (CD34, CD31, CD144, vWF, Flk-1 and CD146) and mesenchymal stromal cell markers (CD29, CD59, and CD90) and then analyzed by flow cytometry. All FDCs were negative for the hematopoeitic cell marker, CD45. Very few (<0.1%) expressed endothelial cell markers (CD34, CD144, vWF, Flk-1) although some CD31 (1.9%) and CD146 (1%) expression was observed. A large fraction of FDCs expressed the mesenchymal stromal cell makers CD59 (64.5%), CD29 (14.3%), and CD90 (5.45%) (Fig.1b).

When cultured in a monolayer in PM, FDCs acquired a fibroblast-like appearance. In fact, when stained for desmin (myogenic cell marker) and vimentin (fibroblast cell marker), FDCs showed minimal positive staining for desmin yet were uniformly positive for vimentin (Fig. 1c). A lack of myotube formation was observed in FDCs when these cells were cultured in myogenic differentiation medium (low serum culturing medium), supporting the low myogenic potential of these cells. A lack of MyoD expression also supports the absence of myogenic cells in the FDCs (Fig. 1c).

Characterization of FACS sorted FDCs ($CD29^+CD146^-$, $CD29^+CD146^+$ and $CD29^-CD146^-$)

FDCs were sorted by FACS immediately following the cells' dissociation. Once hematopoietic cells ($CD45^+$) were excluded, viable cells were gated and further sorted into the following subgroups: (i) $CD29^+CD146^-$ cells (39.2% of the total cell population); (ii) $CD29^+CD146^+$ (1.5% of the total population); (iii) $CD29^-CD146^-$ (21.4% of the total cell population). (Note that there were no $CD29^-CD146^+$ cells detected) (Fig. 2a, b, c). The mean number of viable, $CD45^-$ sorted cells in each subgroup which were recovered for every experiment included $1.18x10^5$ $CD29^+CD146^-$ FDCs, $1.7x10^3$ $CD29^+CD146^+$ FDCs, and $2.75x10^4$ $CD29^-CD146^-$ FDCs. Purities of these three sorted cell populations

were 97.7%, 93.8% and 98.0%, respectively, as confirmed by flow cytometry analysis performed immediately after FACS.

Proliferation of FACS sorted FDCs ($CD29^+CD146^-$, $CD29^+CD146^+$ and $CD29^-CD146^-$)

A significantly higher proliferation rate was observed in $CD29^+CD146^-$ FDCs compared to both $CD29^+CD146^+$ and $CD29^-CD146^-$ FDCs when cultured in DMEM supplemented with 1% FBS and 500ng/ml BMP4 ($P<0.01$). Additionally, $CD29^-CD146^-$ FDCs had a significantly higher rate of proliferation than $CD29^+CD146^+$ FDCs (Fig.2e) ($P<0.01$), as indicated by increased 490nm absorbance in CellTiter 96 AQ_{UEOUS} One Reagent. When cultured in DMEM supplemented with 10% FBS with BMP4, $CD29^+CD146^-$ FDCs, again, had a significantly higher rate of proliferation than both $CD29^+CD146^+$ FDCs and $CD29^-CD146^-$ FDCs ($P<0.01$). However, in this case, no significant difference between $CD29^+CD146^+$ FDCs and $CD29^-CD146^-$ FDCs was observed (Fig. 2d, e). The four populations of cells also displayed different proliferation potentials in both PM and EGM2 after two weeks in culture (supplemental Fig. 1).

Chondrogenic Potential of FACS sorted FDCs ($CD29^+CD146^-$, $CD29^+CD146^+$ and $CD29^-CD146^-$)

The different FDC populations displayed different chondrogenic potentials as determined by extracellular matrix staining by both Safranin O and Alcian blue. The order of decreasing chondrogenic potential was as follows: unsorted FDCs, $CD29^-CD146^-$ FDCs, $CD29^+CD146^-$ FDCs, and $CD29^+CD146^+$ FDCs (Fig. 3a, b, c; supplemental Fig. 2). The round morphology typical of chondrocytes and positive extracellular matrix staining by both Safranin O and Alcian blue was observed in three of the four groups (FDCs, $CD29^+CD146^-$ FDCs and $CD29^-CD146^-$ FDCs) at different time points (day 14, 21 and 28) but a lack of chondrogenesis was observed at any time point tested in the case of $CD29^+CD146^+$ FDCs (Fig 3b, c, d, and e). These results were confirmed by immunostaining for collagen type II (Fig 3f).

Characterization and Chondrogenic Potential of Rat MDCs

MDCs expressed the mesenchymal stromal cell markers CD29 (10 %), CD59 (12.9%), and CD90 (0.6%), whereas few cells expressed CD31 (1%) or CD146 (5%). MDCs were all negative for CD45 and very few (<0.1%) expressed endothelial cell markers (CD34, CD144, vWF, Flk-1) (Fig.4a). MDCs acquired a spindle-shaped or fibroblast-like appearance in monolayer culture in PM, and showed 23 ± 2% positive staining for desmin (myogenic cell marker) and 100% positive staining for vimentin (fibroblast marker)(Fig.4b). A myogenic differentiation assay demonstrated myotube formation in MDCs, as detected by MyoD immunostaining (Fig. 4b). MDCs also demonstrated chondrogenic potential when cultured in chondrogenic medium supplemented with 500ng/ml BMP4 and 10ng/ml TGF-β3 at all measured time points (Fig 4c), indicated by positive extracellular matrix staining for both Safranin O and Alcian blue as well as their round morphology typical of chondrocytes (Fig 4c-e).

Chondrogenic Potential of Mixed FDC and L6 Myoblast Pellets

A chondrogenic assay of pellets with varying ratios of FDCs and L6 myoblasts showed chondrogenic potential decreased with increasing ratio of L6 myoblasts to FDCs numbers (Fig. 5a). Pellets composed entirely of FDCs showed the greatest chondrogenic potential, whereas L6 pellets made entirely with L6 myoblasts demonstrated the least chondrogenic potential (Fig. 5a). Representative images of Safranin O, Alcian blue and collagen type II stained of FDCs and L6 myoblasts pellets indicate the high chondrogenic potential of FDCs while L6 myoblasts display a limited chondrogenic potential (Fig. 5b).

Chondrogenic Potential of Human FDCs

Human FDCs cultured in PM similarly acquired fibroblast-like spindle morphology. Immunostaining showed that very few human FDCs expressed desmin (myogenic cell marker) whereas most of them expressed vimentin (fibroblastic cell marker) (supplemental Fig. 3a). Pellets of human FDCs demonstrated their chondrogenic differentiation potential (supplemental Fig. 3 b, c, d), as indicated by positive Safranin O, Alcian blue, and collagen type II staining.

Discussion:

In the present study, we demonstrated that non-myogenic cells isolated from skeletal muscle fascia possess chondrogenic potential following treatment with BMP4. These FDCs are distinct from myogenic progenitors isolated from skeletal muscle, previously shown by our group to undergo osteogenesis and chondrogenesis (Wright, Peng et al. 2002; Kuroda, Usas et al. 2006). These cells express most mesenchymal stromal cell markers and few endothelial cell markers. They are located in the epimysial fascia and within the muscle (likely the endomysium and perimysium). FDCs can be readily isolated from fascia and expanded in vitro, making them a readily accessible cell source for potential cell based cartilage repair.

All FACS sorted FDC fractions showed chondrogenic differentiation potential except the $CD29^{+}CD146^{+}$ FDCs, which constituted only 1.5% of the FDCs, which indicates that the majority of FDCs have chondrogenic potential following treatment with BMP4. Cell surface marker profiles were examined for potential correlation with the chondrogenic potential of their cell sub-population. Indeed, we observed the following trend of chondrogenic differentiation potential (highest to lowest) for the experimental groups including: FDCs, $CD29^{-}CD146^{-}$ FDCs, $CD29^{+}CD146^{-}$ FDCs and $CD29^{+}CD146^{+}$ FDCs. The increased rate of chondrogenic differentiation of both $CD29^{-}CD146^{-}$ FDCs and $CD29^{+}CD146^{-}$ FDCs indicates that CD29 is not a major determinant cell marker of chondrogenic potential. Moreover, lack of chondrogenic differentiation in $CD29^{+}CD146^{+}$ FDCs, the only isolated cell population positive for CD146, implies vasculature related cells possess the least chondrogenic potential. However, this result did not exclude the possibility that these chondrogenic progenitor cells might originate from the vasculature because the cells may lose their chondrogenic potential after they fully differentiate into vasculature-related cells (CD146 positive). In addition, endothelial cell markers are not stable during in vitro expansion and one cannot exclude the presence of endothelial cells that are negative for endothelial cell markers (Zheng, Cao et al. 2007). Moreover, fascia tissue also rich in blood vessels, which implies that these chondrogenic progenitor cells might reside in the "stem cell niche" surrounding the blood vasculature. The blood cell

walls may harbor a dormant reserve of chondrogenic progenitor that could be recruited when they receive a BMP4 stimulation signal.

Proliferation assays of the different FDC populations obtained after sorting did not correlate with chondrogenic potential; however, the unsorted FDCs endowed with the greatest chondrogenic potential also displayed the highest rate of *in vitro* proliferation in all media conditions tested (Figs 2 d, e). This rapid rate of proliferation may be primarily attributed to the presence of $CD29^{+}CD146^{-}$ cells in the unsorted FDCs since a similar proliferation profile was observed between these two cell populations. The high chondrogenic potential of unsorted FDCs highlights the need of multiple cell types for optimal chondrogenic potential. It is likely that some of the cells within the unsorted fraction are responsible for chondrogenic differentiation while others may be important for releasing signals involved with the maintenance and proliferation of that fraction of cells involved in chondrogenic differentiation. Indeed, the need for multiple cell types for optimal progenitor or stem cell maintenance, proliferation, or differentiation has been observed in a variety of cell types, including embryonic stem cells, bone marrow stromal cells, skeletal muscle cells, etc. (A 2007; Carvalho, Oliveira et al. 2008; Neuhuber, Swanger et al. 2008).

MDCs did not show any significant difference in their cell marker profile via FACS analysis when compared to the FDCs. However, positive staining of the myogenic cell marker desmin (23±2%) and myotube formation by the MDCs indicates that, as expected, a population of myogenic cells exists in MDCs, which was not found in the FDCs. Again, it should be noted that endomysium and perimysium could not be physically isolated from the skeletal muscle; therefore, we would expect this MDC population to represent a heterogeneous population of cells, including myogenic cells and connective tissue derived cells from endomysium and perimysium. In order to clarify whether endomysium and perimysium derived cells play a role in MDC mediated chondrogenesis, mixed pellets of FDCs and L6 rat myoblasts in different ratios (1:0, 4:1, 1:1, 1:4, 0:1 of FDCs to L6 cells), were tested for chondrogenic potential. Indeed our results demonstrated that the L6 myoblasts contributed negatively

to the overall chondrogenic potential of the pellet, supporting our contention that connective tissue derived cells (epimysium, perimysium and endomysium) are required for chondrogenesis. These results are consistent with our previous study, in which a mouse myoblast cell line (C2C12 cells) demonstrated a low chondrogenic potential whereas a fibroblast cell line (NIH/3T3 cells) was found to be highly chondrogenic (Li, Peng et al. 2005).

Human fascia derived cells showed similar characteristics to rat fascia cells in terms of cell surface markers and chondrogenic potential. Cells isolated from various human tissues have demonstrated chondrogenic potential, such as bone marrow (Mackay, Beck et al. 1998), adipose tissue (Estes, Wu et al. 2006), synovium (Sakaguchi, Sekiya et al. 2005), umbilical cord blood (Kogler, Sensken et al. 2004) and human skeletal muscle (Mastrogiacomo, Derubeis et al. 2005); however, the chondrogenic potential of cells isolated from skeletal muscle remains controversial. One study reported that cells isolated from skeletal muscle have minimal chondrogenic potential when compared to the bone marrow, synovium, periosteum and adipose tissue (Sakaguchi, Sekiya et al. 2005). On the other hand, other studies demonstrated that skeletal muscle derived cells (SMDCs) resemble bone marrow stromal cells (BMSCs) and had the potential to form cartilage rudiment *in vitro* (Mastrogiacomo, Derubeis et al. 2005; Zheng, Cao et al. 2007).The discrepancies in these studies may be related to the procedures followed for cell isolation. In the Sakaguchi's study, collagenase D was used to digest the muscle, whereas trypsin was used in the latter study. It is possible that the majority of muscle derived cells in the former study (Sakaguchi, Sekiya et al. 2005) are myogenic cells, while SMDCs are highly fibrogenic in nature and hence we observed they had a high chondrogenic potential (Mastrogiacomo, Derubeis et al. 2005). As expected, cells used in the Mastrogiacomo's study were reported to be more fibrogenic and less myogenic based on their surface marker expression (high vimentin and low desmin) (Mastrogiacomo, Derubeis et al. 2005). Therefore, Mastrogiacomo's study is consistent with our observations that human skeletal muscle fascia derived cells, which are more fibrogenic (high expression of vimentin) and less myogenic (low expression of desmin), contain chondrogenic progenitor cells from skeletal muscle.

The in vivo disappearance of implanted cells that possess chondrogenic potential over a period of 6 months is a challenging aspect for applying the cells in articular cartilage repair. It appears that the majority of the implanted cells differentiate into hypertrophic chondrocytes and then eventually become apoptotic or calcified (Pelttari, Winter et al. 2006). It has been reported that human mesenchymal stromal cells (MSCs), the gold standard for in vitro chondrogenesis, can get through the hypertrophic chondrocyte stage when they are cultured in vitro with BMP2 or BMP4. The chondrogenic differentiation process of human MSCs in vitro is different than the natural development of articular cartilage chondrocyte differentiation in the joint, which acquires an intrinsic and stable chondrocytic stage without hypertrophy and becoming resistant to vascular invasion and calcification (Lian, McKee et al. 1993; Gerstenfeld and Shapiro 1996; Steinert, Proffen et al. 2009); however, the mechanism behind the chondrogenic differentiation cellular arrest process is still not fully understood. In the present study, the chondrogenesis of FDC pellets stimulated with BMP4 showed similar staining results for proteoglycans and glycosaminoglycans (both markers of hyaline cartilage) and the morphology of the chondrocytes was also consistent at 3 different time points (days 14, 21 and 28). No obvious changes, in regard to the sizes of chondrocytes lacuna, were observed when the early and later time points were compared; however, it is possible that there might be a size change associated with the chondrocytes lacuna as the cells become hypertrophic at longer-time points (to be determined in future studies).

We have performed earlier studies where the cells were retrovirally transduced with both BMP4 and sFlt1 (a VEGF antagonist) genes and were tested for their chondrogenic potential, both *in vitro* and *in vivo*, and compared to cells transduced with BMP4 only. The results showed that sFlt1 gene therapy improved the BMP-4 induced chondrogenic gene expression of the cells *in vitro* and improved the persistence of articular cartilage repair both in a cartilage defect model (Kubo, Cooper et al. 2009) and an osteoarthritis model (Matsumoto, Cooper et al. 2009). The posited mechanism for sFlt-1's action is that it prevents chondrocyte hypertrophy and apoptosis by blocking the intrinsic VEGF catabolic pathway *in vitro* and extrinsic VEGF-induced vascular invasion *in vivo*;

however, additional investigation is necessary to work out protocols to aid in the retention of the transplanted cells' chondrocytic stage and keep them from differentiating into hypertrophic chondrocytes.

The two main difference between the FDCs and human MSCs appears to be related to their dose-effect variability to BMP4. Higher doses of BMP4 (500ng/ml) are needed to induce FDCs to differentiate into chondrocytes compared to the relatively lower dose (25ng/ml) of BMP4 required to initiate the differentiation of MSCs (Steinert, Proffen et al. 2009). Furthermore, initiating chondrogenesis in human MSCs does not even require BMP4 stimulation (Li, Kupcsik et al. 2010). In addition, these two population of cells displayed different ostogenic potentials, with the FDCs showing very poor osteogenic potential when cultured in osteogenic medium (data not shown), and the human MSCs being highly prone to differentiating into an osteogenic lineage (Jaiswal, Haynesworth et al. 1997).

In summary, fascia, including the perimysium and endomysium in skeletal muscle, contain cells with high chondrogenic potential. These cells, which lack myogenic potential, express mesenchymal stromal cell markers and low levels of endothelial cell markers; therefore we concluded that non-myogenic cells residing in the fascia of skeletal muscle contain cells with chondrogenic potential. These results support the processes involved in endochondral bone formation within skeletal muscle following BMP stimulation which appears to involve two cell types, fibroblastic cells that are directly involved in chondrogenesis, and myogenic cells, that are involved in the osteogenesis of the cells. Our results also suggest that skeletal muscle fascia represents a novel tissue source from which chondrogenic progenitor cells can be harvested for articular cartilage repair.

ACKNOWLEDGEMENTS

This work was supported in part by grants from the National Institutes of Health (R01-AR049684; RO1-DE13420-06; IU54AR050733-01) and the Department of Defense (AFIRM grant #: W81XWH-08-2-0032) and by the William F. and Jean W. Donaldson Endowed Chair at the Children's Hospital of Pittsburgh, the Henry J. Mankin Endowed Chair at the University of Pittsburgh. We would also like to thank James H. Cummins for his editorial assistance in the preparation of this manuscript. No authors have any potential conflicts of interest to disclose.

References

A, E. M. (2007). "Isolation and propagation of mouse embryonic fibroblasts and preparation of mouse embryonic feeder layer cells." Curr Protoc Stem Cell Biol **Chapter 1**: Unit1C 3.

Bardin, N., F. Anfosso, et al. (2001). "Identification of CD146 as a component of the endothelial junction involved in the control of cell-cell cohesion." Blood **98**(13): 3677-3684.

Carvalho, K. A., L. Oliveira, et al. (2008). "Immunophenotypic expression by flow cytometric analysis of cocultured skeletal muscle and bone marrow mesenchymal stem cells for therapy into myocardium." Transplant Proc **40**(3): 842-844.

Crisan, M., S. Yap, et al. (2008). "A perivascular origin for mesenchymal stem cells in multiple human organs." Cell Stem Cell **3**(3): 301-313.

Dellavalle, A., M. Sampaolesi, et al. (2007). "Pericytes of human skeletal muscle are myogenic precursors distinct from satellite cells." Nat Cell Biol **9**(3): 255-267.

Dienstman, S. R., J. Biehl, et al. (1974). "Myogenic and chondrogenic lineages in developing limb buds grown in vitro." Dev Biol **39**(1): 83-95.

Duda, D. G., K. S. Cohen, et al. (2006). "Differential CD146 expression on circulating versus tissue endothelial cells in rectal cancer patients: implications for circulating endothelial and progenitor cells as biomarkers for antiangiogenic therapy." J Clin Oncol **24**(9): 1449-1453.

Erdbruegger, U., M. Haubitz, et al. (2006). "Circulating endothelial cells: a novel marker of endothelial damage." Clin Chim Acta **373**(1-2): 17-26.

Estes, B. T., A. W. Wu, et al. (2006). "Potent induction of chondrocytic differentiation of human adipose-derived adult stem cells by bone morphogenetic protein 6." Arthritis Rheum **54**(4): 1222-1232.

Figarella-Branger, D., N. Schleinitz, et al. (2006). "Platelet-endothelial cell adhesion molecule-1 and CD146: soluble levels and in situ expression of cellular adhesion molecules implicated in the cohesion of endothelial cells in idiopathic inflammatory myopathies." J Rheumatol **33**(8): 1623-1630.

Gerstenfeld, L. C. and F. D. Shapiro (1996). "Expression of bone-specific genes by hypertrophic chondrocytes: implication of the complex functions of the hypertrophic chondrocyte during endochondral bone development." Journal of cellular biochemistry **62**(1): 1-9.

Gharaibeh, B., A. Lu, et al. (2008). "Isolation of a slowly adhering cell fraction containing stem cells from murine skeletal muscle by the preplate technique." Nat Protoc **3**(9): 1501-1509.

Gimeno, M. J., E. Maneiro, et al. (2005). "Cell therapy: a therapeutic alternative to treat focal cartilage lesions." Transplant Proc **37**(9): 4080-4083.

Jaiswal, N., S. E. Haynesworth, et al. (1997). "Osteogenic differentiation of purified, culture-expanded human mesenchymal stem cells in vitro." Journal of cellular biochemistry **64**(2): 295-312.

Johnstone, B., T. M. Hering, et al. (1998). "In vitro chondrogenesis of bone marrow-derived mesenchymal progenitor cells." Exp Cell Res **238**(1): 265-272.

Kawai, M., H. Hattori, et al. (1994). "Development of hemopoietic bone marrow within the ectopic bone induced by bone morphogenetic protein." Blood Cells **20**(1): 191-199; discussion 200-191.

Kogler, G., S. Sensken, et al. (2004). "A new human somatic stem cell from placental cord blood with intrinsic pluripotent differentiation potential." J Exp Med **200**(2): 123-135.

Kosher, R. A. and B. J. Rodgers (1987). "Separation of the myogenic and chondrogenic progenitor cells of undifferentiated limb mesenchyme." Dev Biol **121**(2): 376-388.

Kragh, J. F., Jr., S. J. Svoboda, et al. (2005). "Epimysium and perimysium in suturing in skeletal muscle lacerations." J Trauma **59**(1): 209-212.

Kubo, S., G. M. Cooper, et al. (2009). "Blocking vascular endothelial growth factor with soluble Flt-1 improves the chondrogenic potential of mouse skeletal muscle-derived stem cells." Arthritis and rheumatism **60**(1): 155-165.

Kuroda, R., A. Usas, et al. (2006). "Cartilage repair using bone morphogenetic protein 4 and muscle-derived stem cells." Arthritis Rheum **54**(2): 433-442.

Kurose, T., Y. Asai, et al. (2006). "Distribution and change of collagen types I and III and elastin in developing leg muscle in rat." Hiroshima J Med Sci **55**(3): 85-91.

Li, G., H. Peng, et al. (2005). "Differential effect of BMP4 on NIH/3T3 and C2C12 cells: implications for endochondral bone formation." J Bone Miner Res **20**(9): 1611-1623.

Li, Q., Y. Yu, et al. (2003). "Differential expression of CD146 in tissues and endothelial cells derived from infantile haemangioma and normal human skin." J Pathol **201**(2): 296-302.

Li, Z., L. Kupcsik, et al. (2010). "Mechanical load modulates chondrogenesis of human mesenchymal stem cells through the TGF-beta pathway." Journal of cellular and molecular medicine **14**(6A): 1338-1346.

Lian, J. B., M. D. McKee, et al. (1993). "Induction of bone-related proteins, osteocalcin and osteopontin, and their matrix ultrastructural localization with development of chondrocyte hypertrophy in vitro." Journal of cellular biochemistry **52**(2): 206-219.

Mackay, A. M., S. C. Beck, et al. (1998). "Chondrogenic differentiation of cultured human mesenchymal stem cells from marrow." Tissue Eng **4**(4): 415-428.

Mastrogiacomo, M., A. R. Derubeis, et al. (2005). "Bone and cartilage formation by skeletal muscle derived cells." J Cell Physiol **204**(2): 594-603.

Matsumoto, T., G. M. Cooper, et al. (2009). "Cartilage repair in a rat model of osteoarthritis through intraarticular transplantation of muscle-derived stem cells expressing bone morphogenetic protein 4 and soluble Flt-1." Arthritis and rheumatism **60**(5): 1390-1405.

Middleton, J., L. Americh, et al. (2005). "A comparative study of endothelial cell markers expressed in chronically inflamed human tissues: MECA-79, Duffy antigen receptor for chemokines, von Willebrand factor, CD31, CD34, CD105 and CD146." J Pathol **206**(3): 260-268.

Neuhuber, B., S. A. Swanger, et al. (2008). "Effects of plating density and culture time on bone marrow stromal cell characteristics." Exp Hematol **36**(9): 1176-1185.

Pelttari, K., A. Winter, et al. (2006). "Premature induction of hypertrophy during in vitro chondrogenesis of human mesenchymal stem cells correlates with calcification and vascular invasion after ectopic transplantation in SCID mice." Arthritis and rheumatism **54**(10): 3254-3266.

Peng, H., A. Usas, et al. (2005). "VEGF improves, whereas sFlt1 inhibits, BMP2-induced bone formation and bone healing through modulation of angiogenesis." J Bone Miner Res **20**(11): 2017-2027.

Qu-Petersen, Z., B. Deasy, et al. (2002). "Identification of a novel population of muscle stem cells in mice: potential for muscle regeneration." J Cell Biol **157**(5): 851-864.

Sakaguchi, Y., I. Sekiya, et al. (2005). "Comparison of human stem cells derived from various mesenchymal tissues: superiority of synovium as a cell source." Arthritis Rheum **52**(8): 2521-2529.

Sasse, J., A. Horwitz, et al. (1984). "Separation of precursor myogenic and chondrogenic cells in early limb bud mesenchyme by a monoclonal antibody." J Cell Biol **99**(5): 1856-1866.

Steinert, A. F., B. Proffen, et al. (2009). "Hypertrophy is induced during the in vitro chondrogenic differentiation of human mesenchymal stem cells by bone morphogenetic protein-2 and bone morphogenetic protein-4 gene transfer." Arthritis research & therapy **11**(5): R148.

Stringa, E., J. M. Love, et al. (1997). "In vitro characterization of chondrogenic cells isolated from chick embryonic muscle using peanut agglutinin affinity chromatography." Exp Cell Res **232**(2): 287-294.

Swalla, B. J. and M. Solursh (1986). "The independence of myogenesis and chondrogenesis in micromass cultures of chick wing buds." Dev Biol **116**(1): 31-38.

Wang, H. S., S. C. Hung, et al. (2004). "Mesenchymal stem cells in the Wharton's jelly of the human umbilical cord." Stem Cells **22**(7): 1330-1337.

Wright, V., H. Peng, et al. (2002). "BMP4-expressing muscle-derived stem cells differentiate into osteogenic lineage and improve bone healing in immunocompetent mice." Mol Ther **6**(2): 169-178.

Wulf, G. G., V. Viereck, et al. (2004). "Mesengenic progenitor cells derived from human placenta." Tissue Eng **10**(7-8): 1136-1147.

Zheng, B., B. Cao, et al. (2007). "Prospective identification of myogenic endothelial cells in human skeletal muscle." Nat Biotechnol.

Figure legends:

Figure 1: Characterization of fascia tissues and FDCs (a) Hematoxylin and eosin stain. Fascia surround skeletal muscle is indicated with black arrows. Vimentin (red) staining of fascia, nuclei- blue (DAPI). CD29 (red) and CD146 (red) staining of fascia. White arrow indicates tubular morphology of CD146 positive blood vessel. (scale bar 50μm). (b) Surface antigens profile of freshly isolated FDCs. (c) FDCs acquire fibroblast shape in vitro. Desmin (red), vimentin (red), MyoD (red) , nuclei-blue (DAPI) (scale bar 50μm)

Figure 2: Cell viability (a) gates were set as indicated on the whole fascia cell suspension. (b) Negative selection of CD45+ cells (c) $CD29^+$ FDCs, $CD29^+CD146^+$ FDCs and $CD29^-CD146^-$ FDCs gated and sorted. (d,e) Proliferation in DMEM with either 1% or 10% FBS (* $p<0.01$)

Figure 3: (a) Macroscopic view of chondrogenic pellets. (b) Safranin O and Alcian blue/nuclear fast red (c) staining at different time points (day 14, 21 and 28) (d) Safranin O staining of FDCs and CD29+CD146+FDCs (scale bar 25μm). (e) Alcian blue staining of FDCs and CD29+CD146+FDCs (scale bar 25μm). (f) Immunostaining for Collagen II of FDCs and CD29+CD146+FDCs (scale bar 25μm).

Figure 4: (a) Surface marker profile of freshly isolated rat MDCs. (b) Desmin (red), vimentin (red), MyoD(red), nuclei (blue-DAPI) (scale bar 50μm). (c) Safranin O (red) and Alcian blue staining (blue) of MDCs pellets at 14, 21 and 28 days. (d,e) Higher magnification, safranin O and Alcian blue/ nuclear fast red (scale bar 25μm).

Figure 5: Chondrogenesis of mixed pellets of FDCs and rat myoblast L6 (a) Safranin-O and Alcian blue staining, pellets of mixed FDCs and rat myoblast L6

chondrogenic differentiation. (b) Higher magnification, safranin-O, Alcian blue and collagen II staining (scale bar 25μm).

Supplemental data

Supplemental figure legends

Supplemental Figure 1: Four populations of cells displayed different growth potentials when cultured in either proliferation medium (PM) or endothelial cell growth medium-2 (EGM2). FDCs demonstrated the greatest proliferation potential while $CD29^{+}CD146^{+}$FDCs displayed the worst proliferation potential.

Supplemental Figure 2: Comparison of pellet volumes among the four cell groups showed that there are significant differences between each of the groups (* $P<0.01$) at day 28.

Supplemental Figure 3: (a) Human FDCs in vitro. Desmin (red), vimentin (red), nuclei (blue-DAPI). (scale bar 50μm). (b,c,d) Safranin-O, Alcian blue and collagen II staining, human FDC pellets (scale bar represents 10μm).

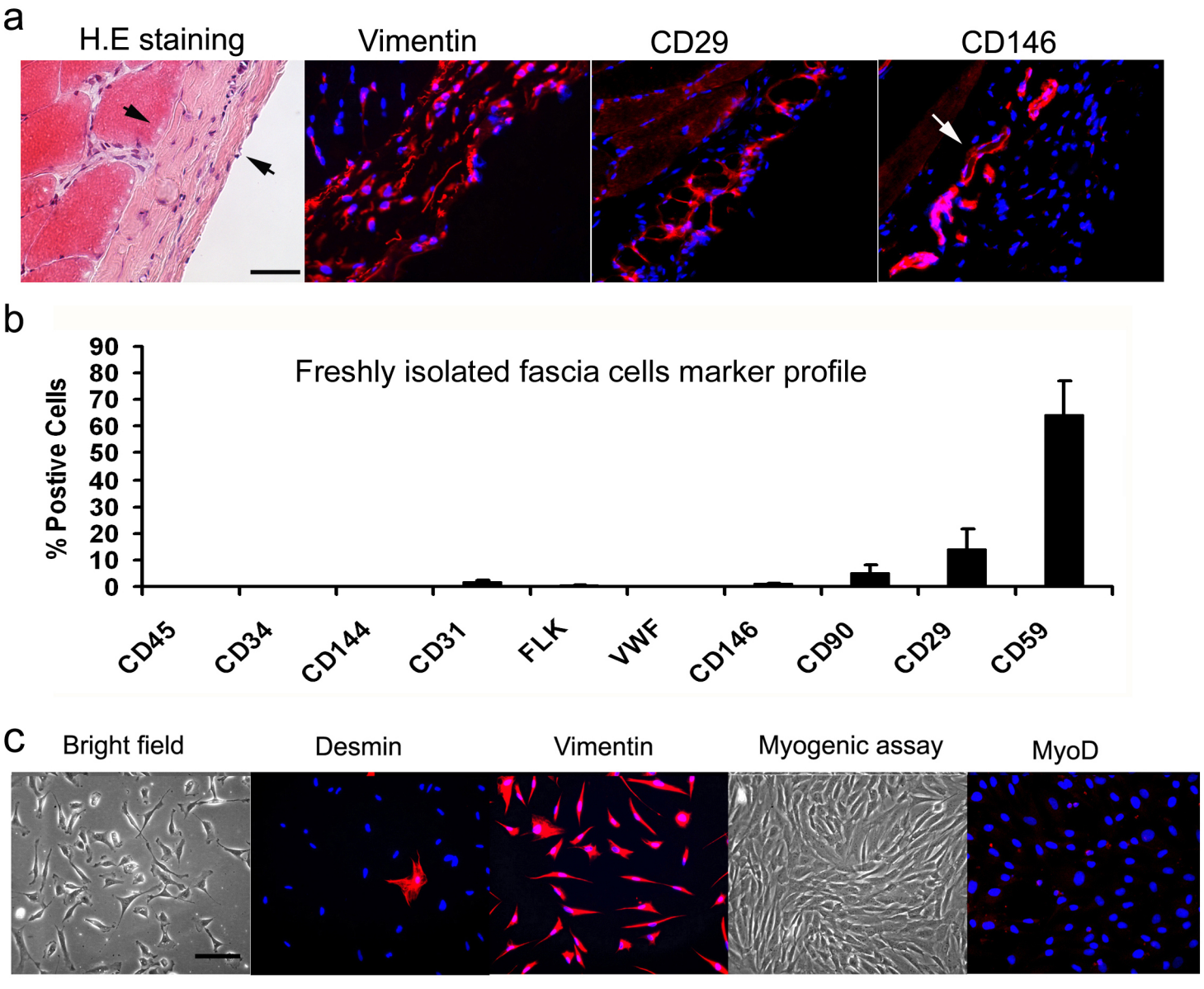
a
H.E staining
Vimentin
CD29
CD146
b
Freshly isolated fascia cells marker profile
% Postive Cells
90
80
70
60
50
40
30
20
10
0
CD45
CD34
CD144
CD31
FLK
VWF
CD146
CD90
CD29
CD59
c
Bright field
Desmin
Vimentin
Myogenic assay
MyoD

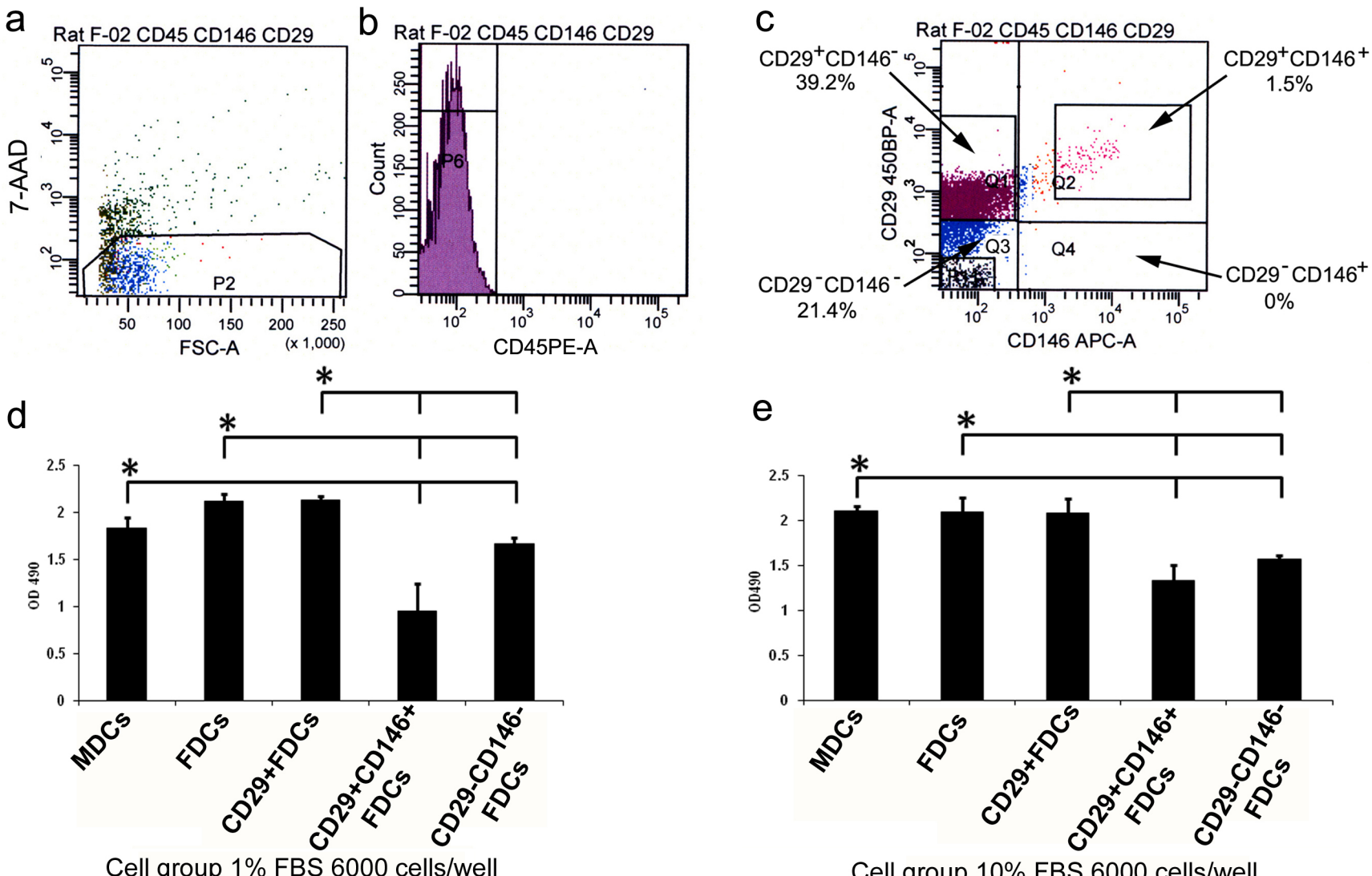
a
Rat F-02 CD45 CD146 CD29
7-AAD
FSC-A
(x 1,000)
P2
b
Rat F-02 CD45 CD146 CD29
Count
P6
CD45PE-A
c
Rat F-02 CD45 CD146 CD29
CD29+CD146-
39.2%
CD29+CD146+
1.5%
CD29 450BP-A
Q1
Q2
Q3
Q4
CD29-CD146-
21.4%
CD29-CD146+
0%
CD146 APC-A
d
OD 490
MDCs
FDCs
CD29+FDCs
CD29+CD146+ FDCs
CD29-CD146- FDCs
Cell group 1% FBS 6000 cells/well
e
OD490
MDCs
FDCs
CD29+FDCs
CD29+CD146+ FDCs
CD29-CD146- FDCs
Cell group 10% FBS 6000 cells/well

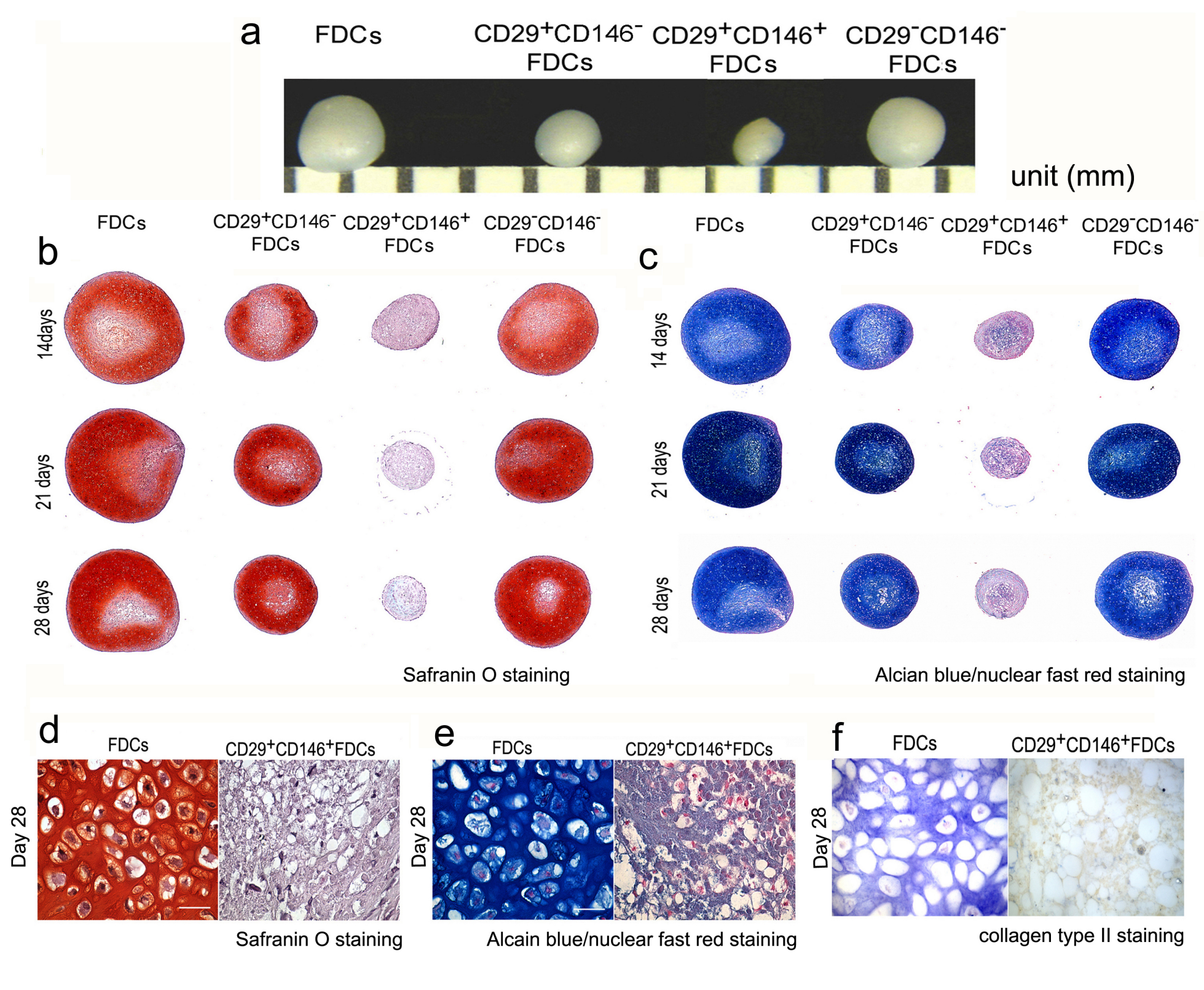
a
FDCs
CD29+CD146- FDCs
CD29+CD146+ FDCs
CD29-CD146- FDCs
unit (mm)
b
FDCs
CD29+CD146- FDCs
CD29+CD146+ FDCs
CD29-CD146- FDCs
14days
21 days
28 days
Safranin O staining
c
FDCs
CD29+CD146- FDCs
CD29+CD146+ FDCs
CD29-CD146- FDCs
14 days
21 days
28 days
Alcian blue/nuclear fast red staining
d
FDCs
CD29+CD146+FDCs
Day 28
Safranin O staining
e
FDCs
CD29+CD146+FDCs
Day 28
Alcain blue/nuclear fast red staining
f
FDCs
CD29+CD146+FDCs
Day 28
collagen type II staining

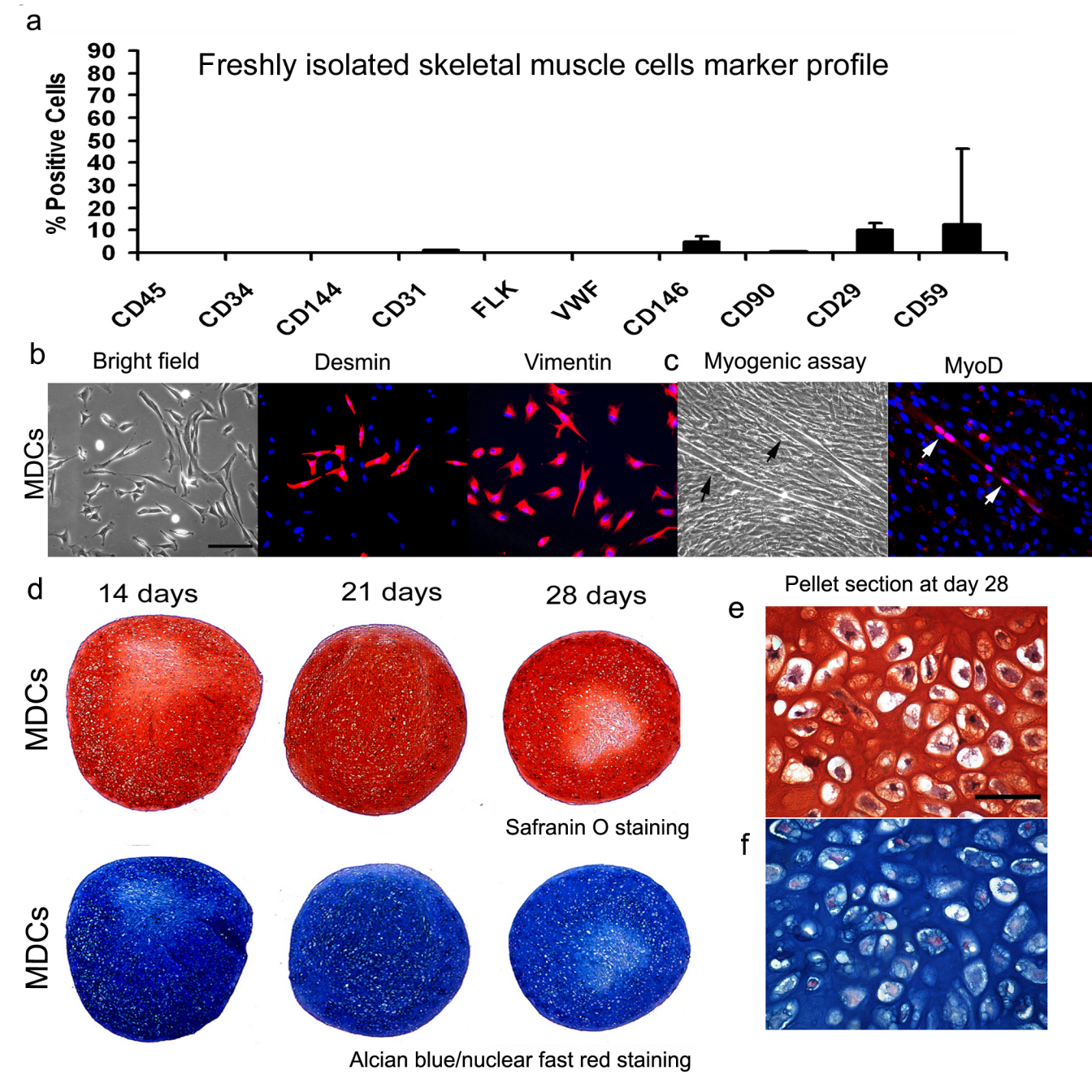
a
Freshly isolated skeletal muscle cells marker profile
% Positive Cells
90
80
70
60
50
40
30
20
10
0
CD45
CD34
CD144
CD31
FLK
VWF
CD146
CD90
CD29
CD59
b
Bright field
Desmin
Vimentin
MDCs
c
Myogenic assay
MyoD
d
14 days
21 days
28 days
MDCs
Safranin O staining
MDCs
Alcian blue/nuclear fast red staining
e
Pellet section at day 28
f

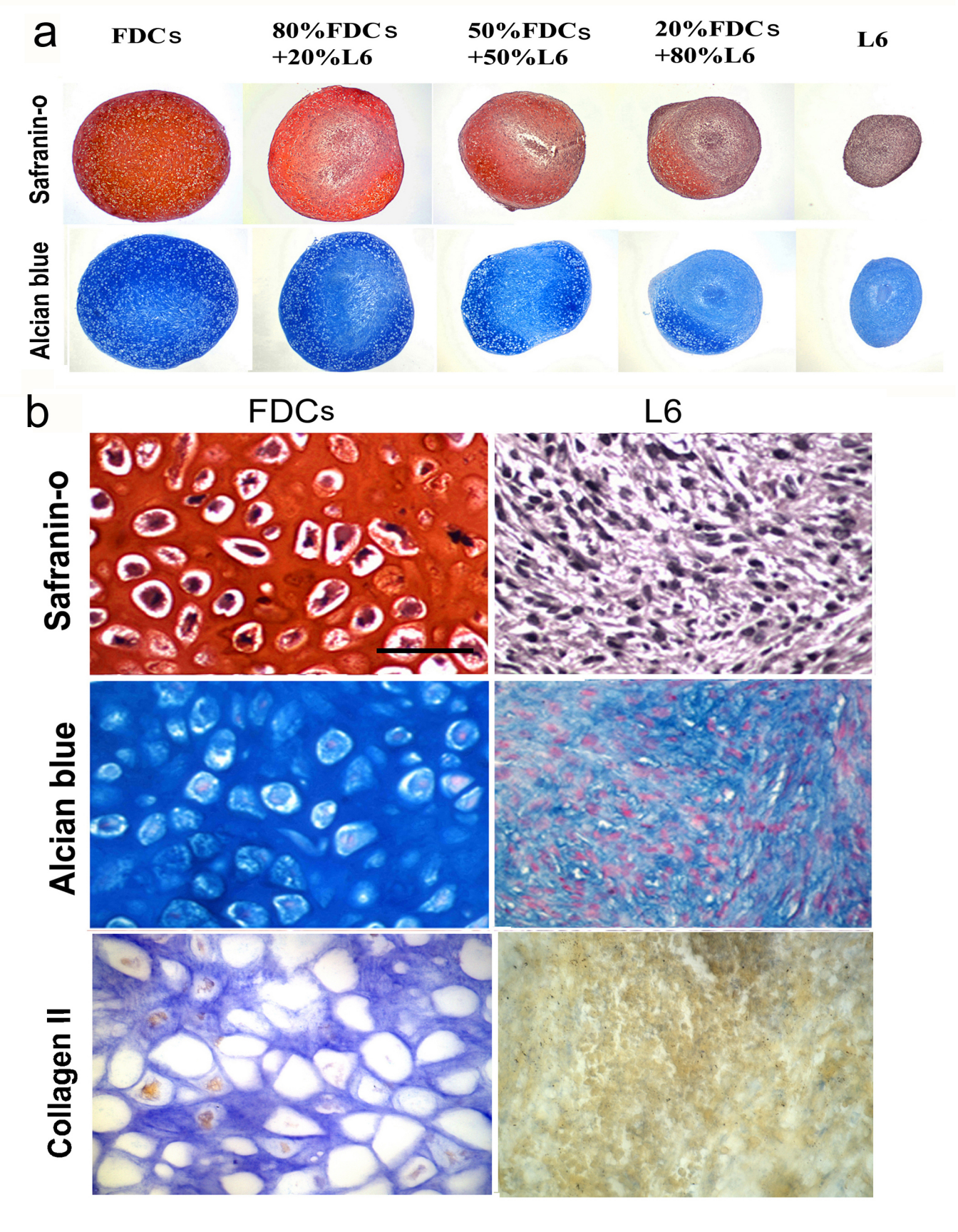
a
FDCs
80%FDCs +20%L6
50%FDCs +50%L6
20%FDCs +80%L6
L6
Safranin-o
Alcian blue
b
FDCs
L6
Safranin-o
Alcian blue
Collagen II

The Influence of Platelet-Rich Plasma on *In-vitro* Proliferation, and on Osteogenic, Chondrogenic, and Myogenic Differentiation of Human Muscle Derived Progenitor Cells

[1]Li H, [1]Usas A, [1]Chen W, [1]Gao X, [1]Huard J

[1] Stem Cell Research Center, Department of Orthopaedic Surgery, University of Pittsburgh School of Medicine, Pittsburgh, PA

Introduction

Platelet-rich plasma (PRP) is an emerging biologic tool for regenerative medicine. It has a significant advantage over other potential therapies in that it contains abundant autologous growth factors and is easy to obtain and to manipulate. The combination of autologous PRP with stem cell therapy is promising in terms of cell expansion and transplantation[1]; however, the interaction of PRP with stem cells and its underlying cellular mechanisms are not fully understood. Human muscle derived progenitor cells (hMDPCs), such as myoendothelial cells and pericytes have been characterized in our lab and by other researchers as multipotent cells that exhibit multilineage developmental potentials and can differentiate into skeletal myofibers, bone, cartilage, and adipocytes both in culture and *in vivo*[2, 3]. They are promising candidates for orthopedics stem cell therapy. In the current study, we evaluated the influence that thrombin-activated human PRP had on the proliferation and osteogenic, chondrogenic and myogenic differentiation potentials of the hMDPCs. We also investigated possible mechanisms involved with PRP's influence in the hMDPCs.

Experimental design and Materials

PRP and PRP releasant preparation: Six human whole blood (WB) donations (Central Blood Bank) were pooled and their buffy coats were used to prepare the PRP. The platelet concentration of the pooled PRP was standardized to 2×10^6 platelets per microliter (10 times above the WB baseline) by centrifugation and re-suspension in platelet poor plasma (PPP) as determined by hemocytometer. The PRP releasant was prepared by activating the PRP with human thrombin (without calcium).

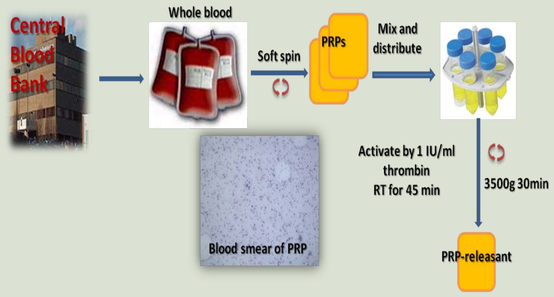

Figure 1. Flow chart of PRP preparation

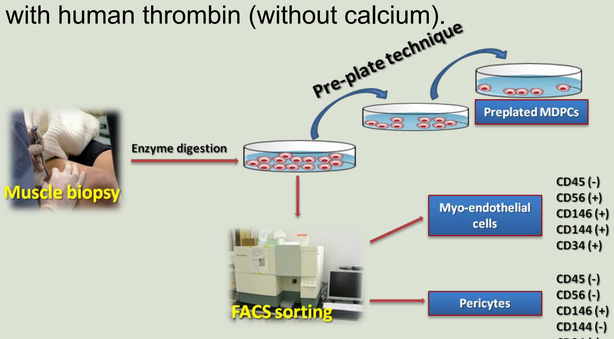

Figure 2. Flow chart of hMDPCs cultivation

Cultivation of hMDPCs: Three different hMDPCs were used for this study. Human pre-plated MDPCs that were isolated by pre-plate technique were purchased from Cook MyoSite, Inc. Myoendothelial cells ($CD45^-$, $CD56^+$, $CD146^-$, $CD144^+$, $CD34^+$) and pericytes ($CD45^-$, $CD56^-$, $CD146^+$, $CD144^-$ $CD34^-$) were obtained by muscle biopsy from three donors, and sorted by FACS. All hMDPCs were isolated and expanded following a standard protocol.

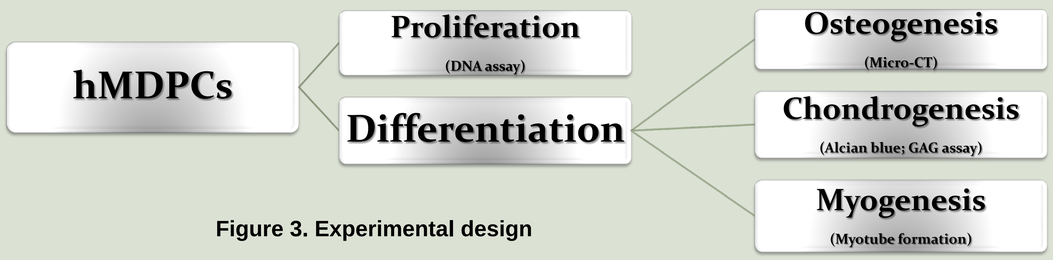

Figure 3. Experimental design

Results

PRP promotes proliferation of hMDPCs: The influence of PRP on the proliferation of hMDPCs was studied with and without FBS, in both short-term and long-term culture conditions. **First**, PRP promoted the proliferation of hMDPCs in a dose-dependent manner when added to conventional proliferation medium (Fig 4 A). **Second**, PRP induced the proliferation of hMDPCs in the absence of FBS in a dose-depend manner (Fig 4 B). **Third**, PRP stimulated the long term proliferation of the hMDPCs which will be beneficial for the *ex-vivo* expansion of the cells (Fig 4 C).

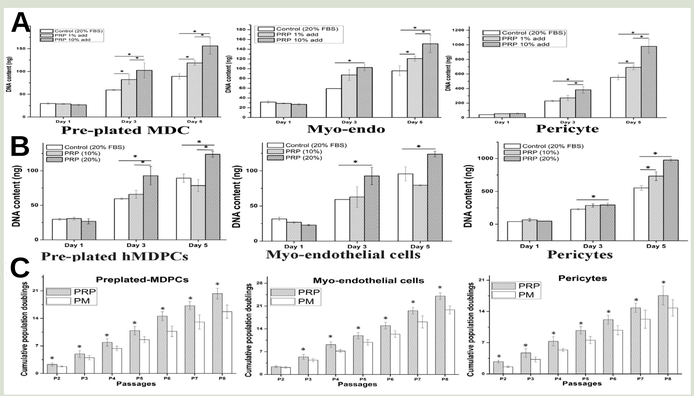

Figure 4. Influence of PRP on the proliferation of hMDPCs. A, Different concentrations of PRP were added into control medium (supplemented with 20% FBS). B, hMDPCs were cultured in basal medium with 10% and 20% PRP in the absent of FBS, 20% FBS served as a control. C, cells were cultured in basal medium supplemented with either 20% FBS and 1% CEE or 20% PRP for up to 8 passages. Cumulative population doubling rates (CPD) were calculated for all passages to compare the effects of different supplements on the proliferative capacity of hMDPCs. $^*P<0.05$

hMDPCs expanded with PRP maintain their differentiation capabilities: The osteogenic, chondrogenic, and myogenic differentiation abilities of all hMDPCs that were expanded within 20% FBS or PRP were tested after passage 8. hMDPCs derived from both culture conditions demonstrated differentiation toward the osteogenic, chondrogenic, and myogenic lineages as assessed by Micro-CT scanning, alcian blue, and f-MHC staining (Fig. 5).

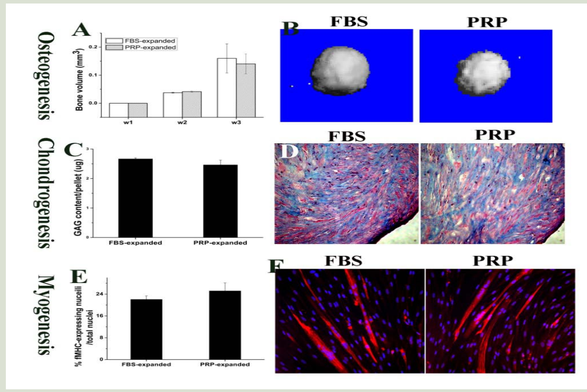

Figure 5. Differentiation ability of hMDPCs was maintained throughout long-term culture with PRP (representative results of pre-plated MDPCs, data of myo-endothelial cells and pericytes are not shown). hMDPCs that expanded either with PRP or FBS differentiated consistently into the osteogenic (A&B), chondrogenic (B&C) and myogenic (D&E) lineages. There were no significant differences between PRP-expanded MDPCs and FBS-expanded MDPCs.

Pluripotent stem cell markers were steadily expressed by the hMDPCs when expanded in PRP: The expression patterns were different among the different hMDPC populations. For most of the stem cell markers, the expression was not altered when cultivated in 20% PRP. For some of the markers, the expression levels were even higher than in the cells expanded in FBS (Fig. 6). The increase and sustained expression of these MSC markers in PRP-treated hMDPCs suggest that PRP may have an effect to keep the cells in a more primordial stage.

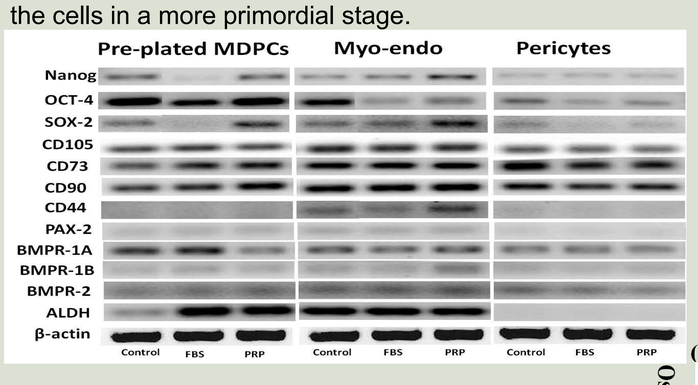

Figure 6. mRNA expression levels of stem cell markers on hMDPCs expanded with FBS or PRP. hMDPCs were cultured with basal medium supplemented with 20% FBS or 20% PRP for up to 3 weeks. The expression of stem cell markers was studied by RT-PCR. Cells cultured at day 0 were used as controls; FBS, hMDPCs cultured in FBS supplemented medium for 3 weeks; PRP, hMDPCs cultured in PRP supplemented medium for 3 weeks.

PRP decreases differentiation efficiency of hMDPCs: Osteogenic, chondrogenic, and myogenic differentiation of hMDPCs were dramatically decreased when PRP was present in the induction medium (Fig. 7). And the inhibition effects were related to the proliferation of the hMDPCs during differentiation induction (data not shown).

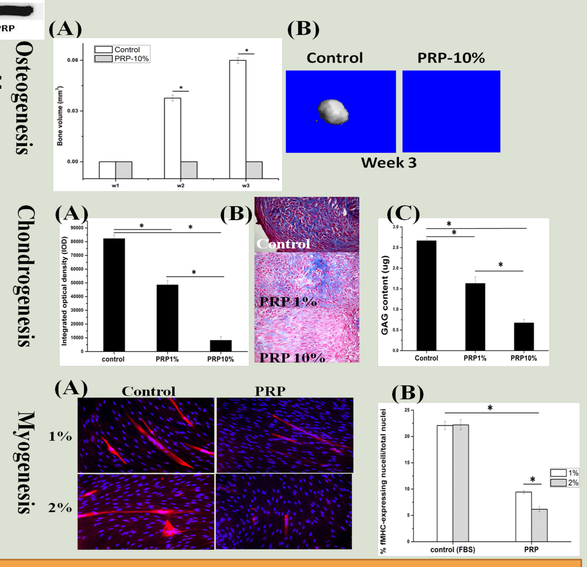

Figure 7. Influence of PRP on differentiation of hMDPCs: hMDPCs (Pre-plated hMDPCs as representative) were cultured in various differentiation medias with or without PRP.

Discussion and Conclusion

This study demonstrates direct effects of PRP on hMDPCs without the additional effect of systemic factors. Together these findings indicate a potential usage of PRP with hMDPCs for tissue engineering. First, PRP can be used as a supplement for *ex vivo* expansion of hMDPCs. Second, PRP could be a possible augmentative agent for *in vivo* stem cell therapy since the growth factors released by PRP can support the proliferation of the hMDPCs and keep them in an early undifferentiated stage at their initial transplantation; once the platelets have lost their activity, the MDPCs will regain their responsiveness to the local microenvironmental stimuli and differentiate into functional tissue cells. If PRP has tissue specific effects on other stem cell populations need further investigation.

References

1. Shahdadfar, A., et al., Stem Cells, 2005. **23**(9): p. 1357-66.
2. Zheng, B., et al., Nat Biotechnol, 2007. **25**(9): p. 1025-34.
3. Crisan, M., et al., Cell Stem Cell, 2008. **3**(3): p. 301-13.